Ectomycorrhizal Fungi Differentially Obtain Nitrogen Derived From Soil Organic Matter: Implications for Community Assembly and Forest Response to Climate Change

By

Peter T. Pellitier

A dissertation submitted in partial fulfillment
of the requirements for the degree of
Doctor of Philosophy
(Resource Policy and Behavior)
University of Michigan
2020

Doctoral Committee:

Professor Donald R. Zak, Chair
Professor Deborah E. Goldberg
Associate Professor Inés Ibáñez
Professor Timothy Y. James

Peter T. Pellitier

ptpell@umich.edu

ORCID iD: 0000-0002-0226-0784

Dedication

This dissertation is dedicated to the memory of Geraldine Land, who was among the first to encourage my passion for Nature. Secondly, I dedicate this work to the senescent patch of old-growth Douglas-Fir forest in South Eugene Oregon, may you forever extend your teachings.

Acknowledgements

I express deep gratitude to Donald Zak for his friendship, steady hand and indomitable passion. I cannot imagine a better guide to the study of Ecology, and I am deeply indebted. It is often the small moments that can retrieve a person, and few individuals have so willingly shared of themselves to help me personally and professionally.

A sincere thanks is also offered to Tim James, a constant source of friendship and peerless in his patience and kindness. I would also like to thank Inés Ibáñez for expanding my understanding of the art of ecological modeling, I will never fear variance again. Finally, I thank Deborah Goldberg for immense ecological wisdom and for her tireless activism.

I am grateful for the comradery and ecological insight offered by William Argiroff and Wes Bickford. My academic brothers made much of this work possible. Additionally I would like to thank Rima Upchurch for her patience, immense scientific savvy, and for gently grabbing the reins when needed. I would also like to thank Sydney Salley, Etienne Herrick, Noor Ahmad, Katie Seguin, Nisha Gudal, Noelle Visser, and Beyonzo for substantial contributions to field and laboratory work. Beth van Dusen provided countless hours of assistance in the laboratory. Darrell Jones III was a major source of inspiration.

I would also like to extend my thanks to Donna Zak, always with generous words and interest in my growth, and also for making sure Don and I come back from the field in one-piece. I also thank the Integrated Training in Microbial Systems program for building community among microbial ecologists, and Rackham for substantial funding to my research. Finally, I

would like to thank Leah Bricker in the School of Education and a special mention to Ken Shindledecker for introducing me to Deep Ecology in high-school.

Finally, I would like to thank my parents, John and Michelle and sisters Natalie and Serena. You've known since the beginning, and I thank you for pushing me to fulfill my passion. Finally, I would like to thank my grandparents near and far: John, Darrell, Lois and Anne for love and understanding.

Table of Contents

List of Tables

List of Figures

Abstract

This dissertation investigates the capacity for ectomycorrhizal fungi to obtain Nitrogen (N), organically bound in soil organic matter (N-SOM). In Chapter 1, I delineate the gene families involved in the decay of SOM, and study their distribution across the ~ 85 independent evolutionary lineages of ECM fungi. I provide evidence that the polyphyletic nature of the ECM lifestyle has resulted in considerable variation in their genetic potential to obtain N-SOM. In addition, I describe several untested physiological conditions that limit our understanding of the contribution of N-SOM to plant growth. In chapters 2 and 3, I study ECM communities arrayed across a natural soil fertility gradient in Northern Michigan using a standardized tree host (*Quercus rubra* L.). I develop and test a whole-plant resource allocation framework that explicitly considers the composition and function of ECM communities and their net effect on plant uptake of organic and inorganic forms of N at the ecosystem scale. In Chapter 2, I employ a trait-based shotgun metagenome enabled approach to study variation in the genomic potential of ECM communities to obtain N-SOM. Foremost, I gathered support for the hypothesis that soil inorganic N availability acts as an environmental filter structuring the assembly of ECM communities and their trait distributions. Specifically, I document that the community weighted mean (CWM) genomic decay potential of ECM communities is inversely correlated with soil inorganic N availability. Furthermore, I tested the hypothesis that *Q. rubra* inhabiting low inorganic N soils, obtain greater quantities of N-SOM than do *Q. rubra* occupying inorganic N rich soils, due to physiological variation in the attributes of their ECM symbionts. I scaled CWM gene counts by the number of ECM infected root-tips present on individual root-systems to document that *Q. rubra* inhabiting low inorganic N soils host greater composite quantities of ECM genes involved in decay. Chapter 3 incorporates dendrochronological tree core data, Bayesian plant growth modeling approaches and molecular characterization of ECM communities and associated foraging morphologies. I show that N-SOM is likely to bolster net primary productivity (NPP) in soils where inorganic N is relatively scarce due to compositional and functional variation of associated ECM communities. Moreover, I compile dendrochronological evidence that trees inhabiting low inorganic N soils, exhibit a positive response to nearly 40 years of increasing ambient [CO_2]. Integrating functional attributes of ECM communities, provides supports for the hypothesized importance of organic N in the global fertilizing effect of CO_2 on NPP. Because ECM fungi that can degrade N-SOM carry a high

carbon cost to their plant host, my results highlight potential tradeoffs in the role of the ECM symbiosis across soil inorganic N gradients. By documenting that N-SOM is unlikely to ubiquitously contribute to plant growth, my dissertation provides unique support for theory of optimal plant N foraging; I suggest that shifts in the functional attributes of ECM communities represent a mechanistic basis for plant flexibility in nutrient foraging strategies. Together, my analyses offers unprecedented molecular insight into the physiology of ECM communities and extends a functional biogeographic perspective that clarifies widespread observations of consistent patterns of ECM community turnover. Finally, my work adds further mechanistic evidence that the plant CO_2 fertilization response is predicated upon the capacity of their ECM symbionts to obtain N-SOM, and clarifies the heterogeneous response of ECM forests to eCO_2.

Chapter 1 Introduction

Historically, plants were thought to exclusively assimilate inorganic N (*i.e.,* NH_4^+ and NO_3^-). Accordingly, the slow saprotrophic release of inorganic N (*i.e.,* net N mineralization) constrained plant growth (Tamm 1991), and modern earth system models (ESM) exclusively parameterize net primary productivity (NPP) using inorganic N (Wieder et al. 2015, Wenzel et al. 2016). While approximately 95% of soil N is complexed in soil organic matter (Schulten and Schnitzer 1997, Rillig et al. 2007), this N pool has been considered biochemically unavailable for plant growth (Vitousek and Howarth 1991, Schimel and Bennett 2004). Independent of temperate-forest-centric studies of N cycling, plant uptake of low molecular weight organic N has been well established for certain boreal plants (Kielland 1994, Näsholm et al. 1998, Jones et al. 2005). Although organic N uptake may contribute to tree growth in certain contexts within temperate ecosystems (Näsholm et al. 2009), there is current debate regarding the importance of N-SOM for plant nutrition, especially the extent to which mycorrhizal fungi provide plant access to the large ecosystem N pool.

Ectomycorrhizal (ECM) fungi represent the primary plant nutrient uptake organ in many forest ecosystems. ECM fungi associate with ~ 60% of the Earth's plant stems (Steidinger et al. 2019) and provision host plants with ~80% of their annual N requirements (Leake et al. 2004). These root-symbionts produce prolific hyphae and greatly increase the volume of soil exploited by fine roots (Smith and Read 2010) and they compose ~ 33% of soil microbial biomass in boreal and temperate forest ecosystems (Högberg and Högberg 2002). The ECM lifestyle has repeatedly evolved ~ 85 times over the past 125 Mya (Hibbett et al. 2000, Tedersoo and Smith 2013) from a

wide phylogenetic range of free-living saprotrophic ancestors in the Basidiomycota, Ascomycota and the Mucoromycota (Smith and Read 2010, Kohler et al. 2015). Integrative understanding of the implications of the polyphyletic evolutionary history of ECM fungi from their free-living saprotrophic ancestors, in an ecosystem context, is a major goal of this dissertation.

The capacity for ECM fungi to assimilate inorganic N, amino acids and amino sugars from soil solution and transfer the N contained therein to their plant hosts is relatively well understood (Abuzinadah and Read 1986, Bending and Read 1996, 1997, Lilleskov et al. 2002a). However, the capacity for ECM fungi to degrade N-SOM is much more contentious (Zak et al. 2019). Originally proposed by Frank (1898), recent whole-genome sequencing efforts have promoted renewed interest in the potential for ECM fungi to decay SOM (Talbot et al. 2008, Martin et al. 2016). Early experiments decisively demonstrated variation in the capacity for ECM fungi to degrade proteins and access amino acids from complex substrates (Abuzinadah and Read 1986, Bending and Read 1996). These experiments also demonstrated, that in comparison to free-living saprotrophic fungi, ECM fungi have significantly reduced capacity to degrade organic N-bearing compounds residing in SOM. Remarkably, however, the past decade has seen the emergence of the generalized paradigm that all ECM fungi deploy decay mechanisms retained from their saprotrophic ancestors to obtain N-SOM (Phillips et al. 2013, Averill et al. 2014). In fact, ECM communities distributed from the tropics to the boreal forest have recently been modelled to function equivalently in their capacity to provision their host plant with N-SOM (Phillips et al. 2013, Averill et al. 2014, Terrer et al. 2018). While the implications of this potential decay physiology are significant and multi-pronged, as I describe and demonstrate in this dissertation, evidence supporting widespread ECM acquisition of N-SOM remains exceptionally weak and theoretically unlikely.

The possibility that plants can 'short-circuit' supply rates of inorganic N (*i.e.,* net N mineralization) by obtaining N-SOM has important implications for soil C cycling (Orwin et al. 2011, Averill et al. 2014, Sterkenburg et al. 2018, Zak et al. 2019), plant coexistence , as well as global productivity responses to elevated atmospheric CO_2 (Terrer et al. 2018, 2019). Plants lack the physiological capacity necessary to degrade SOM and plant access to N-SOM is entirely dependent on the physiology of their ECM mutualists (Lindahl and Tunlid 2015, Zak et al. 2019). Despite the widespread implications of plant uptake of N-SOM, the extent to which ECM fungi can assimilate this N source under field settings remains unknown (Zak et al. 2019). In Chapter 1, I provide a critical review of available evidence and delineate likely ECM gene families required to decay the complex bonds present in SOM (Pellitier and Zak 2018). In addition, I utilize available genomic evidence to summarize the distribution of these gene families across ECM lineages. Critically, I aim to clarify how the genomic background of ancient saprotrophic fungal taxa-- ECM progenitors-- shapes the physiological potential of modern ECM fungi. Moreover, I show how observed experimental heterogeneity in the capacity of ECM fungi to degrade complex organic N sources (Abuzinadah and Read 1986, Bending and Read 1996, 1997) may arise predictably from their polyphyletic evolutionary history. My results demonstrate that ECM fungi do not have equivalently genomic capacity to obtain N-SOM. Embracing intrinsic variation among lineages of ECM fungi opens inquiry into the ecological constraints that mediate plant uptake of N-SOM.

Net primary productivity (NPP) has been globally stimulated by rising anthropogenic [CO_2] and coupled climate-biogeochemical (CCB) models suggest this effect could continue to ~2070 (Wenzel et al. 2016). Trees associating with ECM fungi, in particular, are predicted to experience increased growth as anthropogenic CO_2 continues to accumulate in the Earth's atmosphere (Terrer et al. 2016, 2019). This positive response is thought to be contingent on the putative capacity of their ECM symbiont to 'short-circuit' limiting supply rates of inorganic N, thereby allowing trees to obtain the N bound in SOM. Observational evidence may support such a possibility, because trees associating with arbuscular mycorrhiza, which are entirely dependent on inorganic N sources, display a net neutral response to eCO_2 (Terrer et al. 2016). As a result, plant uptake of N-SOM is believed to be one of the most sensitive model parameters determining the extent to which NPP is boosted by eCO_2 (Terrer et al. 2016, 2019)

Understanding plant uptake of N-SOM under field-conditions is critical because projections of a 12% to 60% increase in NPP under eCO_2 may be overestimated if plants cannot obtain sufficient N (Reich et al. 2006, Wieder et al. 2015). This is because the positive effect of eCO_2 on plant growth is likely to increase plant N demand, despite no significant increase in net N mineralization (Wieder et al. 2015). However, if N-SOM widely contributes to ECM-associated plant N uptake, the terrestrial C sink may continue for decades (Wieder et al. 2015, Terrer et al. 2016). Nonetheless, the contribution of N-SOM to plant growth remains uncertain, and the coarse generality that *all* plants associating with ECM fungi will display an overall *increase* in growth due to eCO_2 requires urgent field-based investigation.

Enhanced understanding of plant uptake of N-SOM can be addressed by building predictive understanding of the assembly rules structuring the functional biogeographic distribution of ECM communities (Violle et al. 2014). Theoretical models of coupled nutrient exchange and plant resource expenditure (Kiers et al. 2011, Hortal et al. 2017) suggest that ECM community assembly is tied to their physiological capacity to assimilate and transfer locally abundant N forms (Kranabetter et al. 2015), including N-SOM (Taylor et al. 2000, Lilleskov et al. 2002b). Indeed, there may be a feedback between ECM N foraging abilities and soil characteristics, because ECM fungi that can access and transfer more N (in whatever form) to their plant hosts may receive more photosynthate in return (Kiers et al. 2011, Nehls et al. 2016, Hortal et al. 2017). As a result, distinct community-assembly trajectories may generate biogeographic variation in the capacity of ECM communities to biochemically modify SOM and provision their hosts with the N bound therein (Read and Perez-Moreno 2003, Koide et al. 2014). This leads to the hypothesis that the capacity for ECM fungi to obtain N-SOM is greatest when inorganic N supply is low.

This framework is contextually supported by available observational data. Underappreciated, but convergent, patterns in ECM community turnover have been repeatedly documented across soil inorganic N gradients, varying in both scale and host type in British Columbia (Kranabetter et al. 2015), Alaska (Lilleskov et al. 2002a), Michigan (Edwards and Zak 2010) , Sweden (Toljander et al. 2006, Bödeker et al. 2014, Sterkenburg et al. 2015, Clemmensen et al. 2015) as well as gradients spanning continental Europe (Taylor et al. 2000, Suz et al. 2014, van der Linde et al. 2018). In further support of this rationale, the ECM genera *Cortinarius*, *Russula,* and *Piloderma,*often occur in forest soils in which the supply of inorganic

N is low (Suz et al. 2014, Sterkenburg et al. 2018). Further, numerous studies consistently find that inorganic N concentrations are inversely correlated with the relative abundance of these ECM genera (Bödeker et al. 2014, van der Linde et al. 2018, Sterkenburg et al. 2018). Intriguingly, representative members of each of these genera are known to possess relatively high quantities of genes (class II peroxides, lytic polysaccharides monooxygenases, and certain glycoside hydrolases) with high oxidative capacity and hence putative capacity to decay SOM and release N from it (Bödeker et al. 2014, Kohler et al. 2015, Pellitier and Zak 2018). Notably, these ECM genera have evolved from white-rot saprotrophic ancestors (Kohler et al. 2015). Accordingly, these ECM genera are among the best candidates to provision N in SOM to their plant hosts. Additional isotopic evidence from *Cortinarius* sporocarps further suggests that members of this genus obtain organic N from SOM (Hobbie and Högberg 2012), and field evidence reveals that the relative abundance of *Cortinarius* spp are positively correlated with Mn-peroxidase activity, a potent extracellular enzyme mediating the oxidation of SOM (Bödeker et al. 2014, Sterkenburg et al. 2018). Shifts in the morphological attributes of ECM hyphae associated with N foraging (Moeller et al. 2014, Defrenne et al. 2019) as well as enzyme and culture assays (Taylor et al. 2000, Lilleskov et al. 2002a, Bödeker et al. 2014, Pierre-Emmanuel et al. 2016) along soil N gradients also implicitly support the hypothesis that ECM communities vary in their capacity to forage for biochemically distinct N forms. In further accordance with this overall rationale, distinct ECM genera are generally dominant members of fungal communities in which quantities of inorganic N are high (Lilleskov et al. 2002b, Edwards and Zak 2010, Clemmensen et al. 2015) and culture-based nutritional studies of particular taxa that occur with fidelity in high inorganic N soils reveal that they cannot degrade complex organic N bearing molecules (Taylor et al. 2000, Lilleskov et al. 2002b, Wolfe et al. 2012).

In Chapter 2, I employ a metagenomics enabled trait-based approach to test the role of inorganic N availability in structuring the assembly of ECM communities. I leveraged principles of plant community ecology in order to gather evidence in support of habitat filtering (Ackerly 2003, Cornwell and Ackerly 2009). Specifically, I evaluated shifts in the community weighted mean (CWM) decay capacity of ECM communities inhabiting individual red-oak (*Quercus rubra L.*) root-systems along a well-defined natural soil inorganic N gradient. Consistent with the previous observational evidence summarized above, I predicted that the CWM abundance of decay genes in ECM communities is inversely correlated with soil inorganic N availability.

Moreover, I sought to test the hypothesis that *Q. rubra* inhabiting low inorganic N soils obtain greater quantities of N-SOM than do *Q. rubra* occupying inorganic N rich soils, due to functional variation in the attributes of their ECM symbionts. Evidence in support of this hypothesis would include observation of *Q. rubra* hosting greater overall quantities of ECM genes involved in decay of SOM in low inorganic N soils.

In Chapter 3, I employed an integrative approach combining molecular characterization of ECM communities and dendrochronological analyses of the same *Quercus rubra* individuals studied in Chapter 2. I sought to shed mechanistic light into the role of organic and inorganic N sources in plant growth response to nearly four decades of historical increases in CO_2 (+ 70 μmol mol^{-1}). Moreover, this study aimed to provide insight into the soil conditions and biotic interactions that give rise to plant assimilation of N-SOM. I employed a Bayesian modeling framework to disentangle plant reliance on organic and inorganic N sources in order to compile evidence in further support of the hypothesis that N-SOM primarily contributes to plant growth in low inorganic N soils. In addition, I tested the hypothesis that plant uptake of N-SOM is required for a positive plant response to eCO_2. Given that existing CCB models parametrize plant growth using inorganic N supplies alone, this study offers mechanistic insight into potential plant response to eCO_2.

The analyses presented in Chapter 2 and 3 are intended to generate integrative , and I discuss their joint interpretation in the Discussion section. Namely, I discuss how mechanisms explaining dendrochronological evidence for uptake of N-SOM and enhanced response to historical increases in CO_2 are supported by metagenomic insights into ECM community assembly. Together, positive support for hypotheses delineated in Chapter 2 and 3 would represent unprecedented support for the importance of N-SOM in the global fertilizing effect of CO_2 on NPP, and the role of ECM fungi in plant uptake of N-SOM.

Works Cited

Abuzinadah, R. A., and D. J. Read. 1986. The Role of Proteins in the Nitrogen Nutrition of Ectomycorrhizal Plants. Utilization of Peptides and Proteins by Ectomycorrhizal Fungi. The New Phytologist 103:481–493

Ackerly, D. D. 2003. Community Assembly, Niche Conservatism, and Adaptive Evolution in Changing Environments. International Journal of Plant Sciences 164:S165–S184.

Averill, C., B. L. Turner, and A. C. Finzi. 2014. Mycorrhiza-mediated competition between plants and decomposers drives soil carbon storage. Nature 505:543–545.

Bending, G. D., and D. J. Read. 1996. Nitrogen mobilization from protein-polyphenol complex by ericoid and ectomycorrhizal fungi. Soil Biology and Biochemistry 28:1603–1612.

Bending, G. D., and D. J. Read. 1997. Lignin and soluble phenolic degradation by ectomycorrhizal and ericoid mycorrhizal fungi. Mycological Research 101:1348–1354.

Bödeker, I. T. M., K. E. Clemmensen, W. de Boer, F. Martin, Å. Olson, and B. D. Lindahl. 2014. Ectomycorrhizal Cortinarius species participate in enzymatic oxidation of humus in northern forest ecosystems. New Phytologist 203:245–256.

Bouma-Gregson, K., M. R. Olm, A. J. Probst, K. Anantharaman, M. E. Power, and J. F. Banfield. 2019. Impacts of microbial assemblage and environmental conditions on the distribution of anatoxin-a producing cyanobacteria within a river network. The ISME Journal 13:1618–1634.

Clemmensen, K. E., R. D. Finlay, A. Dahlberg, J. Stenlid, D. A. Wardle, and B. D. Lindahl. 2015. Carbon sequestration is related to mycorrhizal fungal community shifts during long-term succession in boreal forests. New Phytologist:1525–1536.

Cornwell, W. K., and D. D. Ackerly. 2009. Community assembly and shifts in plant trait distributions across an environmental gradient in coastal California. Ecological Monographs 79:109–126.

Defrenne, C. E., T. J. Philpott, S. H. A. Guichon, W. J. Roach, B. J. Pickles, and S. W. Simard. 2019. Shifts in Ectomycorrhizal Fungal Communities and Exploration Types Relate to

the Environment and Fine-Root Traits Across Interior Douglas-Fir Forests of Western Canada. Frontiers in Plant Science 10:643.
Edwards, I. P., and D. R. Zak. 2010. Phylogenetic similarity and structure of Agaricomycotina communities across a forested landscape. Molecular Ecology 19:1469–1482.
Hibbett, D. S., L.-B. Gilbert, and M. J. Donoghue. 2000. Evolutionary instability of ectomycorrhizal symbioses in basidiomycetes. Nature 407:506–508.
Hobbie, E. A., and P. Högberg. 2012. Nitrogen isotopes link mycorrhizal fungi and plants to nitrogen dynamics. New Phytologist 196:367–382.
Högberg, M. N., and P. Högberg. 2002. Extramatrical ectomycorrhizal mycelium contributes one-third of microbial biomass and produces, together with associated roots, half the dissolved organic carbon in a forest soil. New Phytologist 154:791–795.
Hortal, S., K. L. Plett, J. M. Plett, T. Cresswell, M. Johansen, E. Pendall, and I. C. Anderson. 2017. Role of plant–fungal nutrient trading and host control in determining the competitive success of ectomycorrhizal fungi. The ISME Journal 11:2666–2676.
Jones, D. L., J. R. Healey, V. B. Willett, J. F. Farrar, and A. Hodge. 2005. Dissolved organic nitrogen uptake by plants—an important N uptake pathway? Soil Biology and Biochemistry 37:413–423.
Kielland, K. 1994. Amino Acid Absorption by Arctic Plants: Implications for Plant Nutrition and Nitrogen Cycling. Ecology 75:2373–2383.
Kiers, E. T., M. Duhamel, Y. Beesetty, J. A. Mensah, O. Franken, E. Verbruggen, C. R. Fellbaum, G. A. Kowalchuk, M. M. Hart, A. Bago, T. M. Palmer, S. A. West, P. Vandenkoornhuyse, J. Jansa, and H. Bucking. 2011. Reciprocal Rewards Stabilize Cooperation in the Mycorrhizal Symbiosis. Science 333:880–882.
Kohler, A., A. Kuo, L. G. Nagy, E. Morin, K. W. Barry, F. Buscot, B. Canbäck, C. Choi, N. Cichocki, A. Clum, J. Colpaert, A. Copeland, M. D. Costa, J. Doré, D. Floudas, G. Gay, M. Girlanda, B. Henrissat, S. Herrmann, J. Hess, N. Högberg, T. Johansson, H.-R. Khouja, K. LaButti, U. Lahrmann, A. Levasseur, E. A. Lindquist, A. Lipzen, R. Marmeisse, E. Martino, C. Murat, C. Y. Ngan, U. Nehls, J. M. Plett, A. Pringle, R. A. Ohm, S. Perotto, M. Peter, R. Riley, F. Rineau, J. Ruytinx, A. Salamov, F. Shah, H. Sun, M. Tarkka, A. Tritt, C. Veneault-Fourrey, A. Zuccaro, A. Tunlid, I. V. Grigoriev, D. S. Hibbett, and F. Martin. 2015. Convergent losses of decay mechanisms and rapid turnover of symbiosis genes in mycorrhizal mutualists. Nature Genetics 47:410–415.
Koide, R. T., C. Fernandez, and G. Malcolm. 2014. Determining place and process: functional traits of ectomycorrhizal fungi that affect both community structure and ecosystem function. New Phytologist 201:433–439.
Kranabetter, J. M., B. J. Hawkins, M. D. Jones, S. Robbins, T. Dyer, and T. Li. 2015. Species turnover (β-diversity) in ectomycorrhizal fungi linked to uptake capacity. Molecular Ecology 24:5992–6005.
Leake, J., D. Johnson, D. Donnelly, G. Muckle, L. Boddy, and D. Read. 2004. Networks of power and influence: the role of mycorrhizal mycelium in controlling plant communities and agroecosystem functioning 82:30.
Lilleskov, E. A., T. J. Fahey, T. R. Horton, and G. M. Lovett. 2002a. Belowground Ectomycorrhizal Fungal Community Change Over a Nitrogen Deposition Gradient in Alaska. Ecology 83:104–115.

Lilleskov, E. A., E. A. Hobbie, and T. J. Fahey. 2002b. Ectomycorrhizal fungal taxa differing in response to nitrogen deposition also differ in pure culture organic nitrogen use and natural abundance of nitrogen isotopes. New Phytologist 154:219–231.

Lindahl, B. D., and A. Tunlid. 2015. Ectomycorrhizal fungi – potential organic matter decomposers, yet not saprotrophs. The New Phytologist 205:1443–1447.

van der Linde, S., L. M. Suz, C. D. L. Orme, F. Cox, H. Andreae, E. Asi, B. Atkinson, S. Benham, C. Carroll, N. Cools, B. De Vos, H.-P. Dietrich, J. Eichhorn, J. Gehrmann, T. Grebenc, H. S. Gweon, K. Hansen, F. Jacob, F. Kristöfel, P. Lech, M. Manninger, J. Martin, H. Meesenburg, P. Merilä, M. Nicolas, P. Pavlenda, P. Rautio, M. Schaub, H.-W. Schröck, W. Seidling, V. Šrámek, A. Thimonier, I. M. Thomsen, H. Titeux, E. Vanguelova, A. Verstraeten, L. Vesterdal, P. Waldner, S. Wijk, Y. Zhang, D. Žlindra, and M. I. Bidartondo. 2018. Environment and host as large-scale controls of ectomycorrhizal fungi. Nature 558:243–248.

Louca, S., S. M. S. Jacques, A. P. F. Pires, J. S. Leal, A. L. González, M. Doebeli, and V. F. Farjalla. 2017. Functional structure of the bromeliad tank microbiome is strongly shaped by local geochemical conditions. Environmental Microbiology 19:3132–3151.

Martin, F., A. Kohler, C. Murat, C. Veneault-Fourrey, and D. S. Hibbett. 2016. Unearthing the roots of ectomycorrhizal symbioses. Nature Reviews Microbiology 14:760–773.

Moeller, H. V., K. G. Peay, and T. Fukami. 2014. Ectomycorrhizal fungal traits reflect environmental conditions along a coastal California edaphic gradient. FEMS Microbiology Ecology 87:797–806.

Näsholm, T., A. Ekblad, A. Nordin, R. Giesler, M. Högberg, and P. Högberg. 1998. Boreal forest plants take up organic nitrogen. Nature 392:914–916.

Näsholm, T., K. Kielland, and U. Ganeteg. 2009. Uptake of organic nitrogen by plants. New Phytologist 182:31–48.

Nehls, U., A. Das, and D. Neb. 2016. Carbohydrate metabolism in ectomycorrhizal symbiosis. Molecular mycorrhizal symbiosis 10:161–178.

Orwin, K. H., M. U. F. Kirschbaum, M. G. S. John, and I. A. Dickie. 2011. Organic nutrient uptake by mycorrhizal fungi enhances ecosystem carbon storage: a model-based assessment. Ecology Letters 14:493–502.

Pellitier, P. T., I. Ibáñez, D. R. Zak, W. A. Argiroff, and K. Acharya. in review. Ectomycorrhizal access to organic N enhances plant growth response to rising [CO2]. in review.

Pellitier, P. T., and D. R. Zak. 2018. Ectomycorrhizal fungi and the enzymatic liberation of nitrogen from soil organic matter: why evolutionary history matters. New Phytologist 217:68–73.

Phillips, R. P., E. Brzostek, and M. G. Midgley. 2013. The mycorrhizal-associated nutrient economy: a new framework for predicting carbon–nutrient couplings in temperate forests. New Phytologist 199:41–51.

Pierre-Emmanuel, C., M. François, S. Marc-André, D. Myriam, C. Stéven, Z. Fabio, B. Marc, P. Claude, T. Adrien, G. Jean, and R. Franck. 2016. Into the functional ecology of ectomycorrhizal communities: environmental filtering of enzymatic activities. Journal of Ecology 104:1585–1598.

Read, D. J., and J. Perez-Moreno. 2003. Mycorrhizas and Nutrient Cycling in Ecosystems: A Journey towards Relevance? The New Phytologist 157:475–492.

Reich, P. B., S. E. Hobbie, T. Lee, D. S. Ellsworth, J. B. West, D. Tilman, J. M. H. Knops, S. Naeem, and J. Trost. 2006. Nitrogen limitation constrains sustainability of ecosystem response to CO2. Nature 440:922–925.

Rillig, M. C., B. A. Caldwell, H. A. B. Wösten, and P. Sollins. 2007. Role of proteins in soil carbon and nitrogen storage: controls on persistence. Biogeochemistry 85:25–44.

Schimel, J. P., and J. Bennett. 2004. Nitrogen Mineralization: Challenges of a Changing Paradigm. Ecology 85:591–602.

Schulten, H.-R., and M. Schnitzer. 1997. The chemistry of soil organic nitrogen: a review. Biology and Fertility of Soils 26:1–15.

Smith, S. E., and D. J. Read. 2010. Mycorrhizal symbiosis. Academic press.

Steidinger, B. S., T. W. Crowther, J. Liang, M. E. Van Nuland, G. D. A. Werner, P. B. Reich, G. J. Nabuurs, S. de-Miguel, M. Zhou, N. Picard, B. Herault, X. Zhao, C. Zhang, D. Routh, and K. G. Peay. 2019. Climatic controls of decomposition drive the global biogeography of forest-tree symbioses. Nature 569:404–408.

Sterkenburg, E., A. Bahr, M. B. Durling, K. E. Clemmensen, and B. D. Lindahl. 2015. Changes in fungal communities along a boreal forest soil fertility gradient. New Phytologist 207:1145–1158.

Sterkenburg, E., K. E. Clemmensen, A. Ekblad, R. D. Finlay, and B. D. Lindahl. 2018. Contrasting effects of ectomycorrhizal fungi on early and late stage decomposition in a boreal forest. The ISME Journal 12:2187–2197.

Suz, L. M., N. Barsoum, S. Benham, H.-P. Dietrich, K. D. Fetzer, R. Fischer, P. García, J. Gehrman, F. Kristöfel, M. Manninger, S. Neagu, M. Nicolas, J. Oldenburger, S. Raspe, G. Sánchez, H. W. Schröck, A. Schubert, K. Verheyen, A. Verstraeten, and M. I. Bidartondo. 2014. Environmental drivers of ectomycorrhizal communities in Europe's temperate oak forests. Molecular Ecology 23:5628–5644.

Talbot, J. M., S. D. Allison, and K. K. Treseder. 2008. Decomposers in disguise: mycorrhizal fungi as regulators of soil C dynamics in ecosystems under global change. Functional Ecology 22:955–963.

Tamm, C. O. 1991. Introduction: Geochemical Occurrence of Nitrogen. Natural Nitrogen Cycling and Anthropogenic Nitrogen Emissions. Pages 1–6 *in* C. O. Tamm, editor. Nitrogen in Terrestrial Ecosystems: Questions of Productivity, Vegetational Changes, and Ecosystem Stability. Springer, Berlin, Heidelberg.

Taylor, A. F. S., F. Martin, and D. J. Read. 2000. Fungal Diversity in Ectomycorrhizal Communities of Norway Spruce [Picea abies (L.) Karst.] and Beech (Fagus sylvatica L.) Along North-South Transects in Europe. Pages 343–365 *in* E.-D. Schulze, editor. Carbon and Nitrogen Cycling in European Forest Ecosystems. Springer, Berlin, Heidelberg.

Tedersoo, L., and M. E. Smith. 2013. Lineages of ectomycorrhizal fungi revisited: Foraging strategies and novel lineages revealed by sequences from belowground. Fungal Biology Reviews 27:83–99.

Terrer, C., R. B. Jackson, I. C. Prentice, T. F. Keenan, C. Kaiser, S. Vicca, J. B. Fisher, P. B. Reich, B. D. Stocker, B. A. Hungate, J. Peñuelas, I. McCallum, N. A. Soudzilovskaia, L. A. Cernusak, A. F. Talhelm, K. Van Sundert, S. Piao, P. C. D. Newton, M. J. Hovenden, D. M. Blumenthal, Y. Y. Liu, C. Müller, K. Winter, C. B. Field, W. Viechtbauer, C. J. Van Lissa, M. R. Hoosbeek, M. Watanabe, T. Koike, V. O. Leshyk, H. W. Polley, and O. Franklin. 2019. Nitrogen and phosphorus constrain the CO2 fertilization of global plant biomass. Nature Climate Change 9:684–689.

Terrer, C., S. Vicca, B. A. Hungate, R. P. Phillips, and I. C. Prentice. 2016. Mycorrhizal association as a primary control of the CO $_2$ fertilization effect. Science 353:72–74.
Terrer, C., S. Vicca, B. D. Stocker, B. A. Hungate, R. P. Phillips, P. B. Reich, A. C. Finzi, and I. C. Prentice. 2018. Ecosystem responses to elevated CO2 governed by plant–soil interactions and the cost of nitrogen acquisition. New Phytologist 217:507–522.
Toljander, J. F., U. Eberhardt, Y. K. Toljander, L. R. Paul, and A. F. S. Taylor. 2006. Species composition of an ectomycorrhizal fungal community along a local nutrient gradient in a boreal forest. New Phytologist 170:873–884.
Violle, C., P. B. Reich, S. W. Pacala, B. J. Enquist, and J. Kattge. 2014. The emergence and promise of functional biogeography. Proceedings of the National Academy of Sciences 111:13690–13696.
Vitousek, P. M., and R. W. Howarth. 1991. Nitrogen limitation on land and in the sea: How can it occur? Biogeochemistry 13:87–115.
Wenzel, S., P. M. Cox, V. Eyring, and P. Friedlingstein. 2016. Projected land photosynthesis constrained by changes in the seasonal cycle of atmospheric CO 2. Nature 538:499–501.
Wieder, W. R., C. C. Cleveland, W. K. Smith, and K. Todd-Brown. 2015. Future productivity and carbon storage limited by terrestrial nutrient availability. Nature Geoscience 8:441–444.
Wolfe, B. E., R. E. Tulloss, and A. Pringle. 2012. The Irreversible Loss of a Decomposition Pathway Marks the Single Origin of an Ectomycorrhizal Symbiosis. PLoS ONE 7.
Zak, D. R., P. T. Pellitier, W. Argiroff, B. Castillo, T. Y. James, L. E. Nave, C. Averill, K. V. Beidler, J. Bhatnagar, J. Blesh, A. T. Classen, M. Craig, C. W. Fernandez, P. Gundersen, R. Johansen, R. T. Koide, E. A. Lilleskov, B. D. Lindahl, K. J. Nadelhoffer, R. P. Phillips, and A. Tunlid. 2019. Exploring the role of ectomycorrhizal fungi in soil carbon dynamics. New Phytologist 223:33–39.

Chapter 2 Ectomycorrhizal Fungi and the Enzymatic Liberation of Nitrogen from Soil Organic Matter: Why Evolutionary History Matters

Peter T. Pellitier & Donald R. Zak

Abstract: The view that ectomycorrhizal (ECM) fungi commonly participate in the enzymatic liberation of N from soil organic matter (SOM) has recently been invoked as a key mechanism governing the biogeochemical cycles of forest ecosystems. Here, we provide evidence that not all evolutionary lineages of ECM have retained the genetic potential to produce extracellular enzymes that degrade SOM, calling into question the ubiquity of the proposed mechanism. Further, we discuss several untested conditions that must be empirically validated before it is certain that any lineage of ECM fungi actively expresses extracellular enzymes in order to degrade SOM and transfer N contained therein to its host plant.

Introduction

In many terrestrial ecosystems, nitrogen (N) mineralization is often insufficient to account for annual plant N demand (Näsholm et al. 2009). To rectify this disparity, organic soil N has been hypothesized to be an important component of plant N supply (Neff et al. 2003). Ectomycorrhizal (ECM) fungi play a significant role in provisioning plants with N. Through the production of prolific hyphae, these fungi compose one-third of microbial biomass in boreal and temperate ecosystems (Högberg and Högberg 2002)ECM fungi greatly increase the volume of soil exploited by fine roots and hence increase inorganic N uptake by plants (Smith and Read 2010). Additionally, ECM fungi assimilate amino acids and amino sugars from soil solution (Lilleskov et al. 2002a) degrade proteins(Abuzinadah and Read 1986a, Bending and Read 1996, 1997) and transfer the N contained therein to their plant hosts(Näsholm et al. 2009).

However, ~ 95% of soil N is complexed in the end products of plant and microbial decay, collectively known as soil organic matter (SOM; (Schulten and Schnitzer 1997, Rillig et al. 2007) While saprotrophic fungi and some bacteria possess the capacity to metabolize SOM, the idea that ECM fungi obtain N bound in SOM has recently become generalized in a wide body of literature (Phillips et al. 2013, Averill and Hawkes 2016, Shah et al. 2016). This purported ECM physiology has significant implications for understanding soil biogeochemical cycles (Orwin et al. 2011, Averill and Hawkes 2016), as well as models of plant NPP. Acquisition of N from SOM has been postulated to provide plants with an additional source of growth-limiting N, thereby allowing sustained growth under elevated atmospheric CO_2 (Terrer et al. 2016). The aforementioned studies argue their results arise, at least in part, from the physiological capability of ECM fungi to use lignocellulolytic enzymes that depolymerize SOM and transfer the N therein to the host plant. However, this generalization ignores the fact that ECM fungi have independently and differentially evolved from saprotrophic ancestors dozens of times (Hibbett et al. 2000) causing the degree to which they have retained genes with saprotrophic function to dramatically differ among lineages (Kohler et al. 2015). The unique evolutionary history of each ECM lineage seriously draws into question the assumption that all ECM function similarly to provide host plants with N bound in SOM.

Understanding the capacity for ECM fungi to obtain N from SOM and transfer it to their plant host requires the empirical validation of several conditions outlined in Figure 1. Foremost, the extent to which ECM fungi metabolize SOM is first contingent on whether genes encoding

lignocellulolytic enzymes (*i.e.,* glycoside hydrolases, class II fungal peroxidases, glyoxyl oxidases, and phenol oxidases) were retained during their evolutionary history and are deployed when in symbiosis with plant roots. By critically reviewing pertinent studies and their bearing on the conditions presented in Figure 1, we conclude that, to the best of our knowledge, direct evidence establishing that all these conditions simultaneously occur for any ECM fungi is presently absent from the literature. Finally, we discuss recent biogeochemical observations with respect to the implications derived from our conclusions.

Have ECM fungi retained genes with lignocellulolytic potential from saprotrophic ancestors?

ECM fungi evolved primarily in the Basidiomycetes, but independent ECM lineages also appear in the Ascomycota (Smith and Read 2010). The evolution of genes encoding lignin and manganese peroxidases, however, appear to have primarily evolved in the Basidiomycota (Floudas et al. 2012). Accordingly, Ascomycete ECM fungi, such as the widespread *Cenoccoccum geophilum,* are unlikely to possess the genetic potential to depolymerize SOM.

Although the ancestor to the Agaricomycete clade has been reconstructed as a white rot saprotroph (Hibbett et al. 2000, Floudas et al. 2012), the evolution of the ECM lifestyle was thought to involve large losses of genes mediating the decay of lignocellulose and phenolic compounds in SOM(Plett and Martin 2011, Wolfe et al. 2012, Martin et al. 2016). Recently, however, numerous copies of genes potentially mediating the decay of SOM were observed in some lineages of ECM fungi (Bödeker et al. 2009, Kohler et al. 2015) (Fig. 2). In fact, the largest survey of ECM fungal genomes to date revealed that some ECM possess genes encoding class II peroxidases, glyoxal oxidases, cellobiohydrolases, laccases, and other enzymes which, when present in the genomes of white and brown rot fungi, mediate the saprotrophic decay of plant and microbial detritus as well as SOM (Kohler et al. 2015). Available evidence shows that ectomycorrhizal genomes have fewer lignocellulolytic genes than do their saprotrophic ancestors (Martin et al. 2016). The occurrence of these genes has led some to speculate that ECM fungi actively transcribe them into enzymes that depolymerize complex organic macromolecules in SOM, thereby providing plants access to the large pools of N previously theorized to be unavailable for plant uptake (Bödeker et al. 2014b, Lindahl and Tunlid 2015).

Importantly, the occurrence of genes with saprotrophic function varies widely across lineages of ECM fungi (Fig. 2). For instance, *Amanita muscaria* evolved within a clade of brown rot saprotrophs and consequently has lost the genetic capacity to depolymerize organic matter (Wolfe et al. 2012, Kohler et al. 2015). Similarly, *Laccaria bicolor* has lost most genes encoding enzymes that act on crystalline cellulose and lignin, although its genome does contain 11 copies of lytic polysaccharide monooxygenases (LPMO; (Martin et al. 2008, Kohler et al. 2015). Ectomycorrhizal taxa in the well-known Boletales clade occur within a paraphyletic group of brown rot fungi; these ECM taxa generally lack the genetic potential to degrade the polyphenolic and polysaccharide components of plant cell wall, microbial residues, as well as analogous compounds in SOM (Kohler et al. 2015)(Fig. 2). For the Boletales, it appears that parallel losses of genes mediating saprotrophic decay occurred in each of the three independent originations of a mutualistic lifestyle (Kohler et al. 2015).

By contrast, *Hebeloma cylindrosporum* evolved from a white rot ancestor that uses class II fungal peroxidases to oxidize polyphenolic compounds in SOM (Kohler et al. 2015). *H. cylindrosporum* has retained 3 copies of class II peroxidases, as well as 3 LPMO copies(Kohler et al. 2015)(Fig 2.). Lastly, *Cortinarius glaucopus* has retained the greatest known number of genes with putative saprotrophic function, including 11 Mn-peroxidases derived from white rot saprotrophic ancestors (Bödeker et al. 2014b, Martin et al. 2016). Clearly, the genetic potential to decay SOM varies widely across lineages of ECM fungi, making broad generalizations about the role of these organisms as agents of litter and SOM metabolism tenuous at best.

As each of the aforementioned lineages evolved into ECM fungi, hypothetical selective and drift processes governed the retention or loss of genes involved in the depolymerization of SOM. If ECM fungi evolved under conditions in which the fungi or host plants were consistently N limited, there may have been selective pressure to maintain energetically expensive lignocellulolytic genes that mediate the release of N from SOM. Further, because the ECM lifestyle evolved repeatedly over a relatively large span of evolutionary time, it would be unlikely that each of the dozens of independent transitions to ECM symbiosis resulted in the same whole-genome alterations (*i.e.,* loss of genes with saprotrophic function). This phenomenon has some precedent in the fungal symbionts of ambrosia beetles, in which each of the multiple origins of ambrosia fungi experienced different patterns of gene loss or gain (Cassar and Blackwell 1996). In sum, because ECM fungi have lost genes with saprotrophic function

over their evolutionary history in a differential manner (Martin et al. 2016), we should not expect that they represent a single functional group that uniformly provides host plants with N from SOM.

Are genes with saprotrophic function expressed by ECM fungi when in symbiosis?

In cases where ECM taxa have retained genes encoding enzymes that mediate SOM decay, it remains unclear if these genes are actively transcribed while forming mycorrhiza **(**Fig. 1). Ecological predictions based on the results of whole-genome sequencing suggest that ECM fungi retaining the largest numbers of class II fungal peroxidase genes should have the greatest physiological ability to oxidize the polyphenolic compounds in SOM (Kohler et al. 2015). However, available evidence does not support this hypothesis when it has been tested in culture. Rather, multiple studies have found that the number of Mn-peroxidase genes present in ECM genomes did not predict enzyme activity when grown on SOM extracts (Shah et al. 2016) leaf litter (Talbot et al. 2015).

Insights into the ability of ECM to synthesize lignocellulolytic enzymes and alter the biochemistry of SOM and plant cell wall in culture are intriguing (Rineau et al. 2012, Talbot et al. 2015, Shah et al. 2016); but because transcriptional profiles of ECM fungi vary depending upon whether the fungi are free-living or actively forming mycorrhiza (Martin et al. 2008, Kohler et al. 2015, Liao et al. 2016), these studies cannot conclusively demonstrate that identical physiology occurs when forming mycorrhiza. In fact, although *L. bicolor* has a limited genetic capacity to degrade plant cell wall, it did not transcribe these genes while forming mycorrhiza (Martin et al. 2008). Accordingly, there are few definitive studies demonstrating that ECM fungi express genes encoding saprotrophic enzymes while in symbiotic association with their plant hosts. In an important exception, Bödeker and colleagues (2014) observed that ECM fungi in the genus *Cortinarius* express high levels of Mn-peroxidase in boreal forest soils.

Finally, if genes with saprotrophic potential are expressed under field conditions, it is likely that their expression is context-dependent, determined by a myriad of ecological and edaphic factors including pH, the availability of inorganic N and organic N in soil solution. This phenomenon is well known for saprotrophic fungi (Sinsabaugh 2010, Edwards et al. 2011) and has now been demonstrated for ECM fungi in the field (Bödeker et al. 2014b) For example, when NH_4^+ is added to soils in the field, the expression of ECM genes with lignocellulolytic

capacity are downregulated (Bödeker et al. 2014b). Extrapolations from these patterns suggest that ECM fungi deploying Mn-peroxidases and other energetically expensive lignocellulolytic enzymes do so only when they and or their plant hosts are N limited. Resolving the abiotic conditions and nutritional status of the host plant, as well as symbiont in which these ECM genes reside, will add significant insight to our understanding of this phenomenon.

Do transcribed enzymes operate to obtain N from SOM?

Classic studies demonstrated that certain ECM fungi can obtain N from various organic sources (Abuzinadah and Read 1986a, 1988). Below, we clarify why previous work has not definitively resolved the ability for ECM fungi to obtain N from SOM. Evidence that ECM obtain organic N and transfer it to their host plants comes primarily from studies using pure protein or amino acids as an organic N source (Abuzinadah and Read 1988, Lilleskov et al. 2002a). However, most protein in soil is complexed with SOM or mineral surfaces (Rillig et al. 2007, Nannipieri and Paul 2009), and moreover the macromolecular structure of SOM results in amino acids, amino sugars, and protein being both physically and chemically resistant to enzymes that degrade peptides (Rillig et al. 2007). Thus, studies using pure protein as an N source are unlikely to be ecologically realistic (Jones et al. 2005, Nannipieri and Paul 2009).Recognizing these challenges, Bending and Read (1996) provided N to ECM fungi as a protein-polyphenol complex in pure culture, and observed that ECM fungi displayed significantly reduced uptake of organic N.

An additional level of uncertainty associated with the function of saprotrophic genes in ECM fungi arises from the fact that the enzymes they encode may have alternative functions. ECM transcribing laccase genes, thereby producing phenol oxidase enzymes, have been suggested as important to SOM decay (Talbot and Treseder 2010, Shah et al. 2016). However, laccase genes can transcribe both extra- and intracellular enzymes, the latter of which is involved with rigidifying fungal cell walls, producing melanin, and detoxifying cells (Kües and Rühl 2011). Apart from Mn- and lignin peroxidases whose substrates are inherently extracellular (Baldrian 2006) the occurrence and expression of fungal laccase genes need not imply that ECM express them to operate extracellularly on SOM.

Finally, it has been assumed that the oxidative potential of the enzymes expressed by ECM fungi is equivalent to those produced by saprotrophic fungi (Bödeker et al. 2014b). Nonetheless, genes annotated as Mn-peroxidases in ECM fungi, including *H. cylindrosporum, C.*

glaucopus and *P. croceum* were described as 'atypical' (Kohler et al. 2015, Shah et al. 2016, Martin et al. 2016), suggesting that the conformation of enzymes transcribed from these genes may not allow for the oxidation of lignin and polyphenols. Presently, we simply do not understand the effectiveness of the array of enzymes produced by ECM to oxidize or hydrolyze the wide range of organic bonds in SOM.

Is the organic N derived from SOM transferred to the plant host?

Finally, if some ECM taxa obtain N from SOM, they may not transfer this N to their plant hosts (Fig. 1). For example, Abuzinadah and Read (1986) noted that *Paxillus involutus* obtained N from pure protein, but in so doing sequestered high quantities of this N into its mycelium. This may be a general phenomenon, because current evidence for ECM fungi expressing saprotrophic enzymes in the environment occurs in boreal forests (Bödeker et al. 2014b); other studies in the boreal forest reveal that ECM fungi transfer only small amounts of organic N to their plant hosts (Näsholm et al. 2013, Högberg et al. 2017). In fact, modeling efforts in boreal forest ecosystems suggest that increasing atmospheric CO_2, in direct contrast to Terrer *et al.* (2016), will exacerbate plant N limitation through increases in the biomass and N content of fungal mycelium, even as plants allocate greater amounts of photosynthate belowground (Näsholm et al. 2013, Franklin et al. 2014). We conclude that the role of ECM in enzymatically liberating N from SOM and transferring it to host plants is an open question, and, at present, no *direct evidence* has been gathered to demonstrate that ECM enhance plant N supply by accessing N in SOM.

Concluding Remarks

The rationale we present here highlights the significant complications invoked by the broad assumption that all ECM fungi liberate N from SOM. Until additional experimental evidence accumulates, it is ambiguous, at best, whether ECM fungi can provision their host plants with N from SOM. There is, however, an urgent need to test this possibility under field conditions, as multiple studies suggest this mechanism holds significant implications for the construction of accurate coupled climate-biogeochemical models (Orwin et al. 2011, Averill et al. 2014, Terrer et al. 2016).

We note that the intriguing patterns observed in some recent biogeochemical models likely occur through a plurality of belowground interactions, including the physical and biochemical activity of ECM fungi on their soil surroundings. ECM may contribute to SOM

dynamics through the accumulation of hyphae to exploit soil volume, which can vary substantially in architecture and biomass (Clemmensen et al. 2015); further, hyphal traits such as melanization may render some hyphae more resistant to decay than others (Fernandez et al. 2016). Accumulation of hyphae, and the greater functional exploitation of soil volume for inorganic and simple organic N compounds, is distinct from the idea that certain ECM fungi biochemically alter SOM through the exudation of extracellular lignocellulolytic enzymes. As we have discussed, lineages of ECM fungi that have retained genes with lignocellulolytic capacity are more likely to depolymerize SOM than others. Decay-resistant hyphae and enzymatic activities need not be mutually exclusive, and it is plausible that certain fungal communities contribute to SOM dynamics more than others. Finally, given current knowledge of the turnover of ECM communities across space (Talbot et al. 2014) it is unlikely that ECM lineages with the potential to operate on SOM are distributed uniformly across ecosystems. Therefore, improved understanding of the biogeographic distribution and enzymatic physiology of different lineages of ECM fungi will instruct ecologically realistic models of C and N cycling across ecosystems.

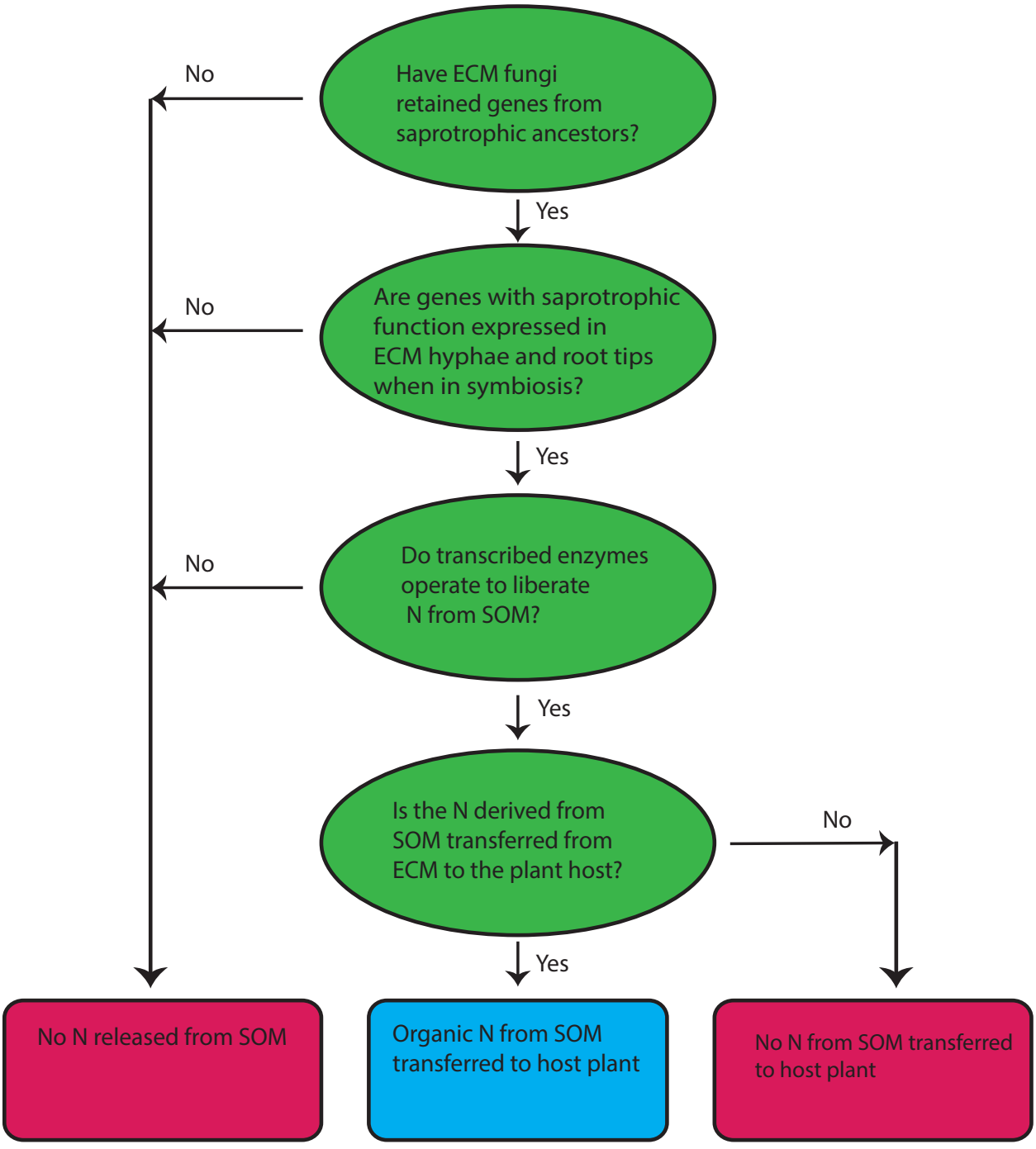

Figure 2-1 Set of minimum conditions necessary for the liberation of organic N from soil organic matter (SOM) by ectomycorrhizal fungi (ECM). See full text for explanation

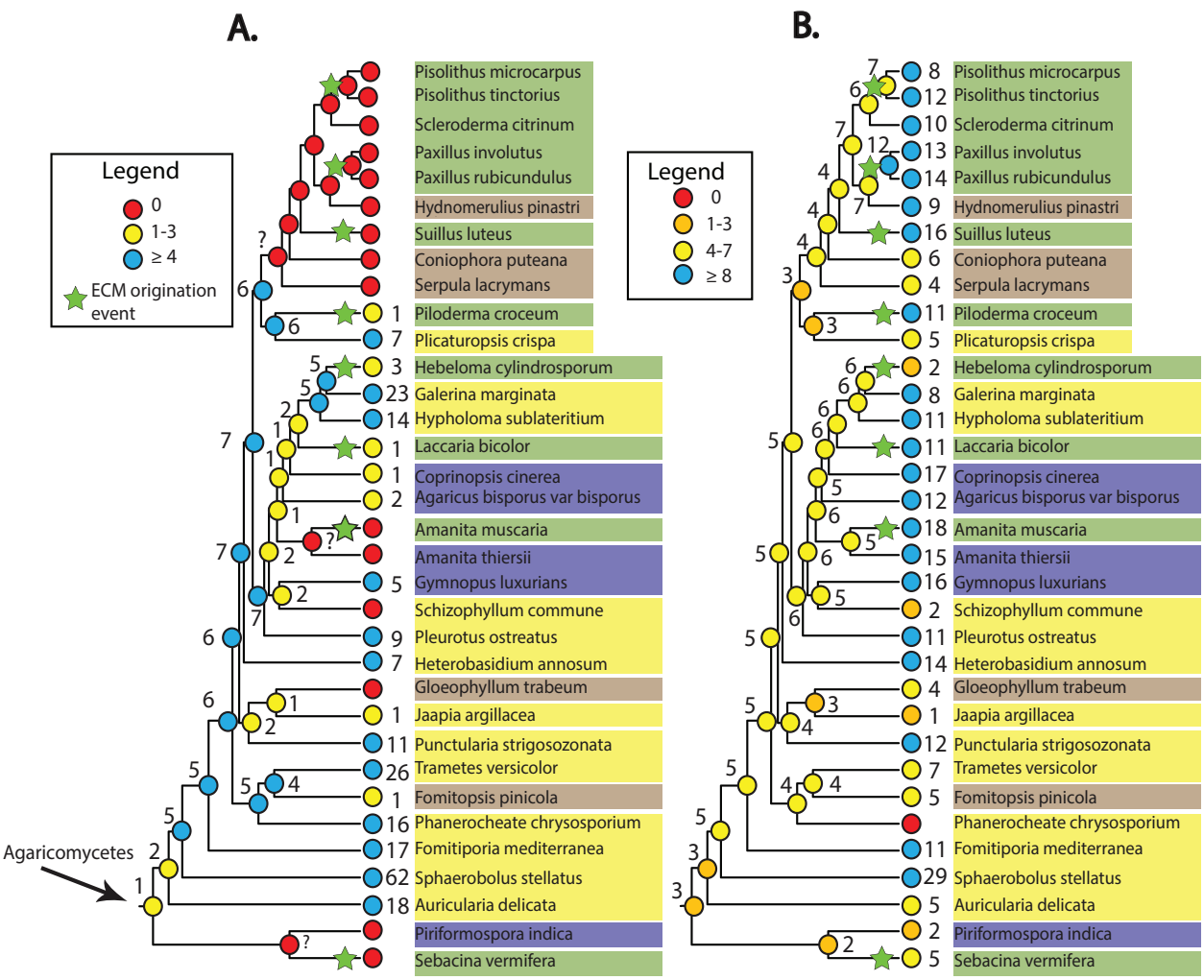

Figure 2-2 Agaricomycete gene copy number for enzymes acting on organic matter, A. class II peroxidases and B. laccase gene copy number. Numbers at tips represent the number of genes observed, numbers at nodes represent reconstructed gene copy number. Question marks indicate uncertain estimates. Ecology of taxa are color coded as follows: Ectomycorrhizal fungi in green, White Rot in yellow, Brown Rot in brown, all others in purple. Legend: average gene copy numbers for Agaricomycotina: Blue: at or above average, Yellow or orange: below average, Red: no copies of the gene family. Nodes with question marks indicate uncertain estimates. Green star: Independent ECM origination. Modified with kind permission from Kohler et al., 2015.

Works Cited

Abuzinadah, R. A., and D. J. Read. 1986. The Role of Proteins in the Nitrogen Nutrition of Ectomycorrhizal Plants. I. Utilization of Peptides and Proteins by Ectomycorrhizal Fungi. The New Phytologist 103:481–493.

Abuzinadah, R. A., and D. J. Read. 1988. Amino acids as nitrogen sources for ectomycorrhizal fungi: Utilization of individual amino acids. Transactions of the British Mycological Society 91:473–479.

Averill, C., and C. V. Hawkes. 2016. Ectomycorrhizal fungi slow soil carbon cycling. Ecology Letters 19:937–947.

Averill, C., B. L. Turner, and A. C. Finzi. 2014. Mycorrhiza-mediated competition between plants and decomposers drives soil carbon storage. Nature 505:543–545.

Baldrian, P. 2006. Fungal laccases – occurrence and properties. FEMS Microbiology Reviews 30:215–242.

Bending, G. D., and D. J. Read. 1996. Nitrogen mobilization from protein-polyphenol complex by ericoid and ectomycorrhizal fungi. Soil Biology and Biochemistry 28:1603–1612.

Bending, G. D., and D. J. Read. 1997. Lignin and soluble phenolic degradation by ectomycorrhizal and ericoid mycorrhizal fungi. Mycological Research 101:1348–1354.

Bödeker, I. T. M., K. E. Clemmensen, W. de Boer, F. Martin, Å. Olson, and B. D. Lindahl. 2014. Ectomycorrhizal *Cortinarius* species participate in enzymatic oxidation of humus in northern forest ecosystems. New Phytologist 203:245–256.

Bödeker, I. T. M., C. M. R. Nygren, A. F. S. Taylor, Å. Olson, and B. D. Lindahl. 2009. ClassII peroxidase-encoding genes are present in a phylogenetically wide range of ectomycorrhizal fungi. The ISME Journal 3:1387–1395.

Cassar, S., and M. Blackwell. 1996. Convergent origins of ambrosia fungi. Mycologia 88:596–601.

Clemmensen, K. E., R. D. Finlay, A. Dahlberg, J. Stenlid, D. A. Wardle, and B. D. Lindahl. 2015. Carbon sequestration is related to mycorrhizal fungal community shifts during long-term succession in boreal forests. New Phytologist:1525–1536.

Edwards, I. P., D. R. Zak, H. Kellner, S. D. Eisenlord, and K. S. Pregitzer. 2011. Simulated Atmospheric N Deposition Alters Fungal Community Composition and Suppresses Ligninolytic Gene Expression in a Northern Hardwood Forest. PLoS ONE 6.

Fernandez, C. W., J. A. Langley, S. Chapman, M. L. McCormack, and R. T. Koide. 2016. The decomposition of ectomycorrhizal fungal necromass. Soil Biology and Biochemistry 93:38–49.

Floudas, D., M. Binder, R. Riley, K. Barry, R. A. Blanchette, B. Henrissat, A. T. Martínez, R. Otillar, J. W. Spatafora, J. S. Yadav, A. Aerts, I. Benoit, A. Boyd, A. Carlson, A. Copeland, P. M. Coutinho, R. P. de Vries, P. Ferreira, K. Findley, B. Foster, J. Gaskell, D. Glotzer, P. Górecki, J. Heitman, C. Hesse, C. Hori, K. Igarashi, J. A. Jurgens, N. Kallen, P. Kersten, A. Kohler, U. Kües, T. K. A. Kumar, A. Kuo, K. LaButti, L. F. Larrondo, E. Lindquist, A. Ling, V. Lombard, S. Lucas, T. Lundell, R. Martin, D. J. McLaughlin, I. Morgenstern, E. Morin, C. Murat, L. G. Nagy, M. Nolan, R. A. Ohm, A. Patyshakuliyeva, A. Rokas, F. J. Ruiz-Dueñas, G. Sabat, A. Salamov, M. Samejima, J. Schmutz, J. C. Slot, F. St. John, J. Stenlid, H. Sun, S. Sun, K. Syed, A. Tsang, A. Wiebenga, D. Young, A. Pisabarro, D. C. Eastwood, F. Martin, D. Cullen, I. V. Grigoriev, and D. S. Hibbett. 2012. The Paleozoic Origin of Enzymatic Lignin Decomposition Reconstructed from 31 Fungal Genomes. Science 336:1715–1719.

Franklin, O., T. Näsholm, P. Högberg, and M. N. Högberg. 2014. Forests trapped in nitrogen limitation – an ecological market perspective on ectomycorrhizal symbiosis. New Phytologist 203:657–666.
Hibbett, D. S., L.-B. Gilbert, and M. J. Donoghue. 2000. Evolutionary instability of ectomycorrhizal symbioses in basidiomycetes. Nature 407:506–508.
Högberg, M. N., and P. Högberg. 2002. Extramatrical ectomycorrhizal mycelium contributes one-third of microbial biomass and produces, together with associated roots, half the dissolved organic carbon in a forest soil. New Phytologist 154:791–795.
Högberg, P., T. Näsholm, O. Franklin, and M. N. Högberg. 2017. Tamm Review: On the nature of the nitrogen limitation to plant growth in Fennoscandian boreal forests. Forest Ecology and Management 403:161–185.
Jones, D. L., J. R. Healey, V. B. Willett, J. F. Farrar, and A. Hodge. 2005. Dissolved organic nitrogen uptake by plants—an important N uptake pathway? Soil Biology and Biochemistry 37:413–423.
Kohler, A., A. Kuo, L. G. Nagy, E. Morin, K. W. Barry, F. Buscot, B. Canbäck, C. Choi, N. Cichocki, A. Clum, J. Colpaert, A. Copeland, M. D. Costa, J. Doré, D. Floudas, G. Gay, M. Girlanda, B. Henrissat, S. Herrmann, J. Hess, N. Högberg, T. Johansson, H.-R. Khouja, K. LaButti, U. Lahrmann, A. Levasseur, E. A. Lindquist, A. Lipzen, R. Marmeisse, E. Martino, C. Murat, C. Y. Ngan, U. Nehls, J. M. Plett, A. Pringle, R. A. Ohm, S. Perotto, M. Peter, R. Riley, F. Rineau, J. Ruytinx, A. Salamov, F. Shah, H. Sun, M. Tarkka, A. Tritt, C. Veneault-Fourrey, A. Zuccaro, A. Tunlid, I. V. Grigoriev, D. S. Hibbett, and F. Martin. 2015. Convergent losses of decay mechanisms and rapid turnover of symbiosis genes in mycorrhizal mutualists. Nature Genetics 47:410–415.
Kües, U., and M. Rühl. 2011. Multiple Multi-Copper Oxidase Gene Families in Basidiomycetes – What for? Current Genomics 12:72–94.
Liao, H.-L., Y. Chen, and R. Vilgalys. 2016. Metatranscriptomic Study of Common and Host-Specific Patterns of Gene Expression between Pines and Their Symbiotic Ectomycorrhizal Fungi in the Genus Suillus. PLOS Genetics 12:e1006348.
Lilleskov, E. A., T. J. Fahey, T. R. Horton, and G. M. Lovett. 2002. Belowground Ectomycorrhizal Fungal Community Change Over a Nitrogen Deposition Gradient in Alaska. Ecology 83:104–115.
Lindahl, B. D., and A. Tunlid. 2015. Ectomycorrhizal fungi – potential organic matter decomposers, yet not saprotrophs. The New Phytologist 205:1443–1447.
Martin, F., A. Aerts, D. Ahrén, A. Brun, E. G. J. Danchin, F. Duchaussoy, J. Gibon, A. Kohler, E. Lindquist, V. Pereda, A. Salamov, H. J. Shapiro, J. Wuyts, D. Blaudez, M. Buée, P. Brokstein, B. Canbäck, D. Cohen, P. E. Courty, P. M. Coutinho, C. Delaruelle, J. C. Detter, A. Deveau, S. DiFazio, S. Duplessis, L. Fraissinet-Tachet, E. Lucic, P. Frey-Klett, C. Fourrey, I. Feussner, G. Gay, J. Grimwood, P. J. Hoegger, P. Jain, S. Kilaru, J. Labbé, Y. C. Lin, V. Legué, F. Le Tacon, R. Marmeisse, D. Melayah, B. Montanini, M. Muratet, U. Nehls, H. Niculita-Hirzel, M. P. O.-L. Secq, M. Peter, H. Quesneville, B. Rajashekar, M. Reich, N. Rouhier, J. Schmutz, T. Yin, M. Chalot, B. Henrissat, U. Kües, S. Lucas, Y. Van de Peer, G. K. Podila, A. Polle, P. J. Pukkila, P. M. Richardson, P. Rouzé, I. R. Sanders, J. E. Stajich, A. Tunlid, G. Tuskan, and I. V. Grigoriev. 2008. The genome of Laccaria bicolor provides insights into mycorrhizal symbiosis. Nature 452:88–92.
Martin, F., A. Kohler, C. Murat, C. Veneault-Fourrey, and D. S. Hibbett. 2016. Unearthing the roots of ectomycorrhizal symbioses. Nature Reviews Microbiology 14:760–773.

Nannipieri, P., and E. Paul. 2009. The chemical and functional characterization of soil N and its biotic components. Soil Biology and Biochemistry 41:2357–2369.
Näsholm, T., P. Högberg, O. Franklin, D. Metcalfe, S. G. Keel, C. Campbell, V. Hurry, S. Linder, and M. N. Högberg. 2013. Are ectomycorrhizal fungi alleviating or aggravating nitrogen limitation of tree growth in boreal forests? New Phytologist 198:214–221.
Näsholm, T., K. Kielland, and U. Ganeteg. 2009. Uptake of organic nitrogen by plants. New Phytologist 182:31–48.
Neff, J. C., F. S. Chapin, and P. M. Vitousek. 2003. Breaks in the cycle: dissolved organic nitrogen in terrestrial ecosystems. Frontiers in Ecology and the Environment 1:205–211.
Orwin, K. H., M. U. F. Kirschbaum, M. G. S. John, and I. A. Dickie. 2011. Organic nutrient uptake by mycorrhizal fungi enhances ecosystem carbon storage: a model-based assessment. Ecology Letters 14:493–502.
Phillips, R. P., E. Brzostek, and M. G. Midgley. 2013. The mycorrhizal-associated nutrient economy: a new framework for predicting carbon–nutrient couplings in temperate forests. New Phytologist 199:41–51.
Plett, J. M., and F. Martin. 2011. Blurred boundaries: lifestyle lessons from ectomycorrhizal fungal genomes. Trends in Genetics 27:14–22.
Rillig, M. C., B. A. Caldwell, H. A. B. Wösten, and P. Sollins. 2007. Role of proteins in soil carbon and nitrogen storage: controls on persistence. Biogeochemistry 85:25–44.
Rineau, F., D. Roth, F. Shah, M. Smits, T. Johansson, B. Canbäck, P. B. Olsen, P. Persson, M. N. Grell, E. Lindquist, I. V. Grigoriev, L. Lange, and A. Tunlid. 2012. The ectomycorrhizal fungus Paxillus involutus converts organic matter in plant litter using a trimmed brown-rot mechanism involving Fenton chemistry. Environmental Microbiology 14:1477–1487.
Schulten, H.-R., and M. Schnitzer. 1997. The chemistry of soil organic nitrogen: a review. Biology and Fertility of Soils 26:1–15.
Shah, F., C. Nicolás, J. Bentzer, M. Ellström, M. Smits, F. Rineau, B. Canbäck, D. Floudas, R. Carleer, G. Lackner, J. Braesel, D. Hoffmeister, B. Henrissat, D. Ahrén, T. Johansson, D. S. Hibbett, F. Martin, P. Persson, and A. Tunlid. 2016. Ectomycorrhizal fungi decompose soil organic matter using oxidative mechanisms adapted from saprotrophic ancestors. New Phytologist 209:1705–1719.
Sinsabaugh, R. L. 2010. Phenol oxidase, peroxidase and organic matter dynamics of soil. Soil Biology and Biochemistry 42:391–404.
Smith, S. E., and D. J. Read. 2010. Mycorrhizal symbiosis. Academic press.
Talbot, J. M., T. D. Bruns, J. W. Taylor, D. P. Smith, S. Branco, S. I. Glassman, S. Erlandson, R. Vilgalys, H.-L. Liao, M. E. Smith, and K. G. Peay. 2014. Endemism and functional convergence across the North American soil mycobiome. Proceedings of the National Academy of Sciences 111:6341–6346.
Talbot, J. M., F. Martin, A. Kohler, B. Henrissat, and K. G. Peay. 2015. Functional guild classification predicts the enzymatic role of fungi in litter and soil biogeochemistry. Soil Biology and Biochemistry 88:441–456.
Talbot, J. M., and K. K. Treseder. 2010. Controls over mycorrhizal uptake of organic nitrogen. Pedobiologia 53:169–179.
Terrer, C., S. Vicca, B. A. Hungate, R. P. Phillips, and I. C. Prentice. 2016. Mycorrhizal association as a primary control of the CO_2 fertilization effect. Science 353:72–74.

Wolfe, B. E., R. E. Tulloss, and A. Pringle. 2012. The Irreversible Loss of a Decomposition Pathway Marks the Single Origin of an Ectomycorrhizal Symbiosis. PLoS ONE 7.

Chapter 3 Ectomycorrhizal Community Assembly and Plant Uptake of Nitrogen Derived From Soil Organic Matter

Peter T. Pellitier & Donald R. Zak

Abstract: The assembly of ectomycorrhizal (ECM) communities is critical to predicting their resultant impact on plant access to growth limiting Nitrogen (N). Plant access to N in soil organic matter (SOM) is predicated upon the decay physiology of their ECM symbionts; this physiology represents a complex trait encoded by a diverse array of gene families. Soil inorganic N availability is known to impact ECM community structure, and here we test the hypothesis that ECM communities occurring in low inorganic N soils, possess greater genetic potential to obtain N-SOM. In turn, N-SOM primarily contributes to plant growth in low inorganic N soils. Here we employed a metagenomics enabled trait-based approach to study the role of environmental filtering in ECM community assembly along a natural soil inorganic N gradient in a temperate upland forest. We quantified the distribution and prevalence of genes involved in the decay and acquisition N-SOM by studying 59 individual ECM communities inhabiting the root-systems of the standardized plant host *Quercus rubra L*. We found that the community weighted mean (CWM) prevalence of key gene families involved in the enzymatic and free-radical modification of SOM were inversely correlated with soil inorganic N availability. We scaled the CWM gene counts by the number of colonized ECM root-tips present on *Q. rubra* individuals. In broad support of optimal plant foraging theory, our results suggest that *Q. rubra* inhabiting low inorganic N soils are likely to obtain significantly more N-SOM than trees inhabiting inorganic N rich soils. Together these findings provide a mechanistic basis for the role of soil inorganic N availability in ECM community assembly, and we highlight that ECM hosts may not have equivalent potential to respond to elevated CO_2 if uptake of N-SOM is required.

Introduction:

Quantifying patterns of trait variation across climatic and edaphic gradients has led to fundamental insight into community assembly processes (Diaz et al. 1998, Cornwell and Ackerly 2009, Kunstler et al. 2016). However, unlike plant and animal communities for which linkages between trait and environmental gradients have been studied for well over a century (Cowles 1899, Diamond 1973, Wright et al. 2004), there is minimal understanding of trait-environment linkages for microbial communities or the underlying processes that may generate them (Nemergut et al. 2013, Louca et al. 2018). Environmental filtering, sometimes deemed ecological selection, limits the establishment of species suitable for a particular environment due to a relatively narrow range of compatible trait-environment interactions (Ackerly and Cornwell 2007, Vellend 2010, Bernard-Verdier et al. 2012). Evidence for the role of environmental filtering in plant community assembly relies on the identification of shifts in species and community weighted trait means across environmental gradients (Diaz et al. 1998, Ackerly 2003). Although, similar approaches have been proposed for microbial communities (Nemergut et al. 2013), relatively few studies have employed trait-based approaches to study microbial community assembly and the role of habitat filtering (Louca et al. 2016, 2017, Bouma-Gregson et al. 2019). Paradoxically, evidence to date suggests that despite hyperdivesity within microbial communities, they appear largely functionally redundant with respect to key biogeochemical transformations (Louca *et al.* 2018).

Microbial 'traits' have primarily been measured using isotopes, gross morphology, and enzyme assays; however, new ultra-high-throughput metagenomic, transcriptomic, and proteomic approaches offer particular promise (Moran et al. 2013, Bouma-Gregson et al. 2019, Malik et al. 2020). Shotgun metagenomic sequencing enable the robust quantification of microbial genes encoding key metabolic pathways (Reed et al. 2014, Bouma-Gregson et al. 2019). Critically, relative counts acquired from assembly-free shotgun metagenomes and standardized by single-copy gene markers, represent proxies for community weighted mean trait values (Fierer et al. 2014, Louca et al. 2018). Studying CWM trait values across ecological gradients has provided essential insight into environmental filters structuring plant community assembly (Ackerly et al. 2002, Bernard-Verdier et al. 2012), but has rarely been employed to test hypotheses of microbial community assembly. While the relative standardized gene abundances

generated by shotgun metagenomes provide a proxy for CWM traits, comparative analyses of microbial assembly and function can be significantly extended if underlying shifts in microbial biomass are integrated (Vandeputte et al. 2017, Regalado et al. 2020). In fact, microbial biomass has been identified as a key factor modulating disease dynamics and ecological interactions (Vandeputte et al. 2017, Regalado et al. 2020). While abundance weighting procedures are often employed in studies of plant trait distributions (Pakeman et al. 2008, Bernard-Verdier et al. 2012), underlying shifts in microbial biomass are rarely directly considered in studies quantifying microbial metagenomic gene potential, limiting wholistic inference of the role of microbial communities on biogeochemical transformations.

Ectomycorrhizal (ECM) fungi form critical nutrient mutualisms with the majority of the Earth's plant roots (Smith and Read 2010, Steidinger et al. 2019) and recent continental-scale surveys have revealed large-scale biogeographic structure among ECM communities (Talbot *et al.* 2014; van der Linde *et al.* 2018; Steidinger *et al.* 2019). Critically, dozens of studies have documented that soil nitrogen (N) availability impacts ECM community composition (Taylor et al. 2000, Lilleskov et al. 2002a, Peay et al. 2015, Sterkenburg et al. 2015), potentially generating observed biogeographical patterns (Read and Perez-Moreno 2003, Steidinger et al. 2019). Saliently, so-called 'nitrophobic' and 'nitrophyllic' ECM taxa exhibit characteristic shifts across soil N gradients (Taylor et al. 2000, Lilleskov et al. 2002a, Smith and Read 2010). However, unlike plant leaf traits, for which ecophysiological measurements have illuminated the functional significance of persistent patterns of trait variation (Ackerly et al. 2002, Cornwell and Ackerly 2009), underlying traits influencing the establishment and persistence of distinct ECM communities across soil N gradients remain unknown.

Variation in the N foraging traits of ECM fungi represents a long-standing but inadequately tested hypothesis explaining shifts in ECM community membership along soil N gradients (Read and Perez-Moreno 2003). ECM fungi differentially evolved from free-living saprotrophic ancestors (Hibbett et al. 2000) and thus likely differ in their capacity to obtain N bound in soil organic matter (N-SOM) (Abuzinadah & Read 1986; Kohler *et al.* 2015; Pierre-Emmanuel *et al.* 2016; Pellitier & Zak 2018; Zak *et al.* 2019). Heterogeneity in the capacity for ECM taxa to obtain N-SOM may act as a key axis governing the assembly of ECM communities across soil N gradients (Pellitier et al. in review, Read and Perez-Moreno 2003, Koide et al. 2014). Shifts in the morphological attributes of ECM hyphae associated with N foraging

(Pellitier et al. in review, Moeller et al. 2014, Defrenne et al. 2019) as well as enzyme and culture assays (Taylor et al. 2000, Lilleskov et al. 2002a, Bödeker et al. 2014a, Pierre-Emmanuel et al. 2016) along soil N gradients, implicitly support the hypothesis that ECM communities vary in their capacity to forage for biochemically distinct N forms. However, support for this hypothesis would challenge the emergent paradigm that globally distributed ECM communities are functionally redundant in their capacity to obtain N-SOM (Phillips et al. 2013, Averill et al. 2014).

The possibility for ECM fungi to obtain N-SOM, and transfer this N to their plant host has been widely invoked to explain patterns in nutrient cycling among ecosystems (Phillips et al. 2013), global patterns of SOM accumulation (Averill et al. 2014, Kyaschenko et al. 2017) as well as forest response to elevated CO_2 (Pellitier et al. in review, Terrer et al. 2016, 2019). Despite dozens of studies investigating the *implications* of this complex fungal trait on various processes, the capacity for ECM communities to obtain N-SOM under field settings remains unknown, as do the ecological conditions under which N-SOM supplements plant growth (Zak et al. 2019).

Developing predictive understanding of plant access to N-SOM may be achieved using trait-based inquiry of the assembly rules structuring the composition and function of ECM communities. Adaptive plant nutrient foraging responses to soil gradients (Kielland 1994, Houlton et al. 2007) may act as a coupled filter structuring the assembly of ECM communities with distinct nutrient foraging attributes. Mechanistically, ECM fungi that can access and transfer more N (in whatever form) to their plant hosts may receive more photosynthate in return (Kiers et al. 2011, Nehls et al. 2016, Hortal et al. 2017). As a result, distinct community assembly trajectories may arise from non-random variation in the capacity of ECM communities to biochemically modify SOM and provision their hosts with the N bound therein (Koide et al. 2014). This leads to the hypothesis that the capacity for ECM fungi to obtain N-SOM is greatest when inorganic N supply is low.

Here, we sought to test for evidence of environmental filtering structuring ECM community assembly using a metagenomics enabled, trait-based approach. First, we aimed to identify shifts in the community weighted mean (CWM) decay capacity of ECM communities inhabiting individual red-oak (*Quercus rubra L.*) root-systems across a natural soil inorganic N gradient. Because the capacity for ECM fungi to obtain N-SOM is predicated upon the decay of

SOM, we reasoned that the CWM decay capacity of ECM communities is inversely related to inorganic N availability. Next, we tested the hypothesis that *Q. rubra* inhabiting low inorganic N soils, obtain greater quantities of N-SOM than do *Q. rubra* occupying inorganic N rich soils, due to functional variation in the attributes of their ECM symbionts. Evidence in support of this hypothesis would include observation of *Q. rubra* hosting greater overall quantities of ECM genes involved in decay of SOM in low inorganic N soils. We gathered evidence for this hypothesis by scaling ECM CWM decay potential by the standardized number of ECM root-tips on individual root-systems along an inorganic N availability, thereby enabling semi-quantitative comparisons of the aggregated effect of ECM community function on plant N nutrition.

Materials and Methods

Site Descriptions

Twelve forest stands were identified in Manistee National Forest in northwestern Lower Michigan. These soils span a natural soil N gradient that has been extensively characterized (Pellitier et al. in review, Zak et al. 1986, Zak and Pregitzer 1990). Natural variation in nutrient cycling among stands is derived from micro-site climatic differences in nutrient and water retention that have developed in the past ~10,000 yrs. Forest stands are even-aged (~100 years old), having all been uniformly harvested in the early 20th century. In each of the 12 stands that span the soil inorganic N gradient, we randomly selected five dominant mature *Q. rubra* individuals (n = 60).

Soil and Site Characterization

In August 2018, 5 root cores were collected radially around the dripline of each focal *Q. rubra* individual in order to harvest fine roots; cores were 10 cm deep and 144 cm^2. Soil and root cores were stored on ice and immediately transported to the laboratory. Soil net N mineralization rates, soil C, soil N, pH, total free primary amines (TFPA) in soil solution as well as gravimetric soil water content, were measured for the homogenized soil cores collected beneath each tree. Briefly, soil inorganic N was extracted from fresh sieved soil using 2M KCl, followed by a 14-day aerobic incubation assay in order to measure rates of soil inorganic N mineralization. NO_3^- and NH_4^+ in soil extracts were analyzed colorometrically (AQ2; Seal Analytical, Mequon, WI).

In addition, all overstory plant stems greater than 5cm diameter breast height (DBH), within 10 m of each focal *Q.rubra* individual, were identified and measured. A total of 1,304 non-focal stems were inventoried. See supplementary methods for further details.

Isolating Ectomycorrhizal Root Tips

Ectomycorrhizal root-tips were isolated from root-cores within 12 days of field sampling. Briefly, ectomycorrhizal root cores were pooled for each individual focal tree. Next, root-tips were manually excised using a dissecting microscope after visually eliminating all non-*Quercus* roots. Definitive ectomycorrhizal tips on *Quercus rubra* were sampled after visual confirmation of ECM mantle and high turgor (Agerer 2001). Root-tip sampling was standardized across samples by visually assessing the tips of at least 90% of all *Quercus* roots in each of the root cores. In total, 14,944 individual ECM root-tips were excised. DNA was extracted from lyophilized root-tips using the Qiagen DNeasy Plant Mini Kit (Hilden, Germany), following manufacturers protocol. DNA was extracted from the totality of each sample, using two or three individual extraction columns; each extraction utilized ~10 mg of lyophilized root-tip per extraction, so as not to bias extraction efficiencies. After confirmation of extraction success using gel electrophoresis, replicate extractions were pooled for each sample. Samples were split into DNA pools for amplicon sequencing and shotgun-metagenomic sequencing. Freeze-thaw cycles were carefully limited throughout the extraction and sequencing protocols in order to prevent shearing.

Fungal Taxonomy

The ITS2 fragment of rRNA was amplified using PCR, following Taylor *et al.* 2016). PCR libraries were barcoded using one-step golay primers, cleaned using AMPure XP, and sequenced using Illumina Mi-Seq (2 x250; San Diego, CA). Sequences were then demultiplexed and quality filtered using DADA2 and QIIME2 pipelines, and clustered into OTU assigned taxonomy using the dynamic UNITE database using a naïve-bayes classifier (Bokulich et al. 2018). Samples were rarefied using 24,021 sequences and assigned taxonomy using the UNITE database (Nilsson et al. 2019). The ectomycorrhizal status of fungal genera was assigned using literature searches, and fungal taxa with uncertain or non-ECM status were removed (~20% of overall sequences). See supplementary materials for further details.

Shotgun Metagenomic Sequence Library Preparation

Prior to metagenomic sequencing library preparation, DNA extracts were quantified (Agilent 4200 TapeStation; Santa Clara, CA) and spiked with a fixed mass (0.4ng) ~1% w/w of synthetic DNA spike-in containing a range of artificial DNA sequences at known concentrations (sequins; Hardwick *et al.* 2018); Sydney, Australia). Libraries were then custom sheared using a Covaris S2 Focused-Ultrasonicator (Woburn, MA), to 200 bp (duty =10%, intensity = 5, cycles/burst = 200, time=120 seconds); previous trials confirmed the efficacy of these settings. Libraries were prepared using the NEB Next Ultra 2 DNA Library Prep kit (Ipswich, MA) with seven cycles of PCR. 59 out of the 60 samples successfully yielded libraries suitable for sequencing. Sequencing libraries were individually barcoded and custom sequencing was conducted on an entire S4 flow cell of the Illumina Nova Seq 6000 instrument (2 x 150bp) at the University of Michigan Advanced Genomics Core.

Metagenomic Sequence Processing and Gene Annotation

In total, 23,203,326,006 sequences were visualized using FastQC, reads were dereplicated, adapters were trimmed, reads with Q >20 were retained, and reads shorter than 40 bp were removed using bbduk (http://jgi.doe.gov). 23,177,098,622 paired-end reads passed initial quality filtering. We used an additional filtering step in order to remove non-fungal sequences using Kraken2 paired-end mode with default parameters (Wood et al. 2019). Sequences were mapped against the standard Kraken2 database containing bacterial, archaeal and UniVec reads (containing sequencing adapters, linkers, and primer sequences), and further supplemented with sequences obtained from published *Quercus rubra* (Konar et al. 2017) and *Qurcus lobata* genomes (Sork et al. 2016) in order to remove plant sequences (contaminants). All reads that mapped to the custom database were removed. On average, 21.7% of sequences per sample were removed during this Kraken2 filtering step. The mean number of sequences remaining in each sample after Kraken mapping was 307,041,274

We used a direct mapping approach to annotate the functional gene composition of each sample. Quality and Kraken2 filtered reads were mapped to functional reference gene databases CAZy (accessed March 2019) (Lombard et al. 2014) and Peroxibase (accessed February 2019) (Fawal et al. 2013). Reads were mapped to CAZy using 'sensitive' mode in DIAMOND v. 0.9.31, with an -e value: 1e-4, following best practices for unmerged reads (Treiber et al. 2020). BWA-MEM was used to map sequences to representatives downloaded from Peroxibase, using default settings (Li and Durbin 2009). The number of mapped reads was averaged for unmerged

forward and reverse reads for each reference gene to avoid double counting, mapped reads were then averaged across all reference sequences for a given gene family. Many gene families are involved in extracellular decay of plant-cell wall and SOM; however some of these are also involved in an morphogenesis and intracellular processes Baldrian 2006; Janusz *et al.* 2017; Blatzer *et al.* 2020). As a result, we screened a core set of genes that appear across a broad range of Dikaryotic fungi that are actively expressed during fungal decay of complex organic substrates (Kohler et al. 2015, Peng et al. 2018, Floudas et al. 2020). In addition, we also studied genes putatively involved in Fenton chemistry, which underlies brown-rot wood decay (Janusz et al. 2017, Op De Beeck et al. 2018). ECM fungi derived from brown-rot saprotrophs may participate in Fenton chemistry, which involves the production of (Eastwood et al. 2011, Janusz et al. 2017).

Finally, we tabulated the number of near-single copy genes, as a proxy for the number of Dikaryotic fungal genomes present in each sample. We used Busco v3, Benchmarking Universal Single-Copy Orthologs, and the OrthoDB v9 orthologous ancestral gene database, which comprised 1312 near-single copy gene variants (Simão et al. 2015, Waterhouse et al. 2018) . Dikaryotic near single-copy genes were chosen because previous study of these ECM communities confirmed that the majority (>95% sequences) are Dikaryotic (Pellitier *unpublished data*). Instead of relying on a single arbitrarily chosen house-keeping gene that may not be at true single-copy abundance in complex environmental samples, we calculated the geometric mean number of 'single-copy' genes present across all orthologs and the standard error for each sample. Filtered forward and reverse reads for each sample were mapped to the Dikaryotic OrthoDB database using DIAMOND as above, and paired-end reads were averaged to prevent double-counting.

Statistical Analysis

Next-generation sequencing libraries are bounded, sometimes deemed 'closed', by the technical limitations of the sequencer, and generate compositional data (Quinn et al. 2018, 2019). We transformed this data using an ecologically intuitive compositional transformation to calculate a log-transformed number of genes per fungal 'average' fungal genome present, by taking the natural logarithm of the number of sequences mapped to a given gene family divided by the geometric mean number of orthologous near single-copy features present in the sample (single-copy genes (Quinn et al. 2018). Gene counts present in a microbial community are necessarily

weighted by the relative, and often unknown, abundance of individual taxa (Fierer et al. 2014), and when counts are standardized on a per genome basis (Quinn et al. 2019), standardized community weighted gene counts can estimate the attributes of the mean, necessarily hypothetical, fungal genome present in a particular sample.

We visualized ECM communities (taxonomic) at both the OTU and genus level, using non-metric multidimensional scaling (NMDS), with Hellinger transformed Bray-Curtis distance matrices. Next, we used the 'rankindex' function in vegan, to study which distance indices best separates the single-copy transformed decay gene matrix along the studied environmental gradients using rank correlations. We visualized variation in the compositional abundance of genes involved in decay of soil SOM using Euclidean distance matrices of the 94 CAZy gene families. Next, we identified a core set of decay genes that were responsive to elements of the studied soil gradient using an iterative approach. We employed a modification of threshold indicator analysis using the 'TITAN2' (Baker and King 2010) to identify gene families that acted as 'indicator' genes; *i.e.,* genes which responded positively or negatively to soil C:N, soil mineralization rates, and soil pH. These specific environmental variables were previously determined to be key determinants of ECM community (OTU) turnover. This approach yielded a total of 22 responsive genes that had a purity and reliability greater than 0.9, metrics that are based on the robustness of the sign and magnitude of gene responses when resampled using 1000 bootstraps (Baker and King 2010). We then visualized the core set of responsive gene families using PCoA with log-transformed Euclidean-distance matrices.

We tested which environmental variables were most strongly correlated with fungal community composition (OTU) using generalized dissimilarity modeling (GDM). GDM can accommodate non-linear responses to environmental gradients, and identify where along gradients community change is slow/rapid. Modeling assemblages of fungal taxa along environmental gradients was accomplished by transforming predictor variables by fitting I-spline functions to the environmental variables and polynomial pieces are connected using knots (Ferrier et al. 2007). We used Bray-Curtis dissimilarity and three I-splines for each predictor (Ferrier et al. 2007, Qin et al. 2020). Environmental predictors by the magnitude of initially included in the model, included net N mineralization rates, pH, soil C and N, C:N, total free primary amines (TFPA), soil moisture, and a Bray-Curtis transformed plant overstory dissimilarity matrix. We separately assessed plant overstory using the frequency of stems of a

particular species, as well as summing the DBH of each overstory species. We used backwards model selection using gdm.varImp to iteratively remove variables that resulted in less than 0.5% change in model deviance (*nperm* = 250; (Bouma-Gregson et al. 2019, Qin et al. 2020). We performed additional testing on the selected GDM to confirm significance of remaining predictors (*nperm* =500).

A range of methods have been proposed to account for variation in microbial biomass across samples (Satinsky et al. 2017, Vandeputte et al. 2017, Regalado et al. 2020); however, each present significant technical limitations. Here we accounted for variation in the biomass of ECM communities, by scaling log-transformed and single-copy standardized gene counts (CWM) using the number of root-tips recovered from each individual root-system. While this approach cannot represent absolute quantification of sequence counts, absolute quantification remains technically challenging and potentially impossible given incalculable heterogeneity in cell-lysis efficiencies (Satinsky et al. 2013). Instead, because we standardized the sampling of ECM root-tips for each tree, colonized root-tips represent active ECM infection and provide a relative measure of ECM biomass (Gardes and Bruns 1996). We used Euclidean distance matrices to visualize differences among samples, using root-tip scaled CWM of all 94 gene families using PCoA.

We employed an extension of GDM's to identify significant predictors of the compositional abundance of 94 gene families within ECM communities. While this is the first known employment of GDM for shotgun metagenomes, it is conceptually similar to modeling genomic variation across environmental gradients using single nucleotide polymorphisms, which are generated using RAD sequencing (Fitzpatrick and Keller 2015) or average nucleotide percentages for assembled genomes (Bouma-Gregson et al. 2019). We used Euclidean dissimilarity matrices of the 94 scaled and unscaled, log-transformed gene-counts (described above). Initial environmental predictors included those described above, as well as a Bray-Curtis dissimilarity matrix of ECM community composition (OTU level), allowing us to disentangle between ECM community composition and soil predictors in driving shifts in ECM community functional gene abundances. We used backwards model selection as described above (*nperm* = 250), and confirmed the significance of remaining predictors (*nperm* = 500). After finalizing model fit, we estimated the proportion of model variance uniquely attributable to soil inorganic N availability, by calculating the difference in the deviance explained by a GDM containing final

variables and a model with all variables except soil inorganic N availability. We then converted this difference to a percentage by dividing by the deviance explained by the finalized GDM (Gossner et al. 2016). All statistical analyses were conducted in R v. 3.5.3

Results

The characteristics of our gradient of soil inorganic N availability have been extensively described elsewhere (Pellitier et al. in review, Zak et al. 1986). Briefly, soil inorganic N availability ranges from 50 to 120 kg N ha^{-1} yr^{-1} (calculated from Zak and Pregitzer 1990), and we confirmed that the underlying soil inorganic gradient is temporally stable across the duration of the growing season by comparing soil samples collected and incubated in both May and August.

We recovered a total of 202 ECM OTU, comprising 45 genera, of which 88% were Basidiomycetes. ECM communities displayed marked compositional variation across the soil inorganic N gradient at both the OTU and genera level (Figure 1a; Figure S1). Shifts in fungal community composition (OTU's) were well explained by soil pH, mineralization rates and C:N (GDM, R2 = 0.34; Figure 1, Figure S3). Overstory trees communities occurring within 10 m of ECM communities were not significant predictors of ECM communities, and were not included in the final model. Because GDM is able to identify where along a gradient the rate of compositional change is greatest, it provides additional insight compared with standard distance-based methods of community analysis (Duhamel et al. 2019). ECM communities exhibited a threshold response to soil pH, ~ 4.3 pH, whereas community responses to soil inorganic N availability and C:N were more continuous (Figure 1).

The number of sequences that passed quality filtering, as well as those remaining after Kraken mapping, did not significantly vary across the mineralization gradient ($P = 0.34$; Figure S3). Moreover, the geometric mean number of single-copy genes detected in each sample (counts per million counts) did not significantly vary across the inorganic N availability gradient (Figure S4); the standard error (SE), a coarse metric of the evenness of genome coverage per community, also did not significantly vary across samples ($P = 0.76$).

Recent transcriptomic studies have confirmed the identity of certain ECM genes putatively involved in the decay of SOM (Sterkenburg et al. 2018, Zak et al. 2019, Nicolás et al. 2019), allowing for a targeted and quantitative study of their presence among ECM communities using shotgun-metagenomic approaches. PCoA was used to visualize variation in the in the

decay genes per fungal genome, which revealed minimal qualitative variation among samples (Figure S4a). A total of 22 responsive gene families exhibited both positive and negative responses with soil inorganic N supply rates, soil C:N, and soil pH (Figure S6-8). Using the subset of 'responsive' gene families, we again used PCoA to distinguish between ECM communities inhabiting high and low inorganic N soils (Figure S4b). We used a step-down modeling procedure using GDM to isolate pH, soil mineralization rates, and soil C:N as predictors of variation in CWM gene abundances. These predictors accounted for 25.3% of model variance. These environmental variables were also best predictors for ECM taxonomic variation among samples.

Using, the scaled gene counts, we observed significant variation in the composition of decay genes across samples and the inorganic N availability gradient (Figures 3-4; Figure S10). This is largely attributable to variation in the abundances of genes, because samples exhibit minimal variation based on community-wide presence or absence alone. We used GDM to detect nonlinear effects of soil parameters on the abundance of scaled gene counts for the 94 gene families (Figure 3). A model including soil mineralization rates, soil pH, gravimetric soil water availability, and soil C:N, accounted for ~16% of model deviance. Of the environmental predictors, soil mineralization rate was the major driver of variation in the composition of ECM genes involved in decay (Figure 3a; $P = 0.014$), whereas other model predictors were insignificant. Soil mineralization rates explained 27% of variance. The effect of soil inorganic N availability on the scaled abundance of ECM decay genes was non-linear; and we detected change point at approximately 0.45 μg N g^{-1} d^{-1} and an accelerating community response with increasing inorganic N supply (Figure 3a). In contrast, soil pH and C:N displayed saturating responses (3b,c). The ECM community dissimilarity (OTU) and overstory plant community dissimilarity explained a negligible proportion of variance (~0.5%) and were not included in the full model. The scaled abundance of previously identified indicator gene families -- genes that exhibited positive or negative responses to soil inorganic N—exhibited significant inverse relationships with soil inorganic N availability (Figure 4). Finally, the relative abundance of the ECM genus *Cortinarius* was positively and significantly correlated with the scaled log-transformed counts of Manganese-peroxidase ($P = 0.05$; $R^2 = 0.12$).

Discussion

We first predicted that soil inorganic N availability serves as an environmental filter structuring the composition and functional attributes of ECM communities. As a consequence of this filter, we reasoned that the prevalence of genes mediating the modification of SOM should be greatest in ECM communities when the supply of inorganic N for plant growth is low. The evidence we accumulated is highly consistent with these ideas, indicating a clear linkage between the composition and function of ECM communities and plant nutrient foraging strategies. For example, the relative CWM abundance of ECM genes involved in the decay of SOM, largely exhibited negative correlations with soil inorganic N availably. Secondly, we found that soil inorganic N availability was a key predictor of compositional variation in the root-tip scaled CWM abundance of ECM decay genes, and that *Q. rubra* inhabiting low inorganic N soils likely obtain greater quantities of N-SOM due to greater composite decay capacity of their ECM symbionts. Although it has been assumed that all ECM communities have the capacity to modify SOM and supply plants with growth-limiting N organically bound within, our results indicate this may only be the case when the rate of inorganic N supply is low in soil.

Consistent with soil inorganic N availability acting as an environmental filter structuring ECM communities, we found evidence supporting a shift in the community-wide trait values of ECM decay capacity. In total, 22 'indicator' gene families, exhibited significant responses to soil C:N, soil inorganic N supply rates and pH. These environmental predictors were previously isolated as the key drivers of community dissimilarity for ECM taxa. While 'indictor' gene families exhibited both positive and negative responses to soil inorganic N availability, genes with extracellular and definitive roles in decay of SOM largely exhibited negative responses to soil inorganic N availability. For example, the CWM abundances of gene families encoding carbohydrate esterases (CE), lytic polysaccharide monooxygenases (LPMO's -- AA9,10,11) and manganese-peroxidases (MnP) displayed marked declines with increasing soil inorganic N availability. LPMO and MnP represent enzymes families with potent capacity to oxidize the bonds present in cellulose, lignin as well as polyphenols in SOM (Villares et al. 2017, Janusz et al. 2017). The contribution of MnP in the ECM decay of SOM is predicated upon the presence of suitable reaction intermediaries (Hammel and Cullen 2008). We found further evidence for reduced capacity of ECM taxa to decay SOM in high inorganic N soils due to the concurrent reduction in genes encoding the production of H_2O_2. For example, CWM of the 'indicator' gene

family AA3-2, encoding glucose oxidases and glucose dehydrogenase which catalyze the production of H_2O_2, declined significantly across the soil inorganic N gradient. The potent activity of MnPs have been extensively implicated as one of the most important fungal enzymes modulating the decay of SOM (Kellner et al. 2014, Janusz et al. 2017, Sterkenburg et al. 2018). Our analyses further corroborate the general role of MnP in ECM acquisition of N-SOM, by independently supporting previous findings documenting that that the activity of MnP in ECM communities, declines with increasing soil inorganic N availability (Bödeker et al. 2014a, Sterkenburg et al. 2018). Due to the technical limitations of shotgun metagenomics, unscaled CWM, or the 'average' ECM genome present within a community represents a particularly conservative measure with which to detect shifts in gene potentials across soil gradients. Although the magnitude of shifts we detected in CWM across our inorganic N supply gradient may appear modest, the slopes of the relationships are remarkably consistent with previous plant community studies identifying significant shifts in community-wide trait means (Ackerly et al. 2002). Together these analyses support the hypothesis that ECM communities differentially assemble in response to soil inorganic N availability.

Although the CWM of gene families, such as CBM13, CE8, GH53, GH62 and GH114, were positively correlated with inorganic N availability, many of these gene families play key roles in morphogenesis, fungal cell wall remodeling and modification of cell-wall polysaccharide branching (Blatzer et al. 2020). Why these specific gene families may be positively associated with inorganic N availability is currently unknown, but the metagenomic patterns may arise as a function of the underlying shifts in the gross morphological attributes of the fungal taxa present (Bloom et al. 1985, Kielland 1994). For example, the relative abundance of ECM taxa possessing short distance exploration types and non-rhizomorphic hyphae were positively correlated with soil inorganic N availability (Pellitier et al. in review).

One potential scenario is that ECM taxa participating in Fenton chemistry via extracellular hydroxyl radicals ($OH^{\bullet}$), and the non-enzymatic acquisition of N-SOM (Shah et al. 2016, Op De Beeck et al. 2018), are evenly distributed or even positively associated with inorganic N availability. As a result, the decay capacity of distinct ECM communities could be relatively equivalent across soil N gradients. While this specific hypothesis not been formally delineated, widespread functional redundancy of ECM communities is often invoked to explain ecosystem patterns (Averill et al. 2014, Terrer et al. 2016). While the genes involved in Fenton

chemistry are still under active investigation, the CWM of two gene families implicated in Fenton decay (cellobiose dehydrogenase and Ferric reductases) (Shah et al. 2016, Janusz et al. 2017), which reduce Fe^{3+} to Fe^{2+}, were inversely related with inorganic N availability. However, the copper radical oxidase family AA5, which encodes an intermediate needed for Fenton decay (Janusz et al. 2017) was an 'indicator' gene family positively associated with inorganic N availability. Taken together, these results further suggests that soil inorganic N availability may act to limit the establishment of ECM taxa with the capacity to obtain N-SOM in soils where inorganic is relatively abundant.

While the CWM of ECM communities provides essential insight into community assembly processes, such a relative measure cannot reveal the composite impact of the ECM community on plant N nutrition if there are significant differences in the biomass of ECM fungi inhabiting the plant host. Scaling the CWM of individual gene families by the number of ECM root-tips detected on each root system provided essential support for the hypothesis that *Q. rubra* inhabiting soils where inorganic N is scarce, obtain greater quantities of N-SOM. The trends observed among unscaled ECM communities were substantially strengthened when scaled by the number of ECM root-tips present on root-systems. The scaled abundance of gene families implicated in decay of SOM exhibited significant reductions with increasing soil inorganic N availability. Put simply, the composite SOM decay potential of ECM communities is substantially higher in low inorganic N soils. These results provides mechanistic insight corroborating the primacy of soil fertility in the role of ECM fungi on plant N nutrition and SOM dynamics (Bödeker et al. 2014a, Sterkenburg et al. 2018). Critically, our results suggest that N-SOM is unlikely to ubiquitously contribute to plant growth, and we suggest that shifts in the functional attributes of ECM communities represent a mechanistic basis for plant flexibility in nutrient foraging strategies. Although the number of ECM root-tips represents an imperfect proxy for ECM biomass, we argue that it likely represents a conservative estimate of variation in ECM biomass across the soil gradient. Specifically, in low inorganic N soils, the majority of ECM root-tips were colonized by medium-distance and rhizomorphic ECM morphotypes (Pellitier et al. in review, Agerer 2001). Excision of ECM root-tips possessing such morphology would necessarily result in the disproportionate loss of extraradical hyphae.

General dissimilarity modeling (GDM) revealed that soil inorganic N availability was the sole significant predictor of compositional variation in the scaled abundance of the 94 gene

families. The non-linear effect detected suggests that the influence of soil inorganic N availability on the decay capacity of ECM communities and potential plant uptake of N-SOM is similar across a range of very low inorganic N availabilities (<0.45μg N g^{-1} d^{-1}). Previously, we used dendrochronological analysis of these same *Q. rubra* individuals, and found that incremental growth in soils below this inorganic N threshold exhibit an enhanced growth response to historic ambient increases in eCO_2, whereas trees inhabiting soils above this inorganic N threshold displayed a modest response (Pellitier et al. in review). Together our coupled metagenomic and dendrochronological evidence corroborates the hypothesized importance of N-SOM in enhanced growth response to eCO_2 (Terrer et al. 2018, 2019). Here, we have unearthed the ecosystem conditions and decay families of the ECM taxa that likely give rise to differential uptake of N-SOM.

The majority of the amplicon sequences detected in this study belonged to the ectomycorrhizal genus *Cortinarius*, and similar to previous studies, the relative abundance of this taxa declined significantly with increasing inorganic N availability (Suz et al. 2014, Sterkenburg et al. 2018). Of all ECM genera, *Cortinarius* has retained the highest known quantities of genes encoding MnP, and it's overall decay potential may rival free-living white-rot saprotrophs (Bödeker et al. 2009, Pellitier and Zak 2018). Here we used scaled and unscaled metagenomic gene counts from a temperate forest ecosystem, to replicate previous ecological inferences. In this study, we found positive correlations between the relative abundance of *Coritinarius* amplicons and abundance of MnP gene in ECM communities; such findings are remarkably similar to the correlations found for *Cortinarius* and MnP mRNA's in a Swedish boreal forest (Bödeker et al. 2014a). Together, this evidence suggests that at least for MnP, the gene potentials measured using metagenomic approaches likely have functional implications for decay of SOM, and further support the role of ECM decay of SOM using MnP (Bödeker et al. 2014a, Sterkenburg et al. 2018).

While we found that the unscaled CWM of many gene families potentially involved in decay, displayed limited variation across communities and our inorganic N availability gradient, this result may not be unexpected from both a technical and ecological perspective. Foremost, many genes putatively involved in decay may also encode a range of additional functions (Baldrian 2006, Kües and Rühl 2011, Blatzer et al. 2020). In addition, certain enzymes are required for the initiation and maintenance of the ectomycorrhizal symbiosis (CAZy) (Plett and

Martin 2011) or cellular maintenance (Baldrian 2006, Blatzer et al. 2020). As a result, we may expect *a priori,* that certain CAzY gene families which are obligate to the ECM lifestyle or which are not subject to strong ecological filtering, will display minimal variation across environmental gradients. Consistent with this premise, we found that the gene family GH5 implicated in host-cell wall degradation and symbiosis development (Plett and Martin 2011) as well as lignin-peroxidase and dye decolorizing peroxidase, which have functions unrelated to the acquisition of N-SOM (Martin et al. 2016) and are not expressed during ECM decay of organic matter (Rineau et al. 2012, Kohler et al. 2015), displayed no significant shift in CWM across the soil gradient. For these reasons, we caution against calculating a composite sum of all CAzY gene families to detect meaningful differences in CWM traits among fungal and bacterial communities (Bahram et al. 2020).

It is important to note that shotgun metagenomic approaches for trait-based study of microbial communities present several challenges that limit their ecological inference. Foremost, the delimitation of microbial phenotypic traits based on genotypic potential (gene counts) remains extremely challenging (Fierer et al. 2014, Zanne et al. 2020, Malik et al. 2020). The inability for microbial ecologists to reveal consistent trait-environment linkages may in part stem from measurement of dormant microbial cells or measurement of genotypic trait potentials at excessively broad genomic scales. Unlike many soil microbial groups for which the majority of cells may be dormant (Jones and Lennon 2010), by exclusively sampling actively mycorrhized root-tips, our analyses only include physiologically active ECM fungi. Microbial communities, including ECM fungi, are often hypothesized to have wide functional redundancy (Burke et al. 2011, Talbot et al. 2014, Louca et al. 2016, 2018). Although portions of our results could be interpreted to support such claims, we argue that apparent functional redundancy within microbial communities is highly dependent upon the scale of genomic inference, and the challenges associated with delineating functional traits from metagenomic gene potentials. Here, ordination of the unscaled CWM of the 94 decay gene families resulted in minimal variation across samples; however, we argue that functional redundancy at such broad levels of function may indeed be inevitable (Louca et al. 2018), just as virtually all plants possess genes encoding photosynthetic machinery. Instead, we found variation among ECM communities when a subset of gene families were considered. Delimitation of functional redundancy across microbial

communities represents an urgent challenge, and the technical challenges associated with current techniques must be considered when drawing ecological inference.

We generated unprecedented metagenomic insight into the capacity of ECM communities to modify SOM, allowing us to gather support for the hypothesis that soil inorganic N availability acts as a key environmental filter structing the composition and functional attributes of ECM communities. We find that CWM capacity of ECM genomes present in low inorganic N soils have greater decay capacity, than those inhabiting high inorganic N soils. Together our results extend decades of research investigating the mechanisms structuring the role of inorganic N in ECM community assembly (Read and Perez-Moreno 2003). By scaling metagenomic gene counts by the number of colonized ECM root-tips present on individual *Q. rubra* root-systems, our results highlight that ECM associated trees do not have equivalent access to N-SOM. Plant uptake of N-SOM may have significant implications for plant response to rising eCO_2 and our results demonstrate that the underappreciated importance of ECM community assembly in plant N nutrition. Taken together, the evidence we have assembled is consistent with the idea that ECM communities are not functionally redundant, and we argue that future trait-based studies of microbial communities must carefully delineate linkages between genotypic co-occurrences and phenotypic traits.

Works Cited

Abuzinadah, R. A., and D. J. Read. 1986. The Role of Proteins in the Nitrogen Nutrition of Ectomycorrhizal Plants. New Phytologist 103:481–493.

Ackerly, D. D. 2003. Community Assembly, Niche Conservatism, and Adaptive Evolution in Changing Environments. International Journal of Plant Sciences 164:S165–S184.

Ackerly, D. D., and W. K. Cornwell. 2007. A trait-based approach to community assembly: partitioning of species trait values into within- and among-community components. Ecology Letters 10:135–145.

Ackerly, D., C. Knight, S. Weiss, K. Barton, and K. Starmer. 2002. Leaf size, specific leaf area and microhabitat distribution of chaparral woody plants: contrasting patterns in species level and community level analyses. Oecologia 130:449–457.

Agerer, R. 2001. Exploration types of ectomycorrhizae. Mycorrhiza 11:107–114.

Averill, C., B. L. Turner, and A. C. Finzi. 2014. Mycorrhiza-mediated competition between plants and decomposers drives soil carbon storage. Nature 505:543–545.

Bahram, M., T. Netherway, F. Hildebrand, K. Pritsch, R. Drenkhan, K. Loit, S. Anslan, P. Bork, and L. Tedersoo. 2020. Plant nutrient-acquisition strategies drive topsoil microbiome structure and function. New Phytologist n/a.

Baker, M. E., and R. S. King. 2010. A new method for detecting and interpreting biodiversity and ecological community thresholds. Methods in Ecology and Evolution 1:25–37.

Baldrian, P. 2006. Fungal laccases – occurrence and properties. FEMS Microbiology Reviews 30:215–242.

Bernard-Verdier, M., M.-L. Navas, M. Vellend, C. Violle, A. Fayolle, and E. Garnier. 2012. Community assembly along a soil depth gradient: contrasting patterns of plant trait convergence and divergence in a Mediterranean rangeland. Journal of Ecology 100:1422–1433.

Blatzer, M., A. Beauvais, B. Henrissat, and J.-P. Latgé. 2020. Revisiting Old Questions and New Approaches to Investigate the Fungal Cell Wall Construction. Springer Berlin Heidelberg, Berlin, Heidelberg.

Bloom, A. J., F. S. Chapin, and H. A. Mooney. 1985. Resource Limitation in Plants-An Economic Analogy. Annual Review of Ecology and Systematics 16:363–392.

Bödeker, I. T. M., K. E. Clemmensen, W. de Boer, F. Martin, Å. Olson, and B. D. Lindahl. 2014. Ectomycorrhizal Cortinarius species participate in enzymatic oxidation of humus in northern forest ecosystems. New Phytologist 203:245–256.

Bödeker, I. T. M., C. M. R. Nygren, A. F. S. Taylor, Å. Olson, and B. D. Lindahl. 2009. ClassII peroxidase-encoding genes are present in a phylogenetically wide range of ectomycorrhizal fungi. The ISME Journal 3:1387–1395.

Bokulich, N. A., M. R. Dillon, E. Bolyen, B. D. Kaehler, G. A. Huttley, and J. G. Caporaso. 2018. q2-sample-classifier: machine-learning tools for microbiome classification and regression. Journal of open research software 3.

Bouma-Gregson, K., M. R. Olm, A. J. Probst, K. Anantharaman, M. E. Power, and J. F. Banfield. 2019. Impacts of microbial assemblage and environmental conditions on the distribution of anatoxin-a producing cyanobacteria within a river network. The ISME Journal 13:1618–1634.

Burke, C., P. Steinberg, D. Rusch, S. Kjelleberg, and T. Thomas. 2011. Bacterial community assembly based on functional genes rather than species. Proceedings of the National Academy of Sciences 108:14288–14293.

Cornwell, W. K., and D. D. Ackerly. 2009. Community assembly and shifts in plant trait distributions across an environmental gradient in coastal California. Ecological Monographs 79:109–126.

Cowles, H. C. 1899. The Ecological Relations of the Vegetation on the Sand Dunes of Lake Michigan. Part I.-Geographical Relations of the Dune Floras. Botanical Gazette 27:95–117.

Defrenne, C. E., T. J. Philpott, S. H. A. Guichon, W. J. Roach, B. J. Pickles, and S. W. Simard. 2019. Shifts in Ectomycorrhizal Fungal Communities and Exploration Types Relate to the Environment and Fine-Root Traits Across Interior Douglas-Fir Forests of Western Canada. Frontiers in Plant Science 10:643.

Diamond, J. M. 1973. Distributional Ecology of New Guinea Birds: Recent ecological and biogeographical theories can be tested on the bird communities of New Guinea. Science 179:759–769.

Diaz, S., M. Cabido, and F. Casanoves. 1998. Plant functional traits and environmental filters at a regional scale. Journal of Vegetation Science 9:113–122.

Duhamel, M., J. Wan, L. M. Bogar, R. M. Segnitz, N. C. Duncritts, and K. G. Peay. 2019. Plant selection initiates alternative successional trajectories in the soil microbial community after disturbance. Ecological Monographs 89:e01367.

Eastwood, D. C., D. Floudas, M. Binder, A. Majcherczyk, P. Schneider, A. Aerts, F. O. Asiegbu, S. E. Baker, K. Barry, M. Bendiksby, M. Blumentritt, P. M. Coutinho, D. Cullen, R. P. de Vries, A. Gathman, B. Goodell, B. Henrissat, K. Ihrmark, H. Kauserud, A. Kohler, K. LaButti, A. Lapidus, J. L. Lavin, Y.-H. Lee, E. Lindquist, W. Lilly, S. Lucas, E. Morin, C. Murat, J. A. Oguiza, J. Park, A. G. Pisabarro, R. Riley, A. Rosling, A. Salamov, O. Schmidt, J. Schmutz, I. Skrede, J. Stenlid, A. Wiebenga, X. Xie, U. Kues, D. S. Hibbett, D. Hoffmeister, N. Hogberg, F. Martin, I. V. Grigoriev, and S. C. Watkinson. 2011. The Plant Cell Wall-Decomposing Machinery Underlies the Functional Diversity of Forest Fungi. Science 333:762–765.

Eng, A., and E. Borenstein. 2018. Taxa-function robustness in microbial communities. Microbiome 6:1–19.

Fawal, N., Q. Li, B. Savelli, M. Brette, G. Passaia, M. Fabre, C. Mathé, and C. Dunand. 2013. PeroxiBase: a database for large-scale evolutionary analysis of peroxidases. Nucleic Acids Research 41:D441–D444.

Ferrier, S., G. Manion, J. Elith, and K. Richardson. 2007. Using generalized dissimilarity modelling to analyse and predict patterns of beta diversity in regional biodiversity assessment. Diversity and Distributions 13:252–264.

Fierer, N., A. Barberán, and D. C. Laughlin. 2014. Seeing the forest for the genes: using metagenomics to infer the aggregated traits of microbial communities. Frontiers in Microbiology 5.

Fitzpatrick, M. C., and S. R. Keller. 2015. Ecological genomics meets community-level modelling of biodiversity: mapping the genomic landscape of current and future environmental adaptation. Ecology Letters 18:1–16.

Floudas, D., J. Bentzer, D. Ahrén, T. Johansson, P. Persson, and A. Tunlid. 2020. Uncovering the hidden diversity of litter-decomposition mechanisms in mushroom-forming fungi. The ISME Journal.

Gardes, M., and T. D. Bruns. 1996. Community structure of ectomycorrhizal fungi in a Pinus muricata forest: above- and below-ground views. Canadian Journal of Botany 74:1572–1583.

Gossner, M. M., T. M. Lewinsohn, T. Kahl, F. Grassein, S. Boch, D. Prati, K. Birkhofer, S. C. Renner, J. Sikorski, T. Wubet, H. Arndt, V. Baumgartner, S. Blaser, N. Blüthgen, C. Börschig, F. Buscot, T. Diekötter, L. R. Jorge, K. Jung, A. C. Keyel, A.-M. Klein, S. Klemmer, J. Krauss, M. Lange, J. Müller, J. Overmann, E. Pašalić, C. Penone, D. J. Perović, O. Purschke, P. Schall, S. A. Socher, I. Sonnemann, M. Tschapka, T. Tscharntke, M. Türke, P. C. Venter, C. N. Weiner, M. Werner, V. Wolters, S. Wurst, C. Westphal, M. Fischer, W. W. Weisser, and E. Allan. 2016. Land-use intensification causes multitrophic homogenization of grassland communities. Nature 540:266–269.

Hammel, K. E., and D. Cullen. 2008. Role of fungal peroxidases in biological ligninolysis. Current Opinion in Plant Biology 11:349–355.

Hardwick, S. A., W. Y. Chen, T. Wong, B. S. Kanakamedala, I. W. Deveson, S. E. Ongley, N. S. Santini, E. Marcellin, M. A. Smith, L. K. Nielsen, C. E. Lovelock, B. A. Neilan, and T. R. Mercer. 2018. Synthetic microbe communities provide internal reference standards for metagenome sequencing and analysis. Nature Communications 9:3096.

Hibbett, D. S., L.-B. Gilbert, and M. J. Donoghue. 2000. Evolutionary instability of ectomycorrhizal symbioses in basidiomycetes. Nature 407:506–508.

Hortal, S., K. L. Plett, J. M. Plett, T. Cresswell, M. Johansen, E. Pendall, and I. C. Anderson. 2017. Role of plant–fungal nutrient trading and host control in determining the competitive success of ectomycorrhizal fungi. The ISME Journal 11:2666–2676.

Houlton, B. Z., D. M. Sigman, E. A. G. Schuur, and L. O. Hedin. 2007. A climate-driven switch in plant nitrogen acquisition within tropical forest communities. Proceedings of the National Academy of Sciences 104:8902–8906.

Janusz, G., A. Pawlik, J. Sulej, U. Świderska-Burek, A. Jarosz-Wilkołazka, and A. Paszczyński. 2017. Lignin degradation: microorganisms, enzymes involved, genomes analysis and evolution. FEMS Microbiology Reviews 41:941–962.

Jones, S. E., and J. T. Lennon. 2010. Dormancy contributes to the maintenance of microbial diversity. Proceedings of the National Academy of Sciences 107:5881–5886.

Kellner, H., P. Luis, M. J. Pecyna, F. Barbi, D. Kapturska, D. Krüger, D. R. Zak, R. Marmeisse, M. Vandenbol, and M. Hofrichter. 2014. Widespread Occurrence of Expressed Fungal Secretory Peroxidases in Forest Soils. PLoS ONE 9.

Kielland, K. 1994. Amino Acid Absorption by Arctic Plants: Implications for Plant Nutrition and Nitrogen Cycling. Ecology 75:2373–2383.

Kiers, E. T., M. Duhamel, Y. Beesetty, J. A. Mensah, O. Franken, E. Verbruggen, C. R. Fellbaum, G. A. Kowalchuk, M. M. Hart, A. Bago, T. M. Palmer, S. A. West, P. Vandenkoornhuyse, J. Jansa, and H. Bucking. 2011. Reciprocal Rewards Stabilize Cooperation in the Mycorrhizal Symbiosis. Science 333:880–882.

Kohler, A., A. Kuo, L. G. Nagy, E. Morin, K. W. Barry, F. Buscot, B. Canbäck, C. Choi, N. Cichocki, A. Clum, J. Colpaert, A. Copeland, M. D. Costa, J. Doré, D. Floudas, G. Gay, M. Girlanda, B. Henrissat, S. Herrmann, J. Hess, N. Högberg, T. Johansson, H.-R. Khouja, K. LaButti, U. Lahrmann, A. Levasseur, E. A. Lindquist, A. Lipzen, R.

Marmeisse, E. Martino, C. Murat, C. Y. Ngan, U. Nehls, J. M. Plett, A. Pringle, R. A. Ohm, S. Perotto, M. Peter, R. Riley, F. Rineau, J. Ruytinx, A. Salamov, F. Shah, H. Sun, M. Tarkka, A. Tritt, C. Veneault-Fourrey, A. Zuccaro, A. Tunlid, I. V. Grigoriev, D. S. Hibbett, and F. Martin. 2015. Convergent losses of decay mechanisms and rapid turnover of symbiosis genes in mycorrhizal mutualists. Nature Genetics 47:410–415.

Koide, R. T., C. Fernandez, and G. Malcolm. 2014. Determining place and process: functional traits of ectomycorrhizal fungi that affect both community structure and ecosystem function. New Phytologist 201:433–439.

Konar, A., O. Choudhury, R. Bullis, L. Fiedler, J. M. Kruser, M. T. Stephens, O. Gailing, S. Schlarbaum, M. V. Coggeshall, M. E. Staton, J. E. Carlson, S. Emrich, and J. Romero-Severson. 2017. High-quality genetic mapping with ddRADseq in the non-model tree Quercus rubra. BMC Genomics 18:417.

Kües, U., and M. Rühl. 2011. Multiple Multi-Copper Oxidase Gene Families in Basidiomycetes – What for? Current Genomics 12:72–94.

Kunstler, G., D. Falster, D. A. Coomes, F. Hui, R. M. Kooyman, D. C. Laughlin, L. Poorter, M. Vanderwel, G. Vieilledent, S. J. Wright, M. Aiba, C. Baraloto, J. Caspersen, J. H. C. Cornelissen, S. Gourlet-Fleury, M. Hanewinkel, B. Herault, J. Kattge, H. Kurokawa, Y. Onoda, J. Peñuelas, H. Poorter, M. Uriarte, S. Richardson, P. Ruiz-Benito, I.-F. Sun, G. Ståhl, N. G. Swenson, J. Thompson, B. Westerlund, C. Wirth, M. A. Zavala, H. Zeng, J. K. Zimmerman, N. E. Zimmermann, and M. Westoby. 2016. Plant functional traits have globally consistent effects on competition. Nature 529:204–207.

Kyaschenko, J., K. E. Clemmensen, E. Karltun, and B. D. Lindahl. 2017. Below-ground organic matter accumulation along a boreal forest fertility gradient relates to guild interaction within fungal communities. Ecology Letters 20:1546–1555.

Li, H., and R. Durbin. 2009. Fast and accurate short read alignment with Burrows–Wheeler transform. Bioinformatics 25:1754–1760.

Lilleskov, E. A., T. J. Fahey, T. R. Horton, and G. M. Lovett. 2002. Belowground Ectomycorrhizal Fungal Community Change Over a Nitrogen Deposition Gradient in Alaska. Ecology 83:104–115.

Lombard, V., H. Golaconda Ramulu, E. Drula, P. M. Coutinho, and B. Henrissat. 2014. The carbohydrate-active enzymes database (CAZy) in 2013. Nucleic Acids Research 42:D490–D495.

Louca, S., S. M. S. Jacques, A. P. F. Pires, J. S. Leal, A. L. González, M. Doebeli, and V. F. Farjalla. 2017. Functional structure of the bromeliad tank microbiome is strongly shaped by local geochemical conditions. Environmental Microbiology 19:3132–3151.

Louca, S., S. M. S. Jacques, A. P. F. Pires, J. S. Leal, D. S. Srivastava, L. W. Parfrey, V. F. Farjalla, and M. Doebeli. 2016. High taxonomic variability despite stable functional structure across microbial communities. Nature Ecology & Evolution 1:0015.

Louca, S., M. F. Polz, F. Mazel, M. B. N. Albright, J. A. Huber, M. I. O'Connor, M. Ackermann, A. S. Hahn, D. S. Srivastava, S. A. Crowe, M. Doebeli, and L. W. Parfrey. 2018. Function and functional redundancy in microbial systems. Nature Ecology & Evolution 2:936–943.

Malik, A. A., J. B. H. Martiny, E. L. Brodie, A. C. Martiny, K. K. Treseder, and S. D. Allison. 2020. Defining trait-based microbial strategies with consequences for soil carbon cycling under climate change. The ISME Journal 14:1–9.

Martin, F., A. Kohler, C. Murat, C. Veneault-Fourrey, and D. S. Hibbett. 2016. Unearthing the roots of ectomycorrhizal symbioses. Nature Reviews Microbiology 14:760–773.
Moeller, H. V., K. G. Peay, and T. Fukami. 2014. Ectomycorrhizal fungal traits reflect environmental conditions along a coastal California edaphic gradient. FEMS Microbiology Ecology 87:797–806.
Moran, M. A., B. Satinsky, S. M. Gifford, H. Luo, A. Rivers, L.-K. Chan, J. Meng, B. P. Durham, C. Shen, V. A. Varaljay, C. B. Smith, P. L. Yager, and B. M. Hopkinson. 2013. Sizing up metatranscriptomics. The ISME Journal 7:237–243.
Nehls, U., A. Das, and D. Neb. 2016. Carbohydrate metabolism in ectomycorrhizal symbiosis. Molecular mycorrhizal symbiosis 10:161–178.
Nemergut, D. R., S. K. Schmidt, T. Fukami, S. P. O'Neill, T. M. Bilinski, L. F. Stanish, J. E. Knelman, J. L. Darcy, R. C. Lynch, P. Wickey, and S. Ferrenberg. 2013. Patterns and Processes of Microbial Community Assembly. Microbiology and Molecular Biology Reviews 77:342–356.
Nicolás, C., T. Martin-Bertelsen, D. Floudas, J. Bentzer, M. Smits, T. Johansson, C. Troein, P. Persson, and A. Tunlid. 2019. The soil organic matter decomposition mechanisms in ectomycorrhizal fungi are tuned for liberating soil organic nitrogen. The ISME Journal 13:977–988.
Nilsson, R. H., K.-H. Larsson, A. F. S. Taylor, J. Bengtsson-Palme, T. S. Jeppesen, D. Schigel, P. Kennedy, K. Picard, F. O. Glöckner, L. Tedersoo, I. Saar, U. Kõljalg, and K. Abarenkov. 2019. The UNITE database for molecular identification of fungi: handling dark taxa and parallel taxonomic classifications. Nucleic Acids Research 47:D259–D264.
Op De Beeck, M., C. Troein, C. Peterson, P. Persson, and A. Tunlid. 2018. Fenton reaction facilitates organic nitrogen acquisition by an ectomycorrhizal fungus. New Phytologist 218:335–343.
Pakeman, R. J., E. Garnier, S. Lavorel, P. Ansquer, H. Castro, P. Cruz, J. Doležal, O. Eriksson, H. Freitas, C. Golodets, J. Kigel, M. Kleyer, J. Lepš, T. Meier, M. Papadimitriou, V. P. Papanastasis, H. Quested, F. Quétier, G. Rusch, M. Sternberg, J.-P. Theau, A. Thébault, and D. Vile. 2008. Impact of abundance weighting on the response of seed traits to climate and land use. Journal of Ecology 96:355–366.
Peay, K. G., S. E. Russo, K. L. McGuire, Z. Lim, J. P. Chan, S. Tan, and S. J. Davies. 2015. Lack of host specificity leads to independent assortment of dipterocarps and ectomycorrhizal fungi across a soil fertility gradient. Ecology Letters 18:807–816.
Pellitier, P. T., I. Ibáñez, D. R. Zak, W. A. Argiroff, and K. Acharya. in review. Ectomycorrhizal access to organic N enhances plant growth response to rising [CO2]. in review.
Pellitier, P. T., and D. R. Zak. 2018. Ectomycorrhizal fungi and the enzymatic liberation of nitrogen from soil organic matter: why evolutionary history matters. New Phytologist 217:68–73.
Peng, M., M. V. Aguilar-Pontes, M. Hainaut, B. Henrissat, K. Hildén, M. R. Mäkelä, and R. P. de Vries. 2018. Comparative analysis of basidiomycete transcriptomes reveals a core set of expressed genes encoding plant biomass degrading enzymes. Fungal Genetics and Biology 112:40–46.
Phillips, R. P., E. Brzostek, and M. G. Midgley. 2013. The mycorrhizal-associated nutrient economy: a new framework for predicting carbon–nutrient couplings in temperate forests. New Phytologist 199:41–51.

Pierre-Emmanuel, C., M. François, S. Marc-André, D. Myriam, C. Stéven, Z. Fabio, B. Marc, P. Claude, T. Adrien, G. Jean, and R. Franck. 2016. Into the functional ecology of ectomycorrhizal communities: environmental filtering of enzymatic activities. Journal of Ecology 104:1585–1598.

Plett, J. M., and F. Martin. 2011. Blurred boundaries: lifestyle lessons from ectomycorrhizal fungal genomes. Trends in Genetics 27:14–22.

Qin, C., K. Zhu, N. R. Chiariello, C. B. Field, and K. G. Peay. 2020. Fire history and plant community composition outweigh decadal multi-factor global change as drivers of microbial composition in an annual grassland. Journal of Ecology 108:611–625.

Quinn, T. P., I. Erb, G. Gloor, C. Notredame, M. F. Richardson, and T. M. Crowley. 2019. A field guide for the compositional analysis of any-omics data. GigaScience 8:giz107.

Quinn, T. P., I. Erb, M. F. Richardson, and T. M. Crowley. 2018. Understanding sequencing data as compositions: an outlook and review. Bioinformatics 34:2870–2878.

Read, D. J., and J. Perez-Moreno. 2003. Mycorrhizas and Nutrient Cycling in Ecosystems: A Journey towards Relevance? The New Phytologist 157:475–492.

Reed, D. C., C. K. Algar, J. A. Huber, and G. J. Dick. 2014. Gene-centric approach to integrating environmental genomics and biogeochemical models. Proceedings of the National Academy of Sciences 111:1879–1884.

Regalado, J., D. S. Lundberg, O. Deusch, S. Kersten, T. Karasov, K. Poersch, G. Shirsekar, and D. Weigel. 2020. Combining whole-genome shotgun sequencing and rRNA gene amplicon analyses to improve detection of microbe–microbe interaction networks in plant leaves. The ISME Journal:1–15.

Rineau, F., D. Roth, F. Shah, M. Smits, T. Johansson, B. Canbäck, P. B. Olsen, P. Persson, M. N. Grell, E. Lindquist, I. V. Grigoriev, L. Lange, and A. Tunlid. 2012. The ectomycorrhizal fungus Paxillus involutus converts organic matter in plant litter using a trimmed brown-rot mechanism involving Fenton chemistry. Environmental Microbiology 14:1477–1487.

Satinsky, B. M., S. M. Gifford, B. C. Crump, and M. A. Moran. 2013. Chapter Twelve - Use of Internal Standards for Quantitative Metatranscriptome and Metagenome Analysis. Pages 237–250 *in* E. F. DeLong, editor. Methods in Enzymology. Academic Press.

Satinsky, B. M., C. B. Smith, S. Sharma, M. Landa, P. M. Medeiros, V. J. Coles, P. L. Yager, B. C. Crump, and M. A. Moran. 2017. Expression patterns of elemental cycling genes in the Amazon River Plume. The ISME Journal 11:1852–1864.

Shah, F., C. Nicolás, J. Bentzer, M. Ellström, M. Smits, F. Rineau, B. Canbäck, D. Floudas, R. Carleer, G. Lackner, J. Braesel, D. Hoffmeister, B. Henrissat, D. Ahrén, T. Johansson, D. S. Hibbett, F. Martin, P. Persson, and A. Tunlid. 2016. Ectomycorrhizal fungi decompose soil organic matter using oxidative mechanisms adapted from saprotrophic ancestors. New Phytologist 209:1705–1719.

Simão, F. A., R. M. Waterhouse, P. Ioannidis, E. V. Kriventseva, and E. M. Zdobnov. 2015. BUSCO: assessing genome assembly and annotation completeness with single-copy orthologs. Bioinformatics 31:3210–3212.

Smith, S. E., and D. J. Read. 2010. Mycorrhizal symbiosis. Academic press.

Sork, V. L., S. T. Fitz-Gibbon, D. Puiu, M. Crepeau, P. F. Gugger, R. Sherman, K. Stevens, C. H. Langley, M. Pellegrini, and S. L. Salzberg. 2016. First Draft Assembly and Annotation of the Genome of a California Endemic Oak. Genes|Genomes|Genetics 6:3485–3495.

Steidinger, B. S., T. W. Crowther, J. Liang, M. E. Van Nuland, G. D. A. Werner, P. B. Reich, G. J. Nabuurs, S. de-Miguel, M. Zhou, N. Picard, B. Herault, X. Zhao, C. Zhang, D. Routh, and K. G. Peay. 2019. Climatic controls of decomposition drive the global biogeography of forest-tree symbioses. Nature 569:404–408.

Sterkenburg, E., A. Bahr, M. B. Durling, K. E. Clemmensen, and B. D. Lindahl. 2015. Changes in fungal communities along a boreal forest soil fertility gradient. New Phytologist 207:1145–1158.

Sterkenburg, E., K. E. Clemmensen, A. Ekblad, R. D. Finlay, and B. D. Lindahl. 2018. Contrasting effects of ectomycorrhizal fungi on early and late stage decomposition in a boreal forest. The ISME Journal 12:2187–2197.

Suz, L. M., N. Barsoum, S. Benham, H.-P. Dietrich, K. D. Fetzer, R. Fischer, P. García, J. Gehrman, F. Kristöfel, M. Manninger, S. Neagu, M. Nicolas, J. Oldenburger, S. Raspe, G. Sánchez, H. W. Schröck, A. Schubert, K. Verheyen, A. Verstraeten, and M. I. Bidartondo. 2014. Environmental drivers of ectomycorrhizal communities in Europe's temperate oak forests. Molecular Ecology 23:5628–5644.

Talbot, J. M., T. D. Bruns, J. W. Taylor, D. P. Smith, S. Branco, S. I. Glassman, S. Erlandson, R. Vilgalys, H.-L. Liao, M. E. Smith, and K. G. Peay. 2014. Endemism and functional convergence across the North American soil mycobiome. Proceedings of the National Academy of Sciences 111:6341–6346.

Taylor, A. F. S., F. Martin, and D. J. Read. 2000. Fungal Diversity in Ectomycorrhizal Communities of Norway Spruce [Picea abies (L.) Karst.] and Beech (Fagus sylvatica L.) Along North-South Transects in Europe. Pages 343–365 *in* E.-D. Schulze, editor. Carbon and Nitrogen Cycling in European Forest Ecosystems. Springer, Berlin, Heidelberg.

Taylor, D. L., W. A. Walters, N. J. Lennon, J. Bochicchio, A. Krohn, J. G. Caporaso, and T. Pennanen. 2016. Accurate Estimation of Fungal Diversity and Abundance through Improved Lineage-Specific Primers Optimized for Illumina Amplicon Sequencing. Applied and Environmental Microbiology 82:7217–7226.

Terrer, C., R. B. Jackson, I. C. Prentice, T. F. Keenan, C. Kaiser, S. Vicca, J. B. Fisher, P. B. Reich, B. D. Stocker, B. A. Hungate, J. Peñuelas, I. McCallum, N. A. Soudzilovskaia, L. A. Cernusak, A. F. Talhelm, K. Van Sundert, S. Piao, P. C. D. Newton, M. J. Hovenden, D. M. Blumenthal, Y. Y. Liu, C. Müller, K. Winter, C. B. Field, W. Viechtbauer, C. J. Van Lissa, M. R. Hoosbeek, M. Watanabe, T. Koike, V. O. Leshyk, H. W. Polley, and O. Franklin. 2019. Nitrogen and phosphorus constrain the CO2 fertilization of global plant biomass. Nature Climate Change 9:684–689.

Terrer, C., S. Vicca, B. A. Hungate, R. P. Phillips, and I. C. Prentice. 2016. Mycorrhizal association as a primary control of the CO_2 fertilization effect. Science 353:72–74.

Terrer, C., S. Vicca, B. D. Stocker, B. A. Hungate, R. P. Phillips, P. B. Reich, A. C. Finzi, and I. C. Prentice. 2018. Ecosystem responses to elevated CO2 governed by plant–soil interactions and the cost of nitrogen acquisition. New Phytologist 217:507–522.

Treiber, M. L., D. H. Taft, I. Korf, D. A. Mills, and D. G. Lemay. 2020. Pre- and post-sequencing recommendations for functional annotation of human fecal metagenomes. BMC Bioinformatics 21:74.

Vandeputte, D., G. Kathagen, K. D'hoe, S. Vieira-Silva, M. Valles-Colomer, J. Sabino, J. Wang, R. Y. Tito, L. De Commer, Y. Darzi, S. Vermeire, G. Falony, and J. Raes. 2017. Quantitative microbiome profiling links gut community variation to microbial load. Nature 551:507–511.

Vellend, M. 2010. Conceptual Synthesis in Community Ecology. The Quarterly Review of Biology 85:183–206.
Villares, A., C. Moreau, C. Bennati-Granier, S. Garajova, L. Foucat, X. Falourd, B. Saake, J.-G. Berrin, and B. Cathala. 2017. Lytic polysaccharide monooxygenases disrupt the cellulose fibers structure. Scientific Reports 7:40262.
Vitousek, P. 1982. Nutrient Cycling and Nutrient Use Efficiency. The American Naturalist 119:553–572.
Waterhouse, R. M., M. Seppey, F. A. Simão, M. Manni, P. Ioannidis, G. Klioutchnikov, E. V. Kriventseva, and E. M. Zdobnov. 2018. BUSCO Applications from Quality Assessments to Gene Prediction and Phylogenomics. Molecular Biology and Evolution 35:543–548.
Wood, D. E., J. Lu, and B. Langmead. 2019. Improved metagenomic analysis with Kraken 2. Genome Biology 20:257.
Wright, I. J., P. B. Reich, M. Westoby, D. D. Ackerly, Z. Baruch, F. Bongers, J. Cavender-Bares, T. Chapin, J. H. C. Cornelissen, M. Diemer, J. Flexas, E. Garnier, P. K. Groom, J. Gulias, K. Hikosaka, B. B. Lamont, T. Lee, W. Lee, C. Lusk, J. J. Midgley, M.-L. Navas, Ü. Niinemets, J. Oleksyn, N. Osada, H. Poorter, P. Poot, L. Prior, V. I. Pyankov, C. Roumet, S. C. Thomas, M. G. Tjoelker, E. J. Veneklaas, and R. Villar. 2004. The worldwide leaf economics spectrum. Nature 428:821–827.
Zak, D. R., P. T. Pellitier, W. Argiroff, B. Castillo, T. Y. James, L. E. Nave, C. Averill, K. V. Beidler, J. Bhatnagar, J. Blesh, A. T. Classen, M. Craig, C. W. Fernandez, P. Gundersen, R. Johansen, R. T. Koide, E. A. Lilleskov, B. D. Lindahl, K. J. Nadelhoffer, R. P. Phillips, and A. Tunlid. 2019. Exploring the role of ectomycorrhizal fungi in soil carbon dynamics. New Phytologist 223:33–39.
Zak, D. R., and K. S. Pregitzer. 1990. Spatial and Temporal Variability of Nitrogen Cycling in Northern Lower Michigan. Forest Science 36:367–380.
Zak, D. R., K. S. Pregitzer, and G. E. Host. 1986. Landscape variation in nitrogen mineralization and nitrification. Canadian Journal of Forest Research 16:1258–1263.
Zanne, A. E., K. Abarenkov, M. E. Afkhami, C. A. Aguilar-Trigueros, S. Bates, J. M. Bhatnagar, P. E. Busby, N. Christian, W. K. Cornwell, T. W. Crowther, H. Flores-Moreno, D. Floudas, R. Gazis, D. Hibbett, P. Kennedy, D. L. Lindner, D. S. Maynard, A. M. Milo, R. H. Nilsson, J. Powell, M. Schildhauer, J. Schilling, and K. K. Treseder. 2020. Fungal functional ecology: bringing a trait-based approach to plant-associated fungi. Biological Reviews.

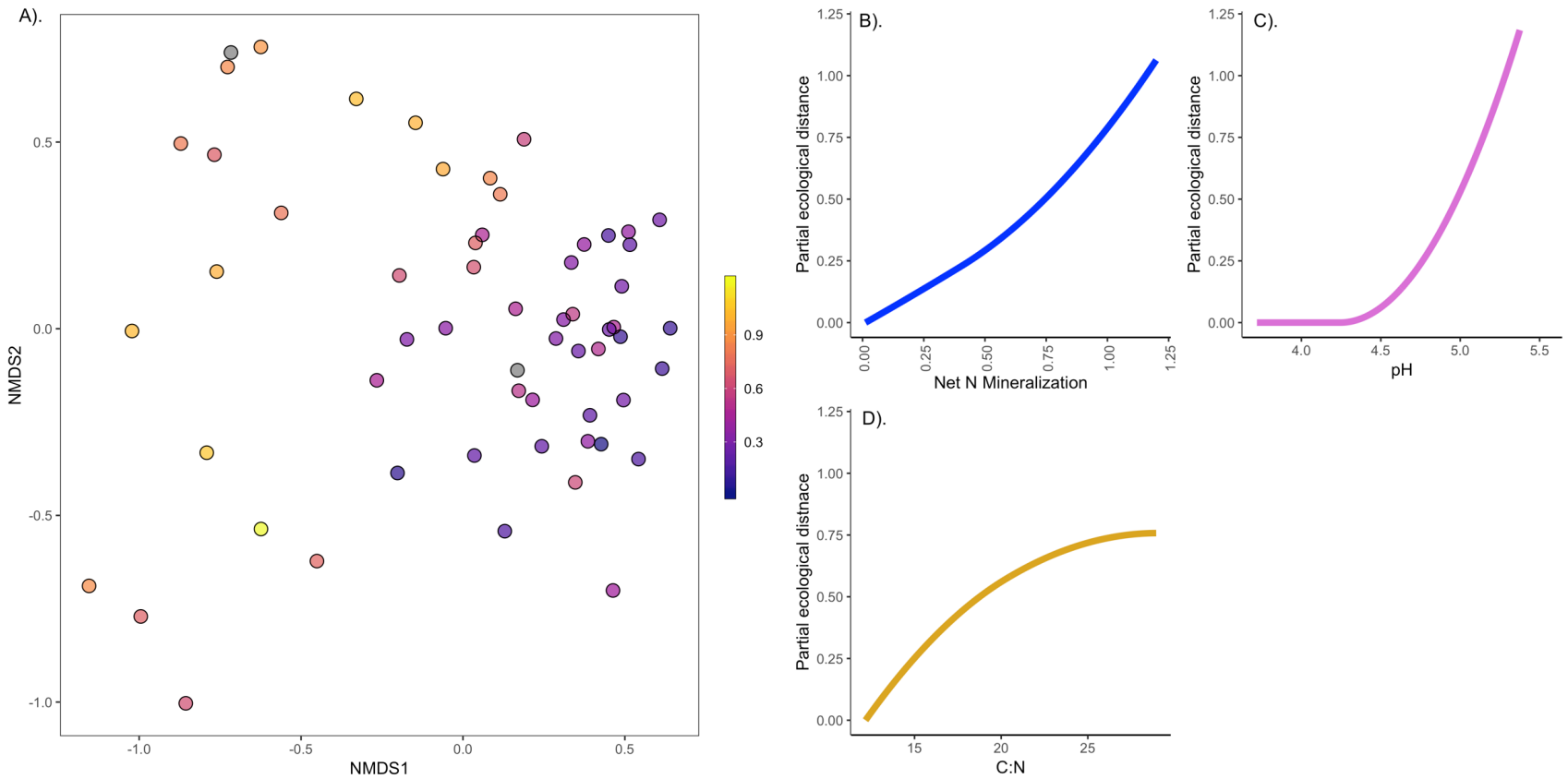

Figure 3-1 Ectomycorrhizal community composition visualized using NMDS. Each point represents ECM communities (OTU) present on individual Quercus rubra *root-systems; counts were Hellinger transformed Bray-Curtis distances. Color bar depicts soil mineralization rates (ug/g/d). (B),(C),(D) Results from the generalized dissimilarity model (GDM), depicting change in compositional turnover along each environmental gradient. The slope and shape of the line shows the rate of community change along the standardized environmental gradient on the x-axis. The maximum height of the regression line indicating the relative proportion of variance explained by each standardized environmental variable. The environmental predictors presented each explained a significant proportion of model deviance.*

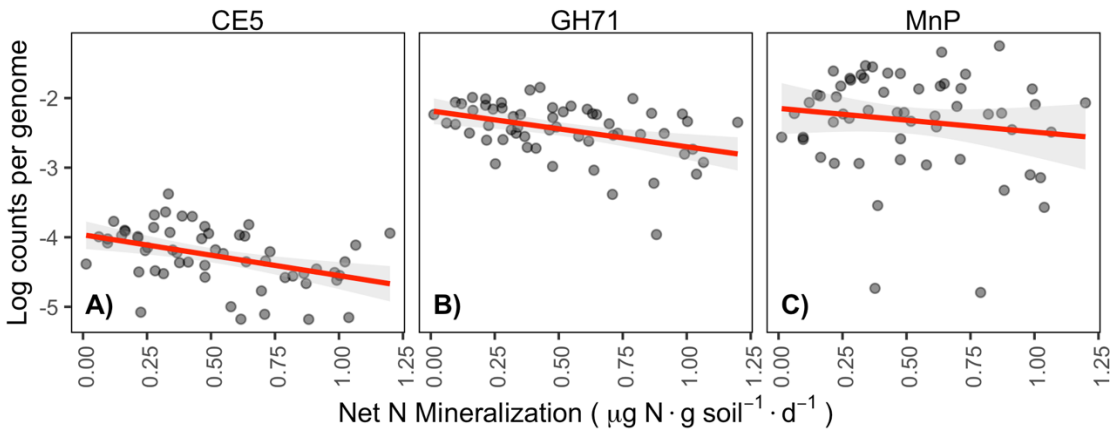

Figure 3-2 Log-transformed unscaled gene counts, depicting community weighted mean (CWM) gene abundances for each ECM community. Panel A). and B). were 'indicator' gene families that exhibited the largest absolute (positive or negative) response to soil inorganic N availability. Red lines indicate linear regression and standard error. CE5 (Carbohydrate Esterase), GH71 (Glycoside Hydrolase), MnP (Manganese-peroxidase).

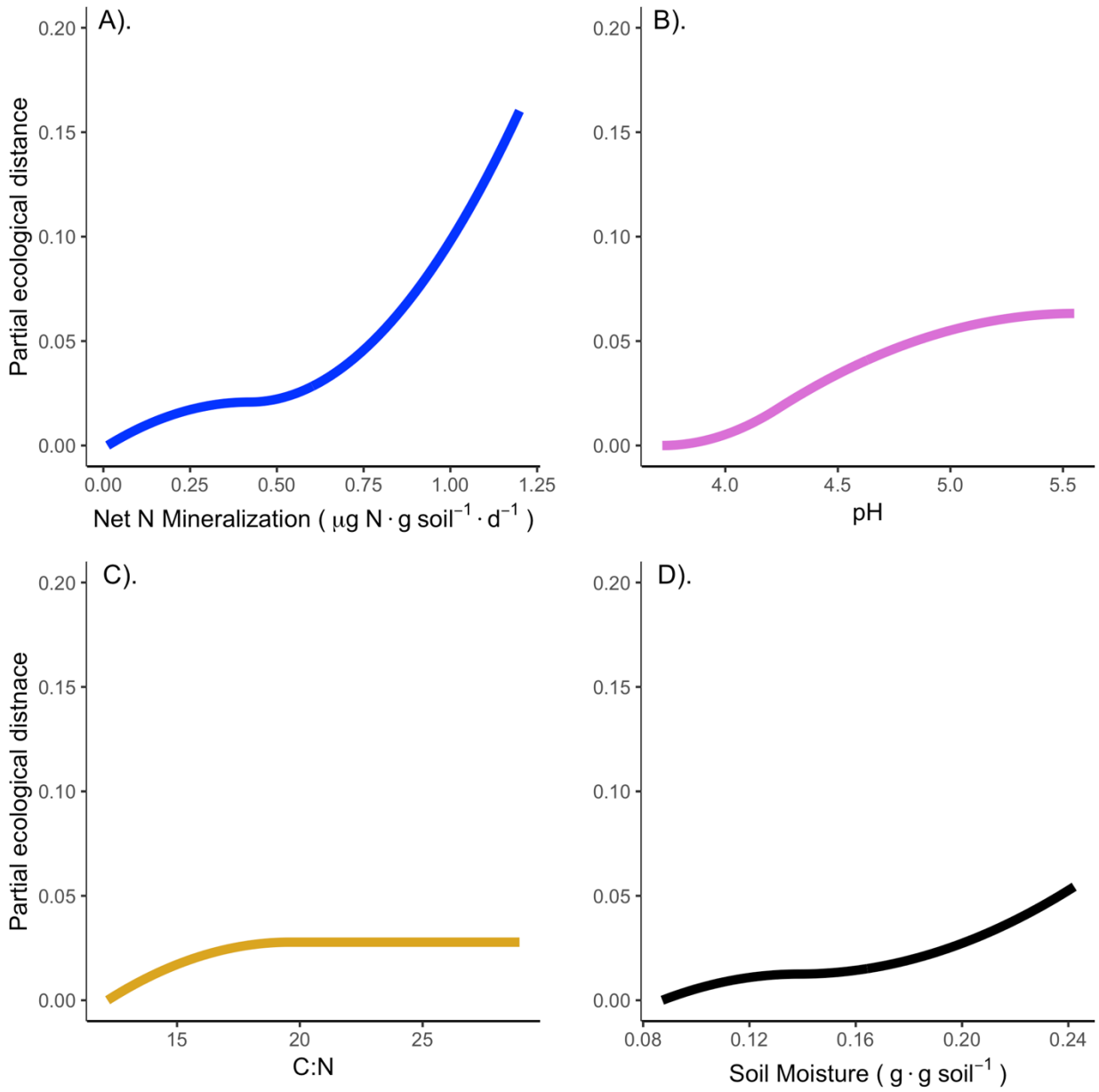

Figure 3-3 Generalized dissimilarity model (GDM) results depicting change in the compositional abundance of genes involved in decay of soil organic matter (SOM)(y-axis). Genes are scaled by the number of colonized ECM root-tips present on individual root-systems. Of the predictors (x-axes), only soil inorganic N availability explained a statistically significant proportion of model deviance. The maximum height of the regression line indicates the relative proportion of variance explained by each standardized environmental variable. The slope of the line shows the rate of gene suite change along the environmental gradient on the x-axis.

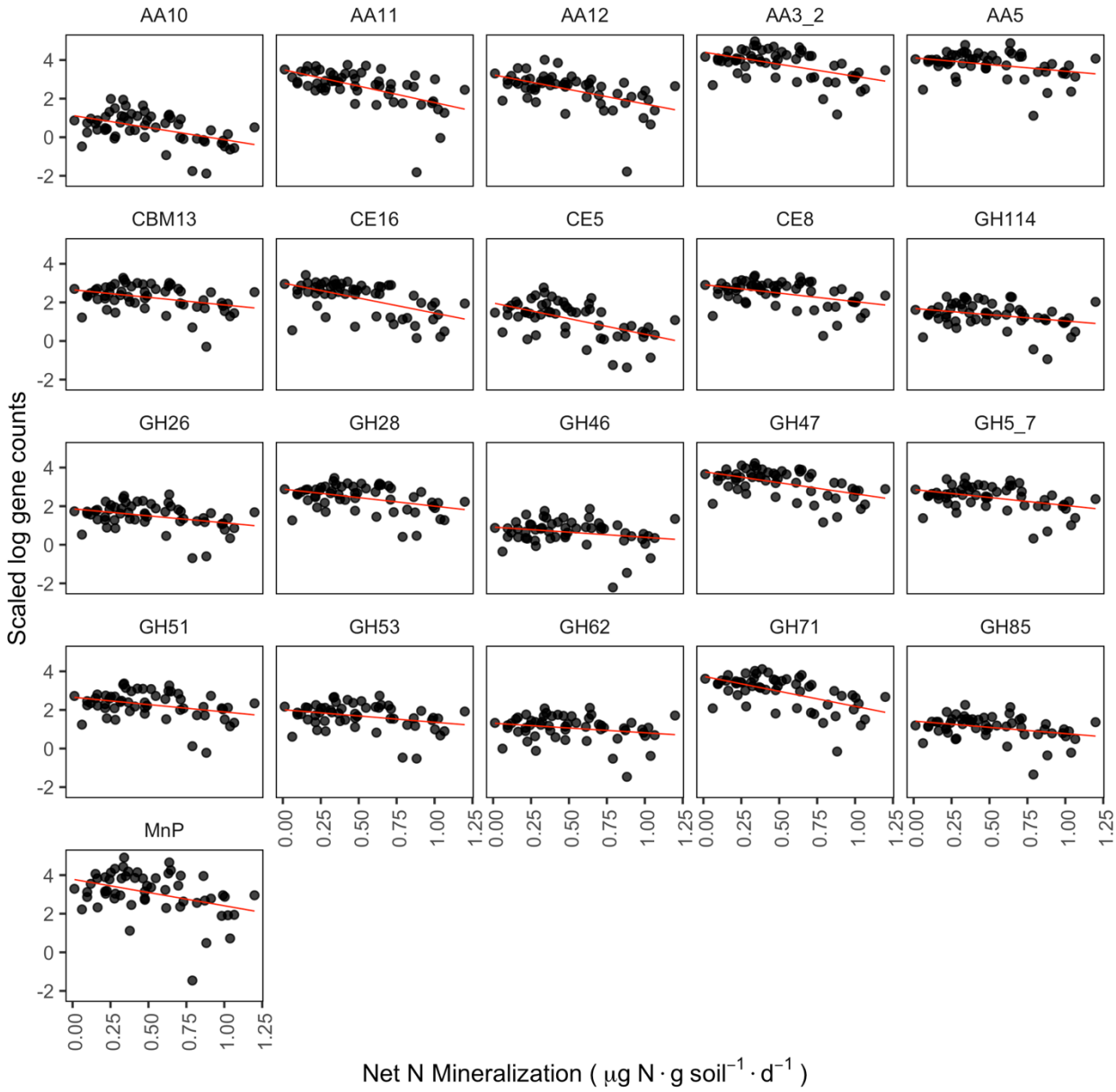

Figure 3-4 Scaled gene abundances of gene families involved in the decay of soil organic matter (SOM)(y-axis), as a function of soil mineralization rates. Log transformed gene counts are scaled by the number of colonized ECM root-tips present on individual root-systems, and were standardized using the number of single copy genes present in each sample. Plotted gene families were previously implicated as 'indicator' genes using unscaled gene counts. MnP was included for plotting but was not revealed as an indicator gene family. Trend lines (red) represent linear regression.

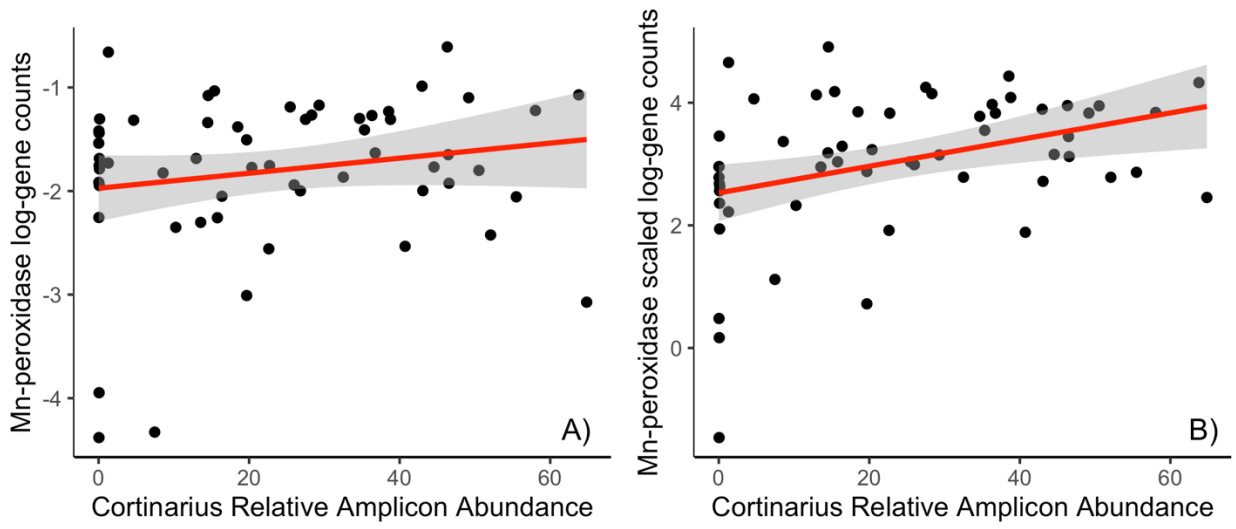

Figure 3-5 Relative abundance of sequences assigned to the ectomycorrhizal genus Cortinarius in relation to the (A) unscaled and (B) scaled, log-transformed abundance of Manganese-peroxidase genes. A). P = *0.13; B).* P= *0.005,* R^2= *0.12. Note distinct y-axes. Cortinarius was the most abundant fungal genus detected across samples.*

Supplementary Figures

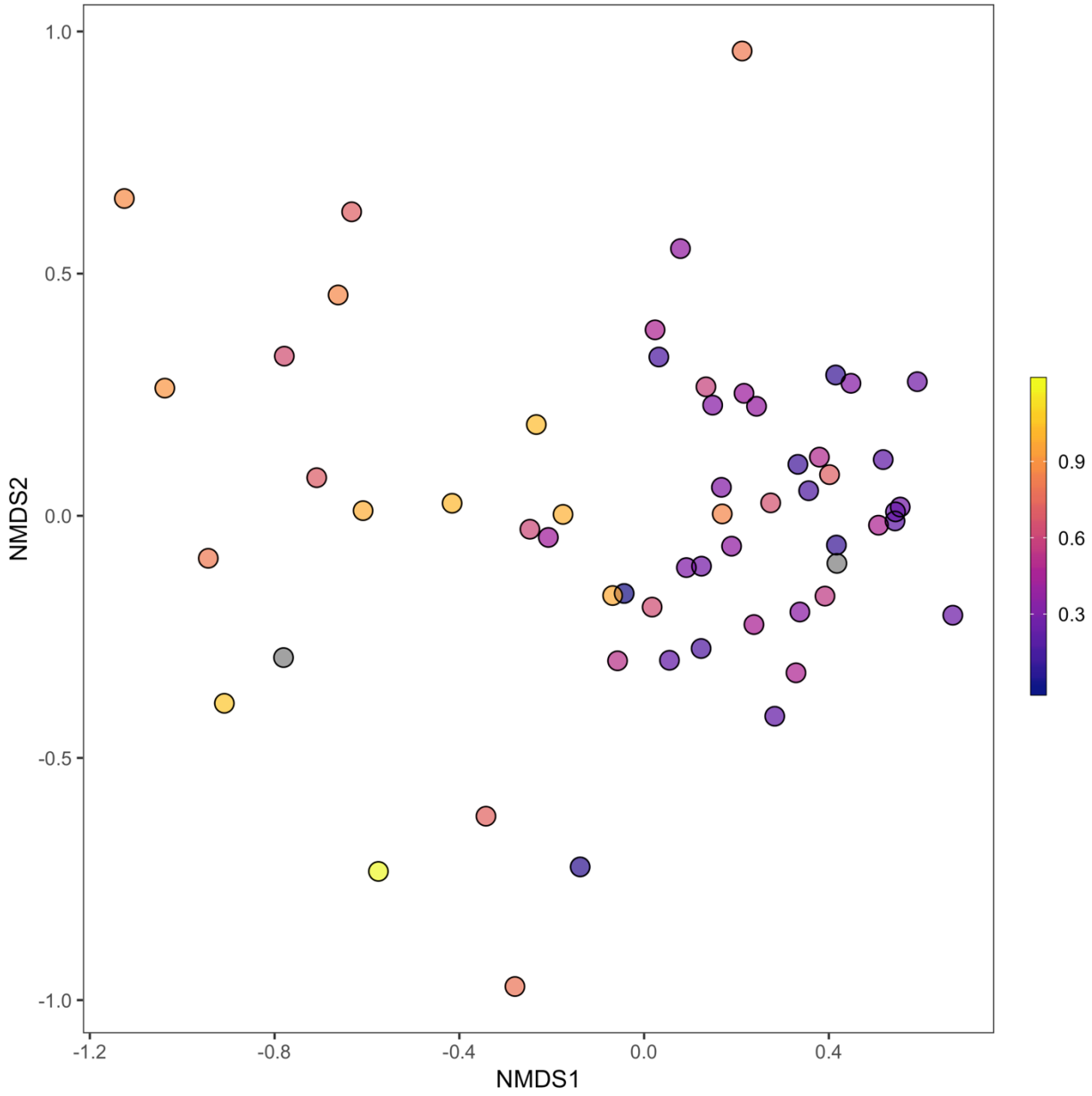

Supplementary Figure 3-1 Ectomycorrhizal community composition visualized using NMDS. Each point represents ECM communities (genera) present on individual Quercus rubra *root-systems; counts were Hellinger transformed Bray-Curtis distances. Color bar depicts soil mineralization rates (ug/g/d).*

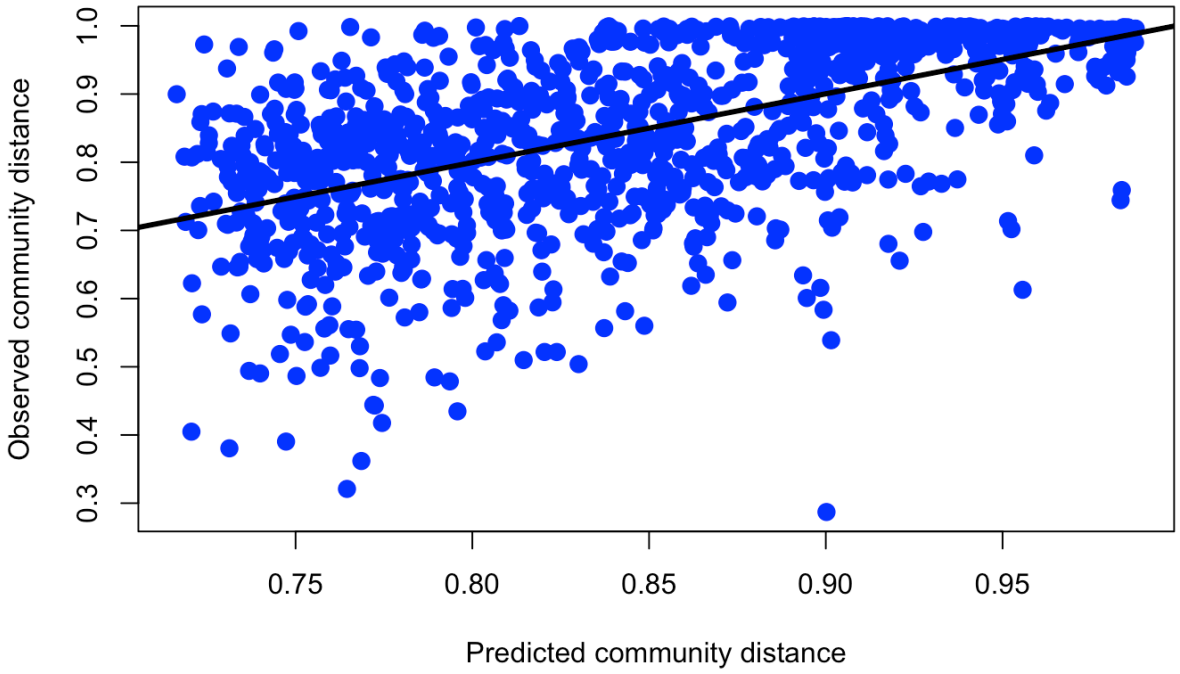

Supplementary Figure 3-2 GDM model output for ECM community modeling. S

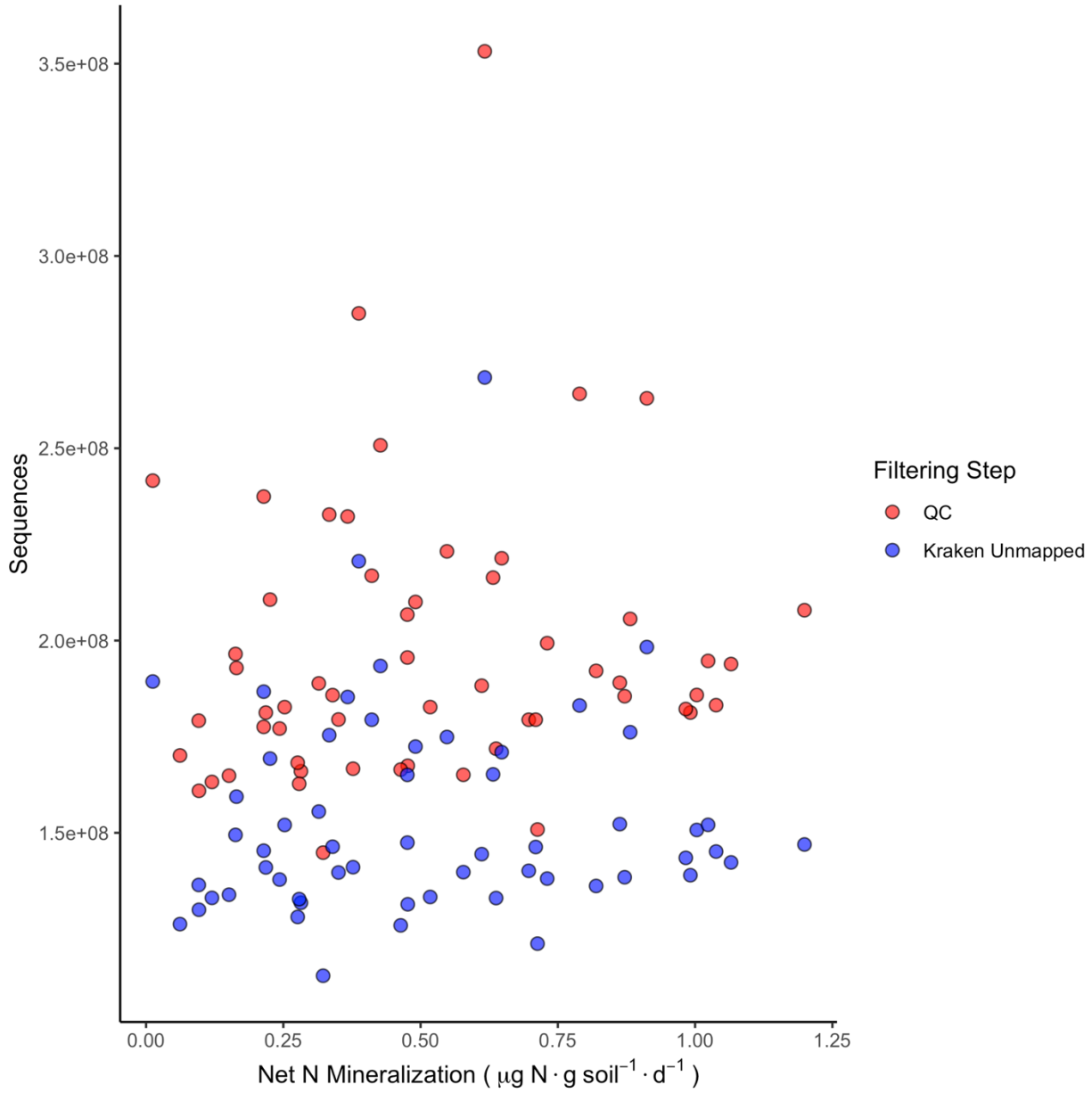

Supplementary Figure 3-3 Sequencing yield for each sample. QC (red) represent quality filtered sequences, see main text. Kraken Unmapped (blue), represent reads that remain after Kraken mapping and removal of contaminant reads (putative fungal reads). No significant relationship for either Filtering Step across the soil mineralization gradient: QC: p-value: 0.36; Kraken: P =0.73. Sample with very high read count was retained, note that normalized CAZy counts are not affected by this high sequence yield

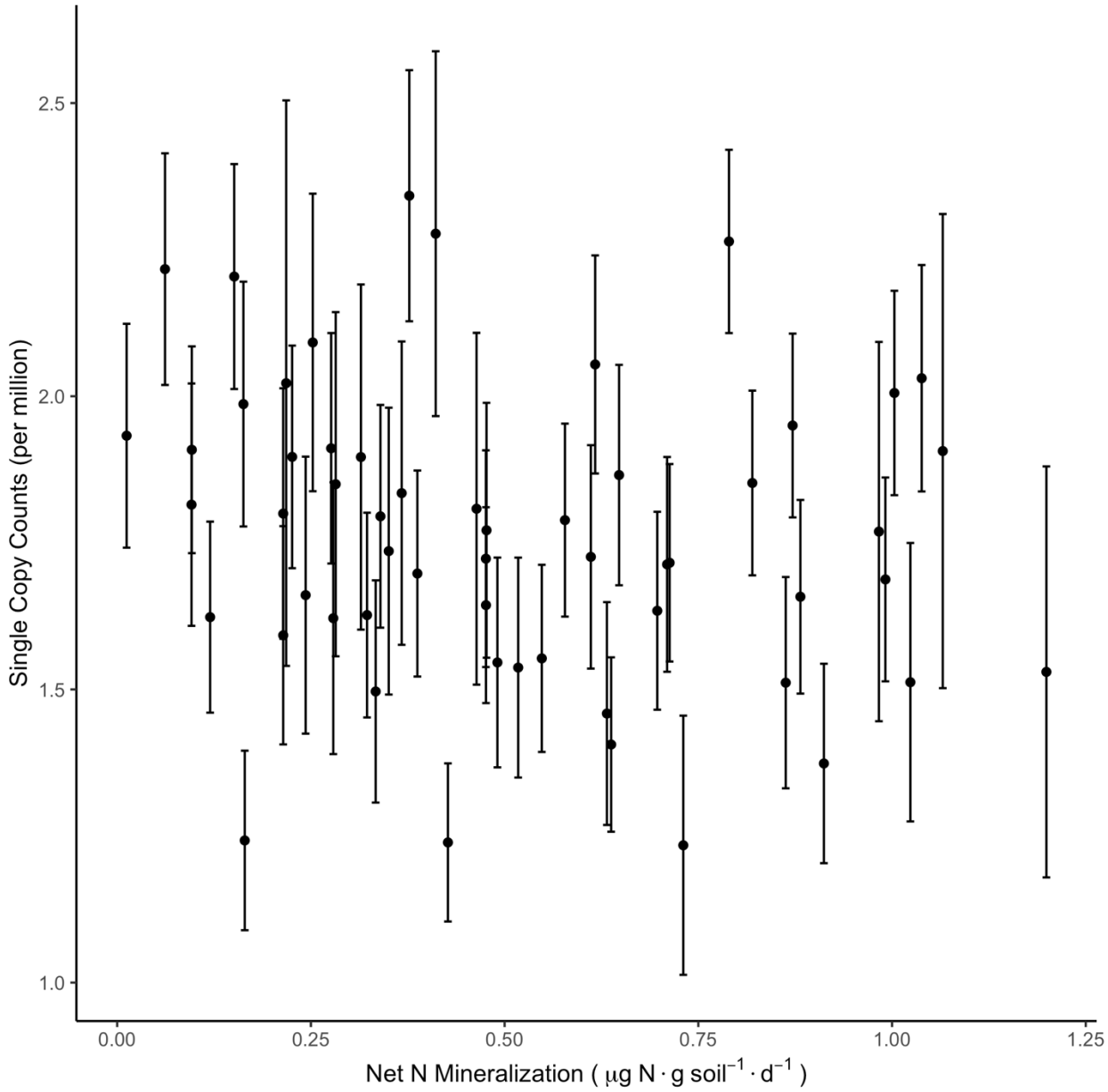

Supplementary Figure 3-4 Fungal genomes per million sequences. The geometric mean number of single copy genes mapped, divided by the sum of all reads mapped in that sample times 1e6. Error bars represent SE of the geometric mean, and may be interpreted as a measure of genome coverage. No significant variation in yield of fungal genomes per sample across the soil mineralization gradient (P = 0.17).

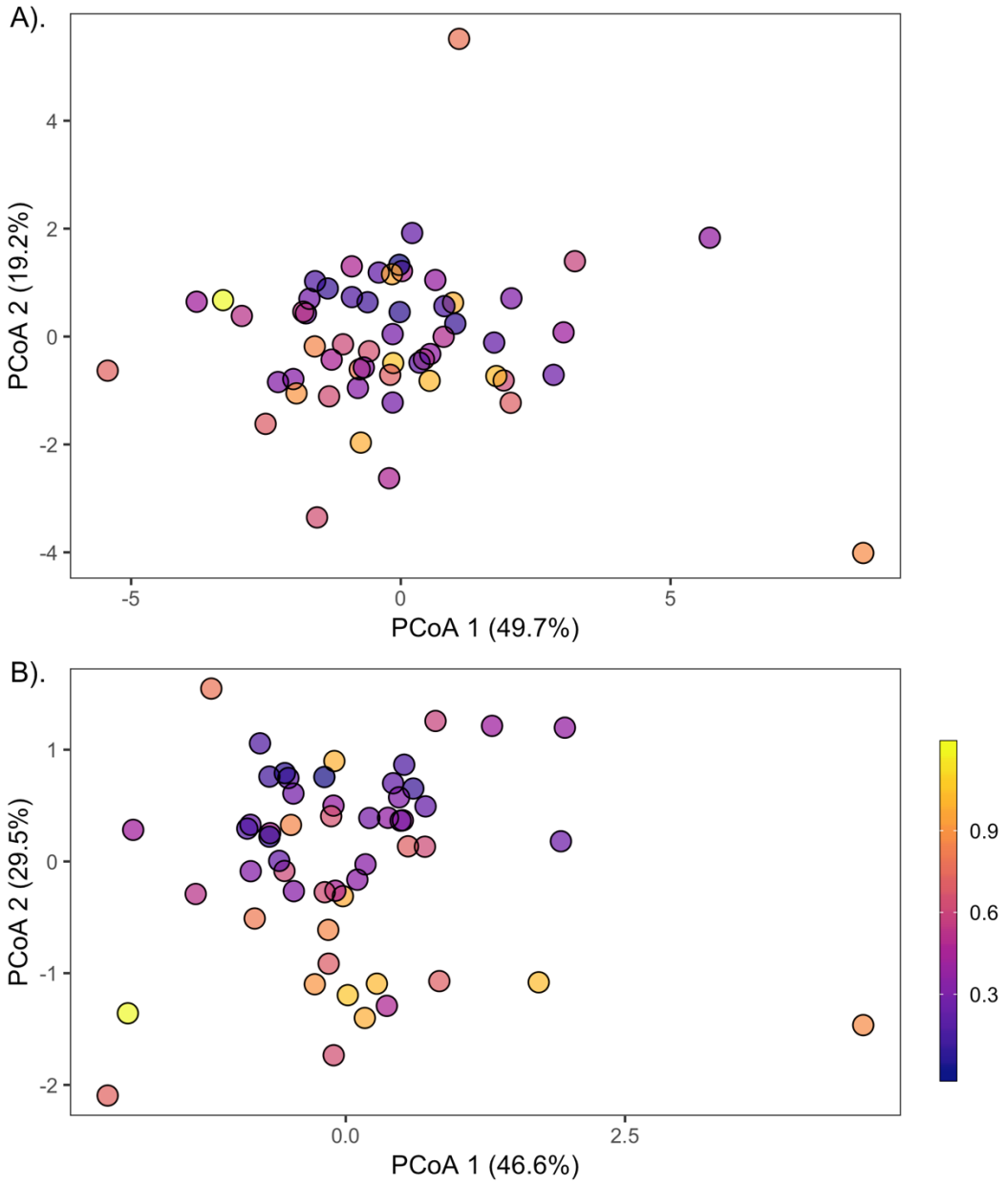

Supplementary Figure 3-5 Principle coordinates analysis, of all studied (94) gene families. Samples are log transformed by the number of individual single copy genomes present. Individual points indicate the composite community of ectomycorrhizal decay genes present on individual root-systems. Gene counts are not scaled. Communities (points) are colored by soil mineralization rates (legend bar) B. Ordination of 22 gene families identified as 'responsive' using the iterative 'indicator' gene analysis. Individual points indicate individual root systems.

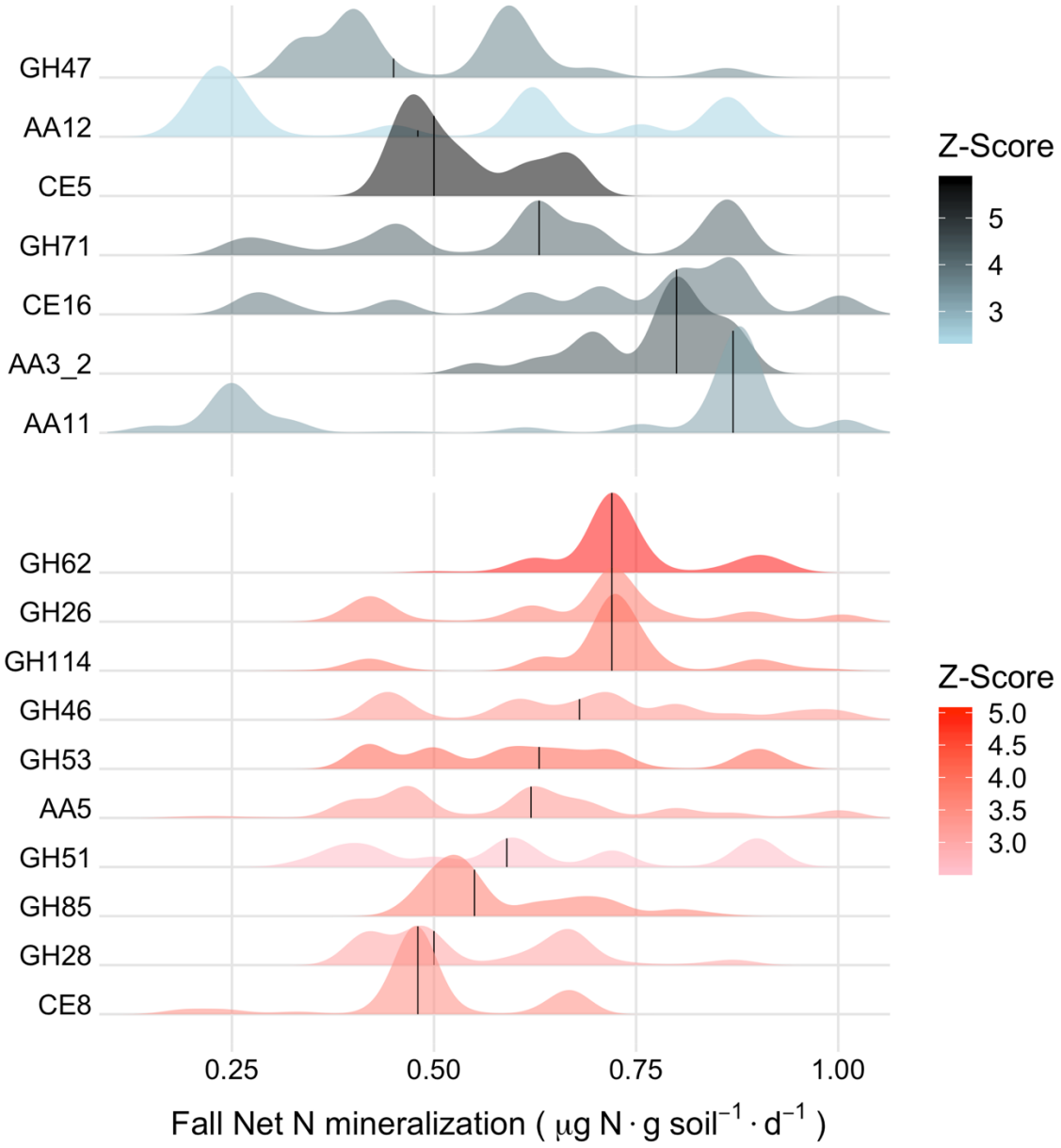

Supplementary Figure 3-6 Unscaled gene families showing change-points for negative (blue), and positive (red), z-scores for 'indicator' gene families that consistently respond to the soil inorganic N gradient. Plot depicts probability density function for all bootstraps (2000). Height of the peak indicates the sensitivity of the change point, for each individual gene families.

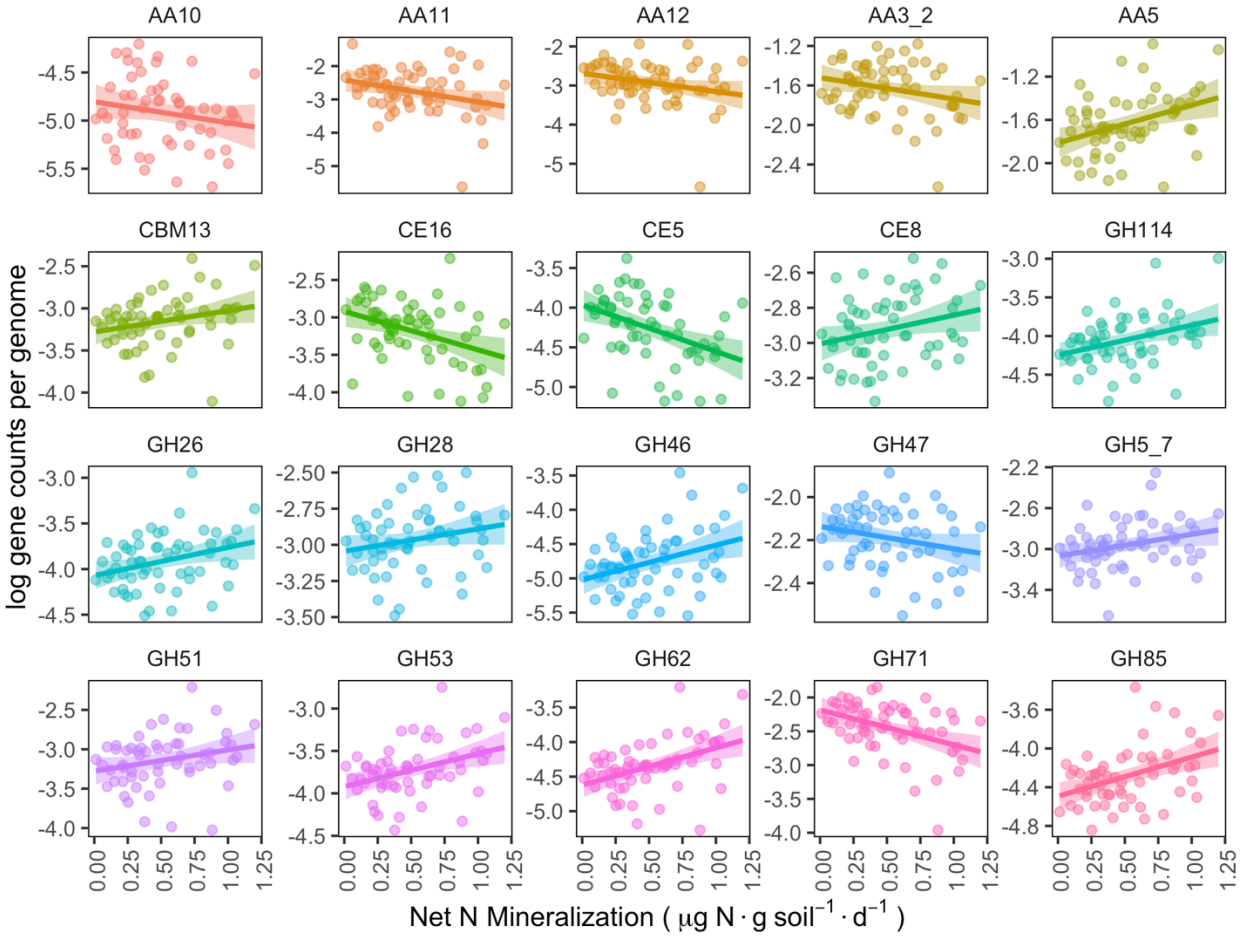

Supplementary Figure 3-7 Linear regressions of the individual 'indicator' gene families implicated using threshold indicator analysis to the soil inorganic N gradient. Note log-scale of the y axis, that varies among panels.

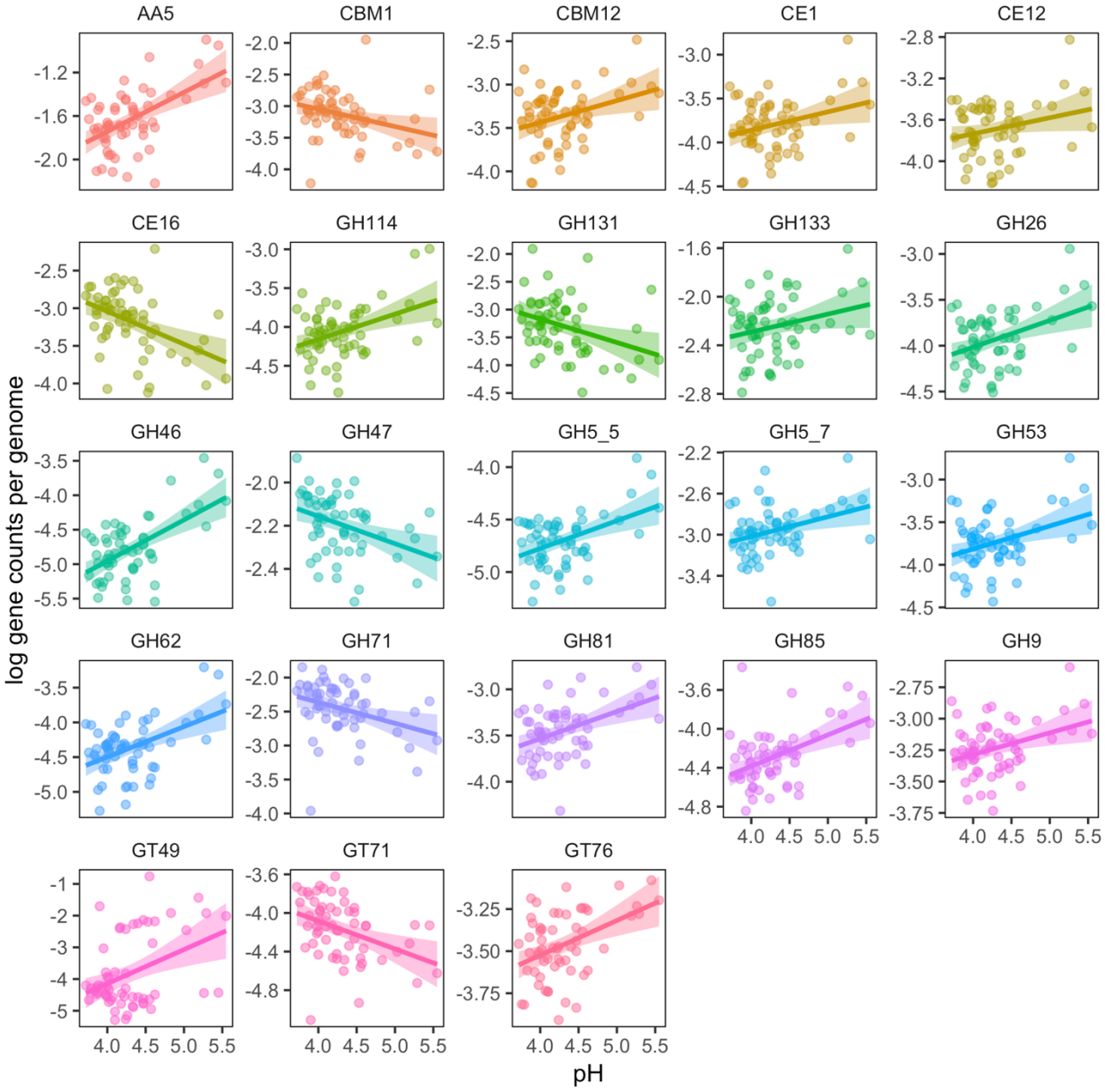

Supplementary Figure 3-8 Linear regressions of the individual 'indicator' gene families implicated using threshold indicator analysis to the pH gradient. Note log-scale of the y axis, that varies among panels.

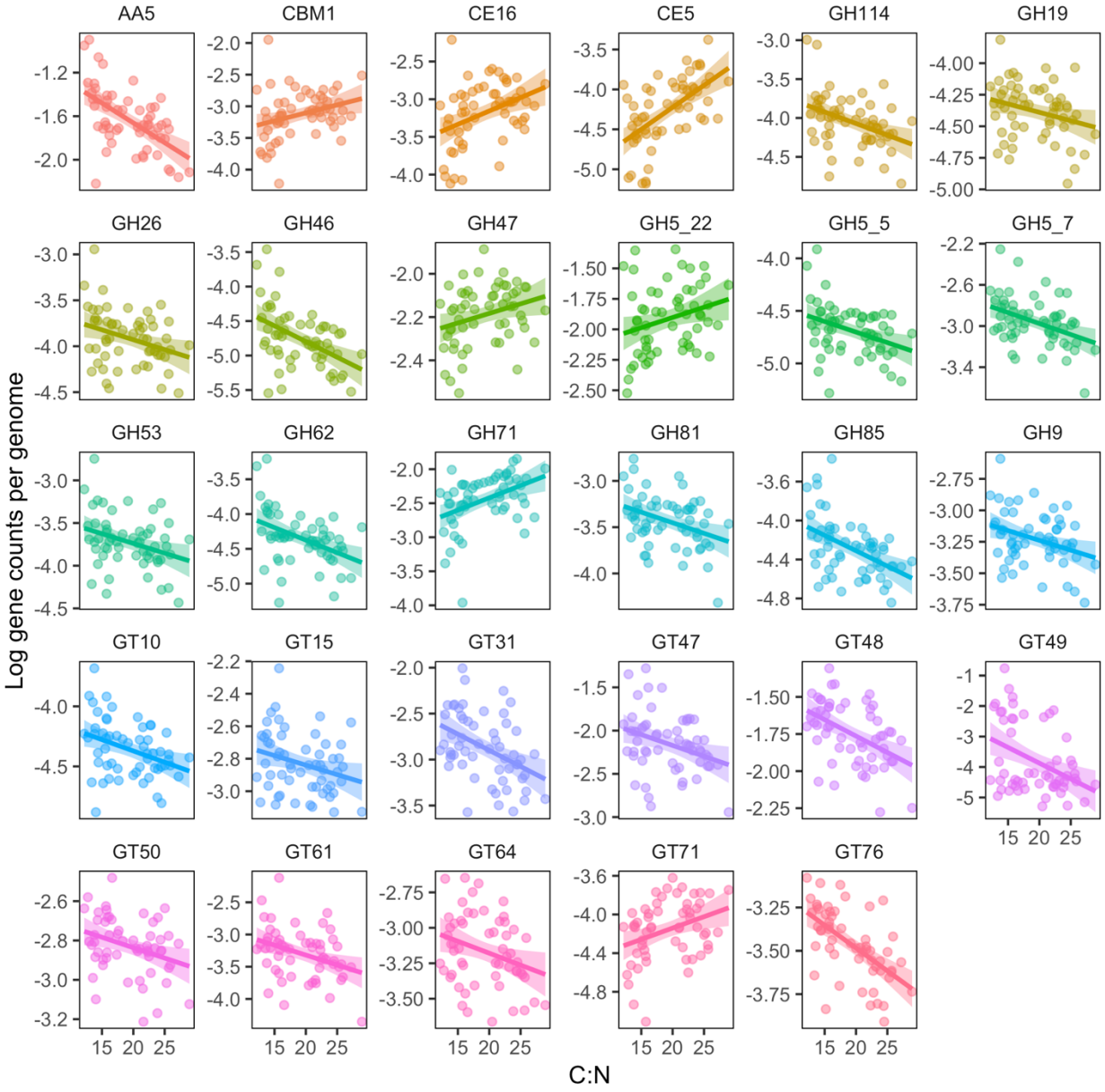

Supplementary Figure 3-9 Linear regressions of the individual 'indicator' gene families implicated using threshold indicator analysis to the C:N gradient. Note log-scale of the y axis, that varies among panels.

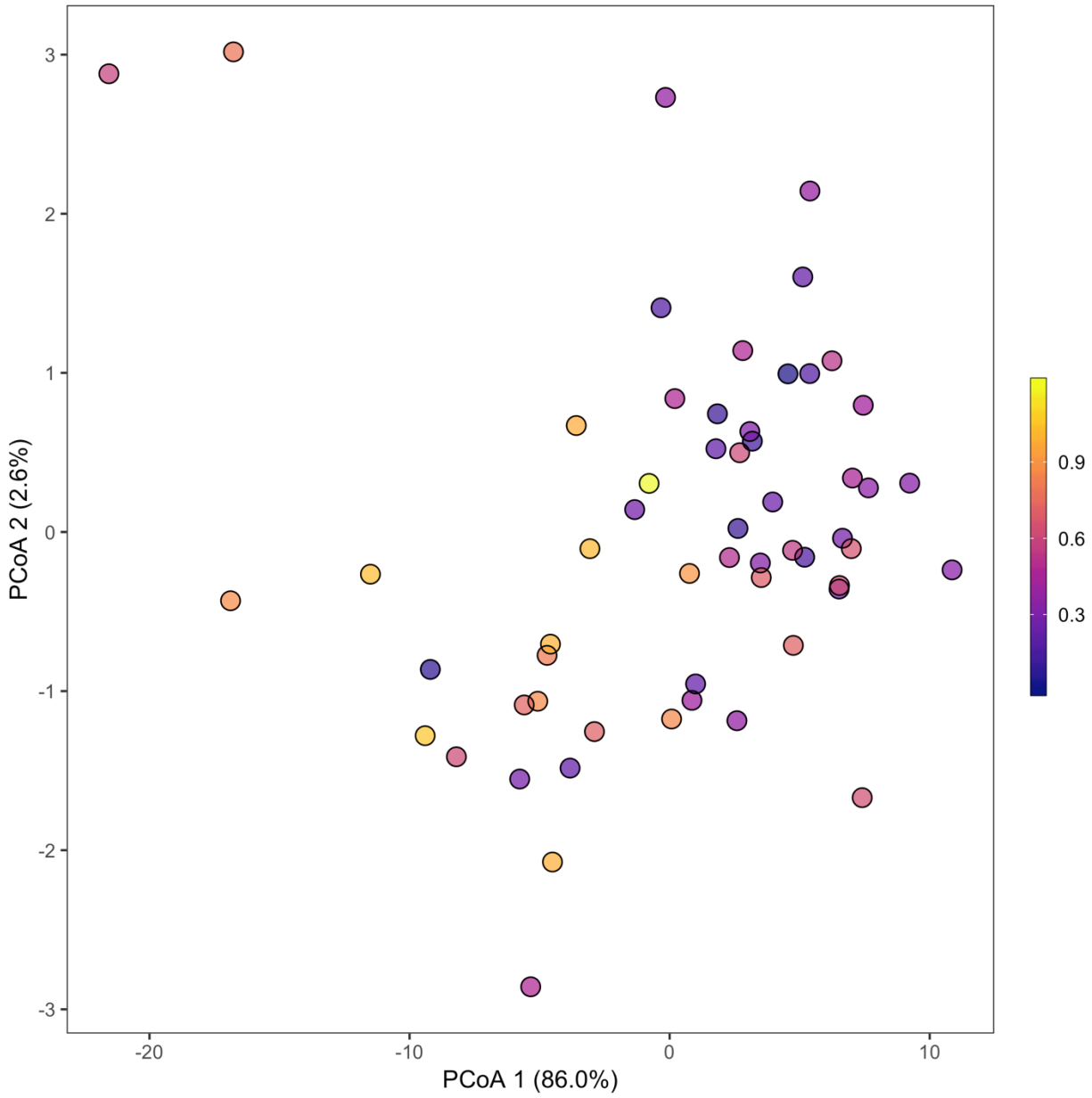

Supplementary Figure 3-10 Trees host ECM communities with heterogeneous decay capacity. PCoA depicting Euclidean distance matrices of single-copy log transformed gene counts, scaled by root-tip abundances per sample.

Chapter 4 Ectomycorrhizal Access To Organic N Enhances Plant Growth Response to Rising [CO_2]

Peter T. Pellitier, Inés Ibáñez, Donald R. Zak, William A. Argiroff, Kirk Acharya

Abstract:

Assimilation of nitrogen (N) bound in soil organic matter (N-SOM) may allow plants to short-circuit growth-limiting supplies of inorganic N, resulting in enhanced growth responses to elevated CO_2 (eCO_2). Plants rely upon symbiotic associations with ectomycorrhizal fungi (ECM) to meet their N requirements, however, assimilation of N-SOM and how that N may affect plant growth response to eCO_2 remains poorly understood. We studied tree growth in a mature temperate forest across a natural soil inorganic N gradient using dendrochronological measures of *Quercus rubra* and molecular characterization of ECM communities inhabiting individual trees. Historical increases in CO_2 (+70 μmol mol^{-1}: 1980-2017) stimulated tree growth in a context-dependent and threshold manner. Paradoxically, the largest relative growth response to CO_2 occurred in soils with low inorganic N supply; paired change-point analyses documented that tree growth in these soils was decoupled from soil inorganic N supply. This response is likely facilitated by the composition and function of ECM communities, because ECM associating with trees in low inorganic N soils were enriched in morphological traits associated with obtaining N-SOM. Together, these analyses suggest that the greatest contribution of N-SOM to plant growth occurs in soils where the supply of soil inorganic N is highly limiting, allowing for the largest relative growth response to eCO_2. Our analyses provide novel insight into the plant-fungal interactions that modulate plant N assimilation and suggest that the global fertilizing effect of eCO_2 on plant growth may be sensitive to an understudied N source, N-SOM.

Introduction

Net primary productivity (NPP) has been globally stimulated by rising anthropogenic [CO_2]

(Campbell et al. 2017) and coupled climate-biogeochemical (CCB) models suggest this effect could continue to ~2070 (Wenzel et al. 2016). This global biogeochemical feedback could determine the accumulation of anthropogenic CO_2 in the atmosphere (Arneth et al. 2010), however, current model projections of NPP under elevated CO_2 (eCO_2) vary widely, from +12 to 60% (Wenzel et al. 2016, Terrer et al. 2019). This discrepancy primarily arises from the manner in which soil nitrogen (N) availability is represented to constrain plant growth; for example, under strong N limitation, models in the current Coupled Model Intercomparison Project (CMIP5) project a modest growth response, whereas models with nearly unconstrained supplies of inorganic N project very high growth responses (Hungate 2003, Wieder et al. 2015, Terrer et al. 2016, 2019). Additional analyses further reveal that supply rates of inorganic N (*i.e.,* NH_4^+ & NO_3^-) are likely insufficient for a decadal and positive plant growth response to eCO_2 (Körner 2003, Reich et al. 2006, Wieder et al. 2015). As a result, the accurate prediction of future NPP, as well as the accumulation of CO_2 in the Earth's atmosphere, is contingent on a deeper understanding of the interplay between soil N availability and its role in constraining plant-growth response to eCO_2 (Zak et al. 2003, Norby and Zak 2011).

Nitrogen organically bound in soil organic matter (N-SOM), by far the largest pool of soil N, has been proposed as an overlooked N source that could allow plants to "short-circuit" limiting supply rates of inorganic N (Näsholm et al. 2009). Although N-SOM is not explicitly incorporated in existing CMIP5 or other CCB models, plant assimilation of N-SOM could provide plants with additional N that may enhance positive growth responses to eCO_2 (Terrer et al. 2016, 2018). Nevertheless, plant assimilation of N-SOM under natural field conditions remains largely unknown and represents a critical knowledge gap (Näsholm et al. 2009, Zak et al. 2019). Plant assimilation of N-SOM is dependent on the activity of ectomycorrhizal (ECM) fungal symbionts (Smith and Read 2010), which associate with ~60% of terrestrial plant stems, the majority of which are trees (Steidinger et al. 2019). Ectomycorrhizal fungi are the primary nutrient absorptive interface between roots and soil, provisioning hosts with the vast majority of their annual N requirements (Smith and Read 2010, Högberg et al. 2010, Koide and Fernandez 2018). ECM-associated plants are predicted to be particularly responsive to eCO_2, because they may be able to access additional growth-limiting N in SOM (Terrer et al. 2016, 2019). However, the extent to which ECM fungi obtain and transfer N-SOM to their plant host under field conditions remains unknown, as does the resultant impact of N-SOM acquisition on plant growth

response to eCO_2 (Zak et al. 2019). Accurate portrayals of plant growth response to eCO_2 is contingent on understanding the factors controlling plant assimilation of both inorganic and N-SOM.

As a result of their polyphyletic evolutionary history (Agerer 2001, Kohler et al. 2015, Pellitier and Zak 2018), ECM fungi vary in their capacity to access and provision their host with N-SOM (Abuzinadah and Read 1986, Hobbie and Högberg 2012). Integrating intrinsic variation among ECM taxa with principles of fungal community assembly (Koide et al. 2014, Bogar and Peay 2017) becomes essential for predicting ECM community function and plant assimilation of N-SOM. For example, ECM taxa vary widely in the hyphal foraging traits associated with organic and inorganic N acquisition (Agerer 2001, Hobbie and Agerer 2010).Therefore, the competitive advantage of particular hyphal morphologies may shift across gradients of inorganic N availability, potentially influencing their distribution in the landscape (Koide et al. 2014). Carbon (C) intensive hyphal morphologies, particularly rhizomorphic and medium- and long-distance extraradical 'exploration types', are associated with N uptake from organic sources, including N-SOM, and these morphological traits may be competitive in soils in which inorganic N is scarce (Hobbie 2006, Moeller et al. 2014, Defrenne et al. 2019). Conversely, in soils where inorganic N is relatively abundant, ECM taxa with metabolically inexpensive, "short" exploration hyphal types, may be dominant community members due to their capacity to maximize plant N return on a lower overall plant C investment (Lilleskov et al. 2002, Hortal et al. 2017, Defrenne et al. 2019). Crucially, if there are tradeoffs in ECM foraging strategies across soil N availability gradients, then plant assimilation of N-SOM may predominately occur in soils in which inorganic N is highly limiting (Read and Perez-Moreno 2003, Koide et al. 2014) (Fig 1). Consequentially, per unit of inorganic N available, trees inhabiting inorganic-N-poor soils may experience the largest relative growth enhancement from eCO_2 due to assimilation of N-SOM via ECM fungi (Fig. 1).

We employed an integrative set of analytical approaches to test key predictions linking ECM communities with plant uptake of N-SOM and their growth response to historical increases in atmospheric CO_2. We first tested if ECM communities occurring in soils where the supply of inorganic N was highly limiting were dominated by hyphal morphologies associated with uptake of N-SOM, and if these traits exhibited turnover across the gradient (Fig. 1). In a second independent analysis, we studied tree-rings to determine how plant growth is coupled with the

supply of inorganic N; we tested the prediction that N-SOM primarily contributes to plant growth when the supply of inorganic N is lowest and highly limiting (Fig. 1). Finally, we took advantage of live trees experiencing nearly four decades of steadily rising ambient [CO_2] to test if tree growth response to eCO_2 was greatest where inorganic N supply is low and putative uptake of N-SOM was high (Fig. 1). We tested these predictions using dendrochronological measures of northern red oak (*Quercus rubra* L.) paired with molecular characterization of ECM communities inhabiting individual trees, across a landscape-level gradient of inorganic N supply (Michigan, USA; Fig. S1). We used a series of change-point model analyses to facilitate co-interpretation of a diverse range of data to gain support of our key predictions (Fig. 1).

Materials and Methods

Study Sites

Twelve forest stands were identified in Manistee National Forest (Manistee and Wexford counties, Michigan, USA; Fig. S1). These soils span a natural soil fertility gradient that has been extensively characterized (Zak et al. 1986, Zak and Pregitzer 1990). Natural variation in nutrient cycling among stands derive from micro-site climatic differences in nutrient and water retention that have developed in the past ~10,000 yrs (Zak et al. 1986, Zak and Pregitzer 1990). Forest stands are even-aged, having all been uniformly harvested in the early 20th century.

Tree Core Sampling and Measurement

In May 2018, we collected two opposing tree-cores at DBH from five focal *Quercus rubra* in each of the 12 forest stands for a total of 60 compiled individual growth chronologies. We digitally measured yearly ring width (growth) and then cross-dated individuals to assemble growth chronologies. See *Supplementary Information* for further details.

Soil and Leaf Sampling

Five root cores were collected radially around the dripline of each study *Q. rubra* individual to a depth of 10 cm using a 144cm^2 soil punch (1440cm^3 root core volume). Five soil cores (5 cm diameter), were sampled as above and homogenized in the field. Root and soil cores were stored on ice. Senesced red oak leaves (Oi horizon) were collected from the forest floor in early May 2019, representing senesced leaves from the 2018 growing season. Full-sun green leaves were collected from the canopy of each study tree in August 2019 using a shotgun.

Soil and Plant properties

Homogenized soil cores were immediately sieved (2 mm) and processed for soil moisture and extractable inorganic NO_3^- and NH_4^+, using a 14-day aerobic N mineralization soil incubation followed by extraction with 2 M KCl (Zak and Pregitzer 1990); extracts were analyzed colorimsetrically both before and after the incubation (AQ2; Seal Analytical, Mequon, WI). Total C and N contents were determined using combustion analysis on a LECO TruMac CN analyzer (LECO Corporation, St. Joseph, MI, USA). Soil pH was determined using 2:1 deionized water and soil slurries. Senesced leaves (Oi horizon), and green leaves (~7 leaves each), were individually deveined, homogenized, dried at 60 °C and ground using a ball mill and analyzed for total N. Total free primary amines in soil solution were determined using unincubated soil KCl extracts according to (Darrouzet-Nardi et al. 2013), with leucine as an internal standard. See *Supplementary Information*.

Collection of Ectomycorrhizal Root Tips

Root cores, stored at 4° C for less than 12 days, were carefully washed in tap water to remove adhering soil and homogenized for each tree. Ectomycorrhizal root tips were excised using a dissecting microscope, after visually eliminating all non-*Quercus* roots. Definitive ectomycorrhizal tips on *Quercus rubra* were sampled after visual confirmation of ECM mantle and high turgor (63). Root-tip sampling was standardized by visually assessing the tips of at least 90% of all *Quercus* roots for each individual tree. Tips from each sample were placed in 2% cetyltrimethylammonium bromide (CTAB) buffer (Smith et al. 2011) and stored at -80 °C prior to DNA extraction.

DNA extraction and PCR

Lyophilized root-tips were homogenized and each root-tip sample was split into 20-25 mg subsamples for extraction. DNA was extracted using the Qiagen DNeasy Plant Mini Kit following manufacturers protocol; subsamples were pooled. The ITS2 region was amplified using Illumina dual-indexed primers 5.8S Fun and ITS4 Fun (Taylor et al. 2016). All PCR was performed in triplicate following (Taylor et al. 2016). Replicate PCR products were pooled and equimolar concentrations were sequenced using a full run of Illumina MiSeq (2 × 250 bp). Raw reads will be available upon acceptance. See *Supplementary Information.*

Bioinformatic Processing and Identification of Fungi

22,606,578 quality raw sequences were demultiplexed and assigned to individual samples. Reverse reads were of insufficient quality for read-joining and were discarded. The DADA2

pipeline was implemented to trim, denoise, detect chimeras, remove PhiX contaminants, and infer absolute sequence variants (ASV) (Callahan et al. 2016). A total of 6,869,462 filtered sequences (mean = 5.64 x 10^5, *SD*= 1.39 x 10^5 sequences per sample) were then assigned to operational taxonomic units (OTU) using the dynamic (97-99% sequence similarity) UNITE database (v.8.0)(Nilsson et al. 2019). Non-singleton OTUs were retained. All sequence processing was performed using QIIME v. 4.2019 (Bokulich et al. 2018, Bolyen et al. 2019). Non-ectomycorrhizal fungal genera were excluded from the analysis using literature searches. The DEEMY (characterization and DEtermination of EctoMYcorrhizae) database (www.deemy.de) was used to gather trait information on the exploration type (*i.e.,* hyphal foraging distance) and rhizomorph formation of ECM fungal species (OTU) present at more than 0.05% relative abundance in the dataset. See *Supplementary Information*.

Statistical Analysis of Soil and Plant Properties and Fungal Communities

Net N mineralization rates were calculated by averaging technical replicates, summing the concentrations of NO_3^- and NH_4^+ prior to and following incubation; net N mineralization was the difference between these values (Zak and Pregitzer 1990). Leaf N translocation was calculated as the difference between green leaf N and senesced leaf N (Oi horizon) for individual trees. To test how the abiotic elements of soil affected the composition of the ECM fungal community, we fitted generalized linear models (GLMs) with the "manyglm" function in mvabund version 4.0.1 (Wang et al. 2012). This analysis was carried out with ectomycorrhizal OTUs only. All abiotic parameters (pH, soil N, C:N, inorganic N availability) were included in the model without interaction components (Cuellar-Gempeler and Leibold 2019) and model residuals checked. The effect of predictor variables was quantified using likelihood-ratio tests (ANOVA, pit trap resampling, 1000 bootstraps) with Bonferonni correction with the 'summary.manyglm' command. Canonical correspondence analysis (CCA) was used to visualize the variation (inertia) explained by the statistically significant soil abiotic attributes using Hellinger-transformed species abundance matrices at the OTU level. We emphasize that the CCA serves as a visualization of the statistically corroborated GLM results (Bálint et al. 2015). Threshold Indicator Analysis was used to detect ECM community level threshold responses – community change points – along the continuous soil N mineralization gradient, using the TITAN2 package (Baker and King 2010) This analysis was conducted with ECM fungi grouped at the genus level that occurred in more than five samples at least five times (Baker and King 2010). We identified

the ECM community change points as the peaks in the cumulative distributions of the negative and positive-z values, using both pure and reliable taxa. Analyses were conducted using R. 3.5.3. See *Supplementary Information*.

Analysis of BAI response to N mineralization rates

Average annual tree radial growth and diameter at breast height (DBH) at the time of sampling were combined to calculate past DBH by subtracting radial growth each year to the previous year's DBH. We then calculated annual tree basal area (BA), $BA=\pi(DBH/2)^2$ and basal area increments (BAI; cm^2/y). BAIs were estimated for each tree (*i*) and year (*y*) as the difference in BA between two consecutive years: $BAI_{i,y}= BA_{i,y} - BA_{i,y-1}$. Fifty four trees yielded high quality BAI estimates. We also accounted for the relationship between tree size (DBH) and growth by including DBH in the analysis of BAI (detrending). Furthermore, because tree growth at any particular year may also be affected by lag effects (growth in previous years) (Peltier and Ibáñez 2015, Ibáñez et al. 2018), we explored how many years back previous growth could have affected current growth, and a lag of one showed the best relationship. We then included BAI of the previous year (as tree level standardized growth, BAIs) in the analysis. To also account for year to year variability in tree growth we included year random effects (YRE). For any particular tree *i* and year *y* BAI analysis likelihood and process models were:

$$BAI_{i,y} \sim logNormal(B_{i,y}, \sigma^2_{i,y})$$

$$B_{i,y} = \alpha_0 + (\alpha_1 + J_i\alpha_2) \cdot Nminer_i + \alpha_3 \cdot \ln(DBH_{i,y}) + \alpha_4 \cdot BAIS_{i,y-1} + YRE_y$$

$$\sigma^2_{i,y} = a + b \cdot ln(DBH_{i,y})$$

We followed a Bayesian approach to estimate parameters. Parameter *J* is an indicator, with value 0 before the change point, and value 1 after. This change point parameter was estimated as: $Change\ point \sim Uniform(0,1.25)$, allowing the change point to fall outside the range of N mineralization sampled (0.06-1.19 μg g^{-1} d^{-1}). Variability around growth estimates (σ_2) was estimated as a function of DBH, since this seems to vary with size (Lines et al. 2012). The rest of the parameters were estimated from non-informative prior distributions, $a \sim logNormal(1,1000), \alpha_*, b \sim Normal(0,10000)$, $YRE_y \sim Normal(0, \sigma^2_{YRE})$,$1/\sigma^2_{YRE} \sim Gamma(0.0001,0.0001)$.

Analysis of BAI response to atmospheric CO_2

We first calculated an index of growth nitrogen efficiency, GNE. This index was estimated for each tree (i) and year (y) as:

$$GNE_{i,y} = \frac{BAI_{i,y}}{Nminr_{\cdot i}}.$$

To easily compare temporal trends in GNE across trees we standardized GNE:

$$(GNES_{i,y} = (GNE_{i,y} - \overline{GNE_i})/SD_{GNEi}$$

We analyzed the past 38 years of growth (1980-2017) for the 54 focal trees to include all trees we had BAI data. We then analyzed GNES as a function of annual atmospheric CO_2 (obtained from NOAA 2019) and year random effects (YRE; to account for year to year variability in environmental conditions other than CO_2). For each tree *i* and year *y*:

$$GNES_{i,y} \sim Normal(G_{i,y}, \sigma_i^2)$$

$$G_{i,y} = \beta_i + \lambda_i \cdot CO_{2_y} + YRE_y$$

We then analyzed the effect of CO_2, slope parameters λ (mean and variance), as a function of N mineralization rate using again a change point analysis. We tried several analyses, including exponential decay and logarithmic functions, and change point analysis with two different intercepts. The best model fitting the data, based on Deviance Inference Criterion (DIC)(Spiegelhalter et al. 2002), was a simple change point analysis. For each tree *i*:

$$\lambda_i \sim Normal(L_i, \sigma_\lambda^2)$$

$$L_i = \theta_0 + (\theta_1 + J_i \cdot \theta_2) \cdot miner_i$$

Parameter *J* is an indicator, with value 0 before the change point, and value 1 after. This change point parameter was estimated as: $Change\ point \sim Uniform(0,1.25)$. Remaining parameters were estimated from non-informative prior distributions,

$$\beta_*, \theta_* \sim Normal(0,10000), YRE_y \sim Normal(0, \sigma_{YRE}^2)\ , 1/\sigma_{YRE}^2 \sim Gamma(0.0001,0.0001).$$

See supplement for additional information and all analysis code.

Results

We reconfirmed the presence of a natural gradient of soil inorganic N availability in a late-successional temperate hardwood forest using a laboratory incubation assay of net N mineralization rates (Zak and Pregitzer 1990) (Fig. S2). Soil was collected below the canopy of 60 focal adult northern red oak trees and supply of soil inorganic N ranged from 0.06 to 1.2 μg N g^{-1} d^{-1} across uniformly sandy soils, Typic Haplorthods (Zak and Pregitzer 1990). This natural

gradient is temporally stable across the duration of the growing season (Pearson r = 0.77; Fig. S2), across years (Argiroff *et al.,* unpublished), and several decades (Zak et al. 1986, Zak and Pregitzer 1990). All trees sampled were uniformly even-aged, because all stands were destructively harvested in the early 1900's. Among these trees, green leaf N content was positively correlated with soil inorganic N availability (R^2_{adj} = 0.36; P <0.01), whereas the amount of N translocated prior to leaf senescence did not significantly vary (P > 0.05; Fig. S3-4). Critically, volumetric water content (P > 0.6), soil C (P >0.6) and texture (Zak and Pregitzer 1990) were not correlated with soil inorganic N availability (Fig. S5-6).

Ectomycorrhizal community composition and morphology

14,944 individual ECM root-tips were collected from 60 oak root-systems, and molecular analyses detected a total of 179 ECM operational taxonomic units (OTU; mean= 27 OTU per tree, SE = 0.95, Fig S7). Rates of net N mineralization were negatively correlated with the number of ECM root-tips encountered on each root system (R^2_{adj} = 0.18, $P < 0.001$, mean= 264.8, SD = 131.9; Fig. S8), and their overall biomass (R^2_{adj} = 0.08, $P < 0.01$, mean=19.6 mg, SD = 11.5; Fig. S9). There was significant turnover in the composition of ECM communities across the soil gradient (Figure 2A). Inorganic N poor soils were dominated by the genera *Cortinarius, Russula*, *Amanita* and *Cenoccocum*; whereas *Hebeloma* and *Tomentella*, were strongly associated with high rates of inorganic N supply (Figure 2A). Threshold indicator analysis was used to identify conditions along the inorganic N supply gradient where ECM communities exhibit the largest turnover in composition (Baker and King 2010). ECM genera that responded negatively to inorganic N availability exhibited the greatest compositional turnover at 0.47 $\mu g\ g^{-1}\ d^{-1}$ (95%CI: 0.41-0.68), whereas those that responded positively showed the largest change point at 0.45 $\mu g\ g^{-1}\ d^{-1}$ (95% CI: 0.36-0.87; Fig. S10-11) (Baker and King 2010). Rhizomorph presence and the degree of extraradical emanating hyphae (exploration types) are ECM root-tip hyphal traits broadly associated with N nutrient foraging strategies (Moeller et al. 2014, Defrenne et al. 2019). We detected a significant interaction-effect between ECM N foraging strategies and their relative sequence abundance, both above and below the soil N availability threshold (ANOVA). This threshold was identified by averaging the two threshold values for ECM community-subsets that responded positively and negatively to inorganic N supply (see above). There were significantly more medium-distance hyphal exploration types

($F_{1,110}$ = 10.94, P <0.001) and rhizomorphic hyphae ($F_{1,110}$ = 8.66, P < 0.01) associated with organic N uptake below the mineralization threshold than above it (Fig. 2B,C).

Tree Growth Response to Inorganic N

We used a change point analysis (Chen and Gupta 2011) within a Bayesian modeling approach to study the effect of inorganic N supplies on yearly plant growth. We asserted that if plant growth is primarily constrained by inorganic N availability (Thomas et al. 2010), we can predict a consistent decrease in growth along a declining gradient of net N mineralization (blue line, Fig. 3A). However, if plant growth in soils with a low supply of inorganic N was supplemented with N-SOM, the slope of this relationship may change (Fig. 3B red line), thereby decoupling observed growth rates from the supply of inorganic N (*i.e.,* net N mineralization).

Basal area increment (i.e., annual circumference growth; BAI) was analyzed as a function of net N mineralization rates, tree size (to detrend size-age effects), growth the year before (to account for lag effects) and as a function of a yearly random effect (to reflect year to year environmental variability; see *Methods;* Fig. S12). Fifty-four trees yielded usable tree-ring data that could be cross-dated (see *Methods*). We detected a change point in plant growth (BAI) at 0.445 ± 0.011 μg g^{-1} d^{-1} (mean ± SD; Fig. 3B). The slope of the relationship between BAI and N mineralization was not significantly different from zero to the left of the change point (Fig. 1C), suggesting that inorganic N was a poor predictor of BAI in soils when inorganic N is in low supply. To the right of the change point, this slope was positive and significantly different from zero (Fig. 1C). Finally, our analyses indicated that these slope values differed (95%CI do not overlap; Fig. 2C).

Plant response to historic rise in CO_2

Thirty-eight years of ring data were used to estimate the response of plant growth (BAI) to increasing ambient concentrations of CO_2. During the sampled growth period (1980-2017), atmospheric CO_2 increased by ~70 μmol mol^{-1} (www.NOAA.gov), serving as a natural gradient of increasing atmospheric [CO_2]. Annual estimates of growth nitrogen efficiencies (GNE) for each tree, $GNE = \frac{BAI}{N\ mineralization}$, were analyzed, after being standardized as a function of yearly atmospheric [CO_2] (Fig. 3A,D; see *Methods;* Fig S12). Slope parameters λ (i.e., eCO_2 effect) for individual trees were then analyzed as a function of net N mineralization (Fig. 3B,E). Our model detected that the relationship between tree growth and the effect of CO_2 changed along the N mineralization gradient at 0.476 ± 0.0002 μg g^{-1} d^{-1} (Fig. 4E). Trees growing in soils below the

change point responded more strongly to rising historic CO_2 concentrations than did trees above it. We found that the slope parameters (θ), to the left and right of the change point were statistically significant and different from one another (Fig. 3F). This independently calculated change-point was remarkably congruent with that detected for BAI and inorganic N availability, as well as the ECM community threshold analysis. All parameter values and analysis code are presented in the *Supplemental Materials.*

Discussion

Here, we document how historical increases in CO_2 have stimulated plant growth in a context-dependent and threshold manner. Notably, our results suggest that plant assimilation of N-SOM augments plant capacity to respond to eCO_2. Coupled analyses of plant growth and ECM community turnover suggest that assimilation of N-SOM is facilitated by specialized ECM communities with medium-distance and rhizomorphic N foraging morphologies. Local site conditions and mutualistic interactions appear to facilitate the assimilation of N-SOM which in turn, mediates plant response to eCO_2.

Our results support the prediction that N-SOM contributes to tree growth when the supply of inorganic N is highly limiting (Read and Perez-Moreno 2003, Koide et al. 2014). *Quercus rubra* growth displayed a stark and highly significant threshold response to inorganic N availability at 0.445μg g^{-1} d^{-1}, and below this threshold, tree growth was decoupled from supply rates of inorganic N. Remarkably, TITAN analysis indicated that ECM communities exhibited the largest compositional turnover at near identical supplies of inorganic N (0.45 and 0.47μg g^{-1} d^{-1}). This compositional shift was associated with turnover in the relative abundance of ECM traits associated with inorganic and N-SOM acquisition. The synchronized response of both plant growth and ECM communities suggests that plant-fungal interactions are modulated by soil conditions which impacts plant access and uptake of both organic and inorganic N forms.

The steep decline in the number of ECM root-tips and their overall biomass on individual tree root-systems across the inorganic N gradient, is broadly consistent with predictions of optimal resource (C) allocation belowground to meet nutrient (N) demand (18,24,39). Indeed, heterogeneous belowground C allocation may impact ECM competition dynamics and community assembly processes (25,40). The strong plant growth response to inorganic N availability to the right of the change point, coupled with the dominance of short-distance and

non-rhizomorphic morphologies comprising less overall fungal biomass, suggests that trees allocate less photosynthate to their ECM mutualists in conditions where inorganic N is plentiful. In contrast, trees allocate more photosynthate to ECM mutualists under conditions where inorganic N is scarce; under these conditions, trees can support ECM taxa with hyphal morphologies that can obtain N-SOM. Our results also offer mechanistic insight for previous findings documenting intra-specific plant specialization on biochemically distinct N forms across soil N availability gradients (Kielland 1994, Nordin et al. 2004, Houlton et al. 2007). Functional redundancy across ECM communities may not be as common as presupposed; instead, coupled compositional and functional changes in ECM communities may drive intra-specific plant flexibility in nutrient assimilation (Kielland 1994, Nordin et al. 2004, Houlton et al. 2007). Taken together, we challenge the paradigm that all plants associating with ECM fungi can gain access to organic N (Averill et al. 2014, Terrer et al. 2016, 2019). Moreover, we argue that improving model representation of plant response to eCO_2 can only be achieved by carefully representing variability in the impact of the ECM symbiosis on plant assimilation of N-SOM (4,45).

NPP in temperate forests is predicted to increase under eCO_2 (Terrer et al. 2019). Here, we provide one of the first natural field tests using dendrochronological insight that both supports and challenges this prediction (Graybill and Idso 1993). Since 1980, atmospheric CO_2 concentrations have risen, ~70 μmol mol^{-1}. During this time, trees growing in soils where inorganic N supplies were below the 0.476 μg g^{-1} d^{-1} threshold displayed a significantly greater growth response to eCO_2 concentrations, per unit of available inorganic N, than those above the threshold (Fig. 4F). This model-independent change-point estimate for the effect of eCO_2 on historic plant growth is remarkably congruent with that detected for tree growth and soil inorganic N availability (Fig 3B). Coupled with observations of turnover in the composition and putative physiology of ECM communities along the inorganic N gradient, we attribute these parallel growth responses as strong evidence for the threshold and asymmetric contribution of N-SOM to plant growth and response to eCO_2.

As one of the first studies to consider organic N assimilation and plant response to eCO_2, our results add nuance to predictions stating that the natural supply of inorganic N is insufficient to engender a decadal and positive NPP effect (Reich et al. 2006, Wieder et al. 2015). Plant growth in soils where the natural supply of inorganic N is relatively high displayed neutral to

weakly positive responses to eCO_2; paradoxically, for trees with relatively high existing growth rates, incremental growth responses to eCO_2 may be unable to accrue due to insufficient inorganic N supply (Luo et al. 2004). This result is consistent with evidence from Free Air CO_2 Enrichment (FACE) experiments that document relatively neutral eCO_2 growth responses across studies, unless additional N is artificially added (Oren et al. 2001, Norby and Zak 2011). In contrast, we found that trees growing in inorganic N poor soils may be stimulated by eCO_2 if they can short-circuit rates of net N mineralization by obtaining N-SOM via ECM symbionts. This positive and sustained net response to eCO_2 occurred primarily for a subset of the trees studied here, particularly individuals with the smallest initial BAI. Although, our results stand in contrast to other tree-ring studies that were unable to detect an effect of CO_2 on historic plant growth (Tognetti et al. 2000, Gedalof and Berg 2010, van der Sleen et al. 2015, Hararuk et al. 2019, Giguère-Croteau et al. 2019), our use of a natural soil fertility gradient, appears to have enhanced our capacity to disentangle the role of inorganic N and N-SOM in plant growth response to eCO_2.

Based on our assessment of soil water content, texture and SOM content, these factors do not account for the detected variation in plant growth response across the gradient. Moreover, previous studies in our study system documented that free-living and symbiotic N fixation are unlikely to provide additional sources of inorganic N that we did not measure (Host and Pregitzer 1992). Further, it is unlikely that greater N-use efficiency could explain the enhanced growth rate we detected in low inorganic N soil; leaf N translocation is a robust proxy for N-use efficiency (Vitousek 1982, Killingbeck 1996) and it did not vary significantly across the gradient (*Supplementary Materials*). FACE studies also find that enhanced N-use efficiency cannot result in a positive response to eCO_2 (Finzi et al. 2007, Walker et al. 2019). The specific biochemical compounds present in N-SOM potentially obtained by ECM fungi and available for plant growth remains an area for further study (Näsholm et al. 2009, Zak et al. 2019). However, differential assimilation of free primary amines from soil solution appears unlikely to produce the divergent plant growth patterns (Fig. S13; *Supplementary Material*), suggesting N-SOM as the primary source of organic N.

We hypothesize that the relative differences detected among fungal communities and coupled soil characteristics have remained temporally stable over several decades, and that our analyses provide representative insight into the complex array of interactions that have generated

divergent growth responses of *Q. rubra* to eCO_2 over the past 38 years. Over the study period, no significant disturbances have altered stand structure or composition (D.R. Zak *pers observation*), and prior data suggests that the underlying soil inorganic N availability gradient studied here has not changed over the past 35 years (Zak and Pregitzer 1990). Available molecular data from a subset of these study sites also suggests that ECM communities have remained compositionally stable over time (Edwards and Zak 2010). By standardizing several well-known variables which can structure ECM communities, host identity, age, soil physical properties (*i.e.,* texture), and soil water availability (Sterkenburg et al. 2015, van der Linde et al. 2018), our study disentangles how plant response to local soil properties (*i.e.,* inorganic N) may act as a complex environmental filter that drives heterogeneity in the membership and function of associated ECM communities. It is unlikely that dispersal limitation or other stochastic processes acting alone can generate the patterns in ECM community composition we have documented and there is little autocorrelative spatial structure among stands distributed along the inorganic N availability gradient (Zak and Pregitzer 1990). Moreover, most of the ECM taxa encountered in our study produce basidiocarps (mushrooms) which can produce spores that can travel across the breadth of the study area (Golan and Pringle 2017).

The general importance and occurrence of plant assimilation of N-SOM across ecosystems, and the role of N-SOM in plant growth response to eCO_2 remains unknown, but represents a critical area of future research. Recent quantitative global maps of the distribution of ECM plant hosts, and soil N limitation could potentially allow for spatially explicit representations of plant-growth response to eCO_2 (Steidinger et al. 2019, Du et al. 2020). Fulfilling this promise will require greater understanding of plant-fungal interactions across soil conditions, specifically the extent to which ECM symbionts provide host plants with N-SOM. The accurate representation of plant growth response to eCO_2 and the terrestrial C sink in coupled climate biogeochemical models appears to be contingent on incorporating this previously unrecognized ecological dynamic.

Works Cited

Abuzinadah, R. A., and D. J. Read. 1986. The Role of Proteins in the Nitrogen Nutrition of Ectomycorrhizal Plants. New Phytologist 103:481–493.

Agerer, R. 2001. Exploration types of ectomycorrhizae. Mycorrhiza 11:107–114.

Arneth, A., S. P. Harrison, S. Zaehle, K. Tsigaridis, S. Menon, P. J. Bartlein, J. Feichter, A. Korhola, M. Kulmala, D. O'Donnell, G. Schurgers, S. Sorvari, and T. Vesala. 2010. Terrestrial biogeochemical feedbacks in the climate system. Nature Geoscience 3:525–532.

Averill, C., B. L. Turner, and A. C. Finzi. 2014. Mycorrhiza-mediated competition between plants and decomposers drives soil carbon storage. Nature 505:543–545.

Baker, M. E., and R. S. King. 2010. A new method for detecting and interpreting biodiversity and ecological community thresholds. Methods in Ecology and Evolution 1:25–37.

Bálint, M., L. Bartha, R. B. O'Hara, M. S. Olson, J. Otte, M. Pfenninger, A. L. Robertson, P. Tiffin, and I. Schmitt. 2015. Relocation, high-latitude warming and host genetic identity shape the foliar fungal microbiome of poplars. Molecular Ecology 24:235–248.

Bloom, A. J., F. S. Chapin, and H. A. Mooney. 1985. Resource Limitation in Plants-An Economic Analogy. Annual Review of Ecology and Systematics 16:363–392.

Bogar, L., and K. Peay. 2017. Processes Maintaining the Coexistence of Ectomycorrhizal Fungi at a Fine Spatial Scale. Pages 79–105 *in* L. Tedersoo, editor. Biogeography of Mycorrhizal Symbiosis. Springer.

Bokulich, N. A., M. R. Dillon, E. Bolyen, B. D. Kaehler, G. A. Huttley, and J. G. Caporaso. 2018. q2-sample-classifier: machine-learning tools for microbiome classification and regression. Journal of open research software 3.

Bolyen, E., J. R. Rideout, M. R. Dillon, N. A. Bokulich, C. C. Abnet, G. A. Al-Ghalith, H. Alexander, E. J. Alm, M. Arumugam, F. Asnicar, Y. Bai, J. E. Bisanz, K. Bittinger, A. Brejnrod, C. J. Brislawn, C. T. Brown, B. J. Callahan, A. M. Caraballo-Rodríguez, J. Chase, E. K. Cope, R. Da Silva, C. Diener, P. C. Dorrestein, G. M. Douglas, D. M. Durall, C. Duvallet, C. F. Edwardson, M. Ernst, M. Estaki, J. Fouquier, J. M. Gauglitz, S. M. Gibbons, D. L. Gibson, A. Gonzalez, K. Gorlick, J. Guo, B. Hillmann, S. Holmes, H. Holste, C. Huttenhower, G. A. Huttley, S. Janssen, A. K. Jarmusch, L. Jiang, B. D. Kaehler, K. B. Kang, C. R. Keefe, P. Keim, S. T. Kelley, D. Knights, I. Koester, T. Kosciolek, J. Kreps, M. G. I. Langille, J. Lee, R. Ley, Y.-X. Liu, E. Loftfield, C. Lozupone, M. Maher, C. Marotz, B. D. Martin, D. McDonald, L. J. McIver, A. V. Melnik, J. L. Metcalf, S. C. Morgan, J. T. Morton, A. T. Naimey, J. A. Navas-Molina, L. F. Nothias, S. B. Orchanian, T. Pearson, S. L. Peoples, D. Petras, M. L. Preuss, E. Pruesse, L. B. Rasmussen, A. Rivers, M. S. Robeson, P. Rosenthal, N. Segata, M. Shaffer, A. Shiffer, R. Sinha, S. J. Song, J. R. Spear, A. D. Swafford, L. R. Thompson, P. J. Torres, P. Trinh, A. Tripathi, P. J. Turnbaugh, S. Ul-Hasan, J. J. J. van der Hooft, F. Vargas, Y. Vázquez-Baeza, E. Vogtmann, M. von Hippel, W. Walters, Y. Wan, M. Wang, J. Warren, K. C. Weber, C. H. D. Williamson, A. D. Willis, Z. Z. Xu, J. R. Zaneveld, Y. Zhang, Q. Zhu, R. Knight, and J. G. Caporaso. 2019. Reproducible, interactive, scalable and extensible microbiome data science using QIIME 2. Nature Biotechnology 37:852–857.

Callahan, B. J., P. J. McMurdie, M. J. Rosen, A. W. Han, A. J. A. Johnson, and S. P. Holmes. 2016. DADA2: High-resolution sample inference from Illumina amplicon data. Nature Methods 13:581–583.

Campbell, J. E., J. A. Berry, U. Seibt, S. J. Smith, S. A. Montzka, T. Launois, S. Belviso, L. Bopp, and M. Laine. 2017. Large historical growth in global terrestrial gross primary production. Nature 544:84–87.

Chen, J., and A. K. Gupta. 2011. Parametric Statistical Change Point Analysis: With Applications to Genetics, Medicine, and Finance. Springer Science & Business Media.

Crowther, T. W., J. van den Hoogen, J. Wan, M. A. Mayes, A. D. Keiser, L. Mo, C. Averill, and D. S. Maynard. 2019. The global soil community and its influence on biogeochemistry. Science 365:eaav0550.

Cuellar-Gempeler, C., and M. A. Leibold. 2019. Key colonist pools and habitat filters mediate the composition of fiddler crab–associated bacterial communities. Ecology 100:e02628.

Darrouzet-Nardi, A., M. P. Ladd, and M. N. Weintraub. 2013. Fluorescent microplate analysis of amino acids and other primary amines in soils. Soil Biology and Biochemistry 57:78–82.

Defrenne, C. E., T. J. Philpott, S. H. A. Guichon, W. J. Roach, B. J. Pickles, and S. W. Simard. 2019. Shifts in Ectomycorrhizal Fungal Communities and Exploration Types Relate to the Environment and Fine-Root Traits Across Interior Douglas-Fir Forests of Western Canada. Frontiers in Plant Science 10:643.

Du, E., C. Terrer, A. F. A. Pellegrini, A. Ahlström, C. J. van Lissa, X. Zhao, N. Xia, X. Wu, and R. B. Jackson. 2020. Global patterns of terrestrial nitrogen and phosphorus limitation. Nature Geoscience.

Edwards, I. P., and D. R. Zak. 2010. Phylogenetic similarity and structure of Agaricomycotina communities across a forested landscape. Molecular Ecology 19:1469–1482.

Finzi, A. C., R. J. Norby, C. Calfapietra, A. Gallet-Budynek, B. Gielen, W. E. Holmes, M. R. Hoosbeek, C. M. Iversen, R. B. Jackson, M. E. Kubiske, J. Ledford, M. Liberloo, R. Oren, A. Polle, S. Pritchard, D. R. Zak, W. H. Schlesinger, and R. Ceulemans. 2007. Increases in nitrogen uptake rather than nitrogen-use efficiency support higher rates of temperate forest productivity under elevated CO2. Proceedings of the National Academy of Sciences 104:14014–14019.

Gedalof, Z., and A. A. Berg. 2010. Tree ring evidence for limited direct CO2 fertilization of forests over the 20th century. Global Biogeochemical Cycles 24.

Giguère-Croteau, C., É. Boucher, Y. Bergeron, M. P. Girardin, I. Drobyshev, L. C. R. Silva, J.-F. Hélie, and M. Garneau. 2019. North America's oldest boreal trees are more efficient water users due to increased [CO_2], but do not grow faster. Proceedings of the National Academy of Sciences 116:2749–2754.

Golan, J. J., and A. Pringle. 2017. Long-Distance Dispersal of Fungi. Microbiology Spectrum 5:24.

Graybill, D. A., and S. B. Idso. 1993. Detecting the aerial fertilization effect of atmospheric CO2 enrichment in tree-ring chronologies. Global Biogeochemical Cycles 7:81–95.

Hararuk, O., E. M. Campbell, J. A. Antos, and R. Parish. 2019. Tree rings provide no evidence of a CO2 fertilization effect in old-growth subalpine forests of western Canada. Global Change Biology 25:1222–1234.

Hobbie, E. A. 2006. Carbon Allocation to Ectomycorrhizal Fungi Correlates with Belowground Allocation in Culture Studies. Ecology 87:563–569.

Hobbie, E. A., and R. Agerer. 2010. Nitrogen isotopes in ectomycorrhizal sporocarps correspond to belowground exploration types. Plant and Soil 327:71–83.
Hobbie, E. A., and P. Högberg. 2012. Nitrogen isotopes link mycorrhizal fungi and plants to nitrogen dynamics. New Phytologist 196:367–382.
Högberg, M. N., M. J. I. Briones, S. G. Keel, D. B. Metcalfe, C. Campbell, A. J. Midwood, B. Thornton, V. Hurry, S. Linder, T. Näsholm, and P. Högberg. 2010. Quantification of effects of season and nitrogen supply on tree below-ground carbon transfer to ectomycorrhizal fungi and other soil organisms in a boreal pine forest. New Phytologist 187:485–493.
Hortal, S., K. L. Plett, J. M. Plett, T. Cresswell, M. Johansen, E. Pendall, and I. C. Anderson. 2017. Role of plant–fungal nutrient trading and host control in determining the competitive success of ectomycorrhizal fungi. The ISME Journal 11:2666–2676.
Host, G. E., and K. S. Pregitzer. 1992. Geomorphic influences on ground-flora and overstory composition in upland forests of northwestern lower Michigan. Canadian Journal of Forest Research 22:1547–1555.
Houlton, B. Z., D. M. Sigman, E. A. G. Schuur, and L. O. Hedin. 2007. A climate-driven switch in plant nitrogen acquisition within tropical forest communities. Proceedings of the National Academy of Sciences 104:8902–8906.
Hungate, B. A. 2003. Nitrogen and Climate Change. Science 302:1513–1514.
Ibáñez, I., D. R. Zak, A. J. Burton, and K. S. Pregitzer. 2018. Anthropogenic nitrogen deposition ameliorates the decline in tree growth caused by a drier climate. Ecology 99:411–420.
Kielland, K. 1994. Amino Acid Absorption by Arctic Plants: Implications for Plant Nutrition and Nitrogen Cycling. Ecology 75:2373–2383.
Killingbeck, K. T. 1996. Nutrients in Senesced Leaves: Keys to the Search for Potential Resorption and Resorption Proficiency. Ecology 77:1716–1727.
Koide, R. T., C. Fernandez, and G. Malcolm. 2014. Determining place and process: functional traits of ectomycorrhizal fungi that affect both community structure and ecosystem function. New Phytologist 201:433–439.
Koide, R. T., and C. W. Fernandez. 2018. The continuing relevance of "older" mycorrhiza literature: insights from the work of John Laker Harley (1911–1990). Mycorrhiza 28:577–586.
Kohler A, A. Kuo, L. G. Nagy, E. Morin, K. W. Barry, F. Buscot, B. Canbäck, C. Choi, N. Cichocki, A. Clum, J. Colpaert, A. Copeland, M. D. Costa, J. Doré, D. Floudas, G. Gay, M. Girlanda, B. Henrissat, S. Herrmann, J. Hess, N. Högberg, T. Johansson, H.-R. Khouja, K. LaButti, U. Lahrmann, A. Levasseur, E. A. Lindquist, A. Lipzen, R. Marmeisse, E. Martino, C. Murat, C. Y. Ngan, U. Nehls, J. M. Plett, A. Pringle, R. A. Ohm, S. Perotto, M. Peter, R. Riley, F. Rineau, J. Ruytinx, A. Salamov, F. Shah, H. Sun, M. Tarkka, A. Tritt, C. Veneault-Fourrey, A. Zuccaro, A. Tunlid, I. V. Grigoriev, D. S. Hibbett, and F. Martin. 2015. Convergent losses of decay mechanisms and rapid turnover of symbiosis genes in mycorrhizal mutualists. Nature Genetics 47:410–415
Körner, C. 2003. Carbon limitation in trees. Journal of Ecology 91:4–17.
Lilleskov, E. A., T. J. Fahey, T. R. Horton, and G. M. Lovett. 2002. Belowground Ectomycorrhizal Fungal Community Change Over a Nitrogen Deposition Gradient in Alaska. Ecology 83:104–115.
van der Linde, S., L. M. Suz, C. D. L. Orme, F. Cox, H. Andreae, E. Asi, B. Atkinson, S. Benham, C. Carroll, N. Cools, B. De Vos, H.-P. Dietrich, J. Eichhorn, J. Gehrmann, T.

Grebenc, H. S. Gweon, K. Hansen, F. Jacob, F. Kristöfel, P. Lech, M. Manninger, J. Martin, H. Meesenburg, P. Merilä, M. Nicolas, P. Pavlenda, P. Rautio, M. Schaub, H.-W. Schröck, W. Seidling, V. Šrámek, A. Thimonier, I. M. Thomsen, H. Titeux, E. Vanguelova, A. Verstraeten, L. Vesterdal, P. Waldner, S. Wijk, Y. Zhang, D. Žlindra, and M. I. Bidartondo. 2018. Environment and host as large-scale controls of ectomycorrhizal fungi. Nature 558:243–248.

Luo, Y., B. Su, W. S. Currie, J. S. Dukes, A. Finzi, U. Hartwig, B. Hungate, R. E. McMurtrie, R. Oren, W. J. Parton, D. E. Pataki, R. M. Shaw, D. R. Zak, and C. B. Field. 2004. Progressive Nitrogen Limitation of Ecosystem Responses to Rising Atmospheric Carbon Dioxide. BioScience 54:731–739.

Moeller, H. V., K. G. Peay, and T. Fukami. 2014. Ectomycorrhizal fungal traits reflect environmental conditions along a coastal California edaphic gradient. FEMS Microbiology Ecology 87:797–806.

Näsholm, T., K. Kielland, and U. Ganeteg. 2009. Uptake of organic nitrogen by plants. New Phytologist 182:31–48.

Nilsson, R. H., K.-H. Larsson, A. F. S. Taylor, J. Bengtsson-Palme, T. S. Jeppesen, D. Schigel, P. Kennedy, K. Picard, F. O. Glöckner, L. Tedersoo, I. Saar, U. Kõljalg, and K. Abarenkov. 2019. The UNITE database for molecular identification of fungi: handling dark taxa and parallel taxonomic classifications. Nucleic Acids Research 47:D259–D264.

Norby, R. J., and D. R. Zak. 2011. Ecological Lessons from Free-Air CO2 Enrichment (FACE) Experiments. Annual Review of Ecology, Evolution, and Systematics 42:181–203.

Nordin, A., I. K. Schmidt, and G. R. Shaver. 2004. Nitrogen Uptake by Arctic Soil Microbes and Plants in Relation to Soil Nitrogen Supply. Ecology 85:955–962.

Oren, R., D. S. Ellsworth, K. H. Johnsen, N. Phillips, B. E. Ewers, C. Maier, K. V. R. Schäfer, H. McCarthy, G. Hendrey, S. G. McNulty, and G. G. Katul. 2001. Soil fertility limits carbon sequestration by forest ecosystems in a CO 2 -enriched atmosphere. Nature 411:469–472.

Pellitier, P. T., and D. R. Zak. 2018. Ectomycorrhizal fungi and the enzymatic liberation of nitrogen from soil organic matter: why evolutionary history matters. New Phytologist 217:68–73.

Peltier, D. M. P., and I. Ibáñez. 2015. Patterns and variability in seedling carbon assimilation: implications for tree recruitment under climate change. Tree Physiology 35:71–85.

Pickles, B. J., D. R. Genney, I. C. Anderson, and I. J. Alexander. 2012. Spatial analysis of ectomycorrhizal fungi reveals that root tip communities are structured by competitive interactions. Molecular Ecology 21:5110–5123.

Read, D. J., and J. Perez-Moreno. 2003. Mycorrhizas and Nutrient Cycling in Ecosystems: A Journey towards Relevance? The New Phytologist 157:475–492.

Reich, P. B., S. E. Hobbie, T. Lee, D. S. Ellsworth, J. B. West, D. Tilman, J. M. H. Knops, S. Naeem, and J. Trost. 2006. Nitrogen limitation constrains sustainability of ecosystem response to CO2. Nature 440:922–925.

van der Sleen, P., P. Groenendijk, M. Vlam, N. P. R. Anten, A. Boom, F. Bongers, T. L. Pons, G. Terburg, and P. A. Zuidema. 2015. No growth stimulation of tropical trees by 150 years of CO2 fertilization but water-use efficiency increased. Nature Geoscience 8:24–28.

Smith, M. E., T. W. Henkel, M. C. Aime, A. K. Fremier, and R. Vilgalys. 2011. Ectomycorrhizal fungal diversity and community structure on three co-occurring leguminous canopy tree species in a Neotropical rainforest. New Phytologist 192:699–712.

Smith, S. E., and D. J. Read. 2010. Mycorrhizal symbiosis. Academic press.

Spiegelhalter, D. J., N. G. Best, B. P. Carlin, and A. V. D. Linde. 2002. Bayesian measures of model complexity and fit. Journal of the Royal Statistical Society: Series B (Statistical Methodology) 64:583–639.

Steidinger, B. S., T. W. Crowther, J. Liang, M. E. Van Nuland, G. D. A. Werner, P. B. Reich, G. J. Nabuurs, S. de-Miguel, M. Zhou, N. Picard, B. Herault, X. Zhao, C. Zhang, D. Routh, and K. G. Peay. 2019. Climatic controls of decomposition drive the global biogeography of forest-tree symbioses. Nature 569:404–408.

Sterkenburg, E., A. Bahr, M. B. Durling, K. E. Clemmensen, and B. D. Lindahl. 2015. Changes in fungal communities along a boreal forest soil fertility gradient. New Phytologist 207:1145–1158.

Taylor, D. L., W. A. Walters, N. J. Lennon, J. Bochicchio, A. Krohn, J. G. Caporaso, and T. Pennanen. 2016. Accurate Estimation of Fungal Diversity and Abundance through Improved Lineage-Specific Primers Optimized for Illumina Amplicon Sequencing. Applied and Environmental Microbiology 82:7217–7226.

Terrer, C., R. B. Jackson, I. C. Prentice, T. F. Keenan, C. Kaiser, S. Vicca, J. B. Fisher, P. B. Reich, B. D. Stocker, B. A. Hungate, J. Peñuelas, I. McCallum, N. A. Soudzilovskaia, L. A. Cernusak, A. F. Talhelm, K. Van Sundert, S. Piao, P. C. D. Newton, M. J. Hovenden, D. M. Blumenthal, Y. Y. Liu, C. Müller, K. Winter, C. B. Field, W. Viechtbauer, C. J. Van Lissa, M. R. Hoosbeek, M. Watanabe, T. Koike, V. O. Leshyk, H. W. Polley, and O. Franklin. 2019. Nitrogen and phosphorus constrain the CO2 fertilization of global plant biomass. Nature Climate Change 9:684–689.

Terrer, C., S. Vicca, B. A. Hungate, R. P. Phillips, and I. C. Prentice. 2016. Mycorrhizal association as a primary control of the CO_2 fertilization effect. Science 353:72–74.

Terrer, C., S. Vicca, B. D. Stocker, B. A. Hungate, R. P. Phillips, P. B. Reich, A. C. Finzi, and I. C. Prentice. 2018. Ecosystem responses to elevated CO2 governed by plant–soil interactions and the cost of nitrogen acquisition. New Phytologist 217:507–522.

Thomas, R. Q., C. D. Canham, K. C. Weathers, and C. L. Goodale. 2010. Increased tree carbon storage in response to nitrogen deposition in the US. Nature Geoscience 3:13–17.

Tognetti, R., P. Cherubini, and J. L. Innes. 2000. Comparative stem-growth rates of Mediterranean trees under background and naturally enhanced ambient CO2 concentrations: RESEARCH Tree-ring responses to long-term elevated CO2 concentrations. New Phytologist 146:59–74.

Vitousek, P. 1982. Nutrient Cycling and Nutrient Use Efficiency. The American Naturalist 119:553–572.

Walker, A. P., M. G. De Kauwe, B. E. Medlyn, C. M. Iversen, S. Asao, B. Guenet, A. Harper, T. Hickler, B. A. Hungate, A. K. Jain, Y. Luo, X. Lu, M. Lu, K. Luus, J. P. Megonigal, R. Oren, E. Ryan, S. Shu, A. Talhelm, Y.-P. Wang, J. M. Warren, C. Werner, J. Xia, B. Yang, D. R. Zak, and R. J. Norby. 2019. Decadal biomass increment in early secondary succession woody ecosystems is increased by CO2 enrichment. Nature Communications 10:454.

Wang, Y., U. Naumann, S. T. Wright, and D. I. Warton. 2012. mvabund– an R package for model-based analysis of multivariate abundance data. Methods in Ecology and Evolution 3:471–474.

Wenzel, S., P. M. Cox, V. Eyring, and P. Friedlingstein. 2016. Projected land photosynthesis constrained by changes in the seasonal cycle of atmospheric CO 2. Nature 538:499–501.

Wieder, W. R., C. C. Cleveland, W. K. Smith, and K. Todd-Brown. 2015. Future productivity and carbon storage limited by terrestrial nutrient availability. Nature Geoscience 8:441–444.

Zak, D. R., W. E. Holmes, A. C. Finzi, R. J. Norby, and W. H. Schlesinger. 2003. Soil Nitrogen Cycling Under Elevated Co2: A Synthesis of Forest Face Experiments. Ecological Applications 13:1508–1514.

Zak, D. R., P. T. Pellitier, W. Argiroff, B. Castillo, T. Y. James, L. E. Nave, C. Averill, K. V. Beidler, J. Bhatnagar, J. Blesh, A. T. Classen, M. Craig, C. W. Fernandez, P. Gundersen, R. Johansen, R. T. Koide, E. A. Lilleskov, B. D. Lindahl, K. J. Nadelhoffer, R. P. Phillips, and A. Tunlid. 2019. Exploring the role of ectomycorrhizal fungi in soil carbon dynamics. New Phytologist 223:33–39.

Zak, D. R., and K. S. Pregitzer. 1990. Spatial and Temporal Variability of Nitrogen Cycling in Northern Lower Michigan. Forest Science 36:367–380.

Zak, D. R., K. S. Pregitzer, and G. E. Host. 1986. Landscape variation in nitrogen mineralization and nitrification. Canadian Journal of Forest Research 16:1258–1263.

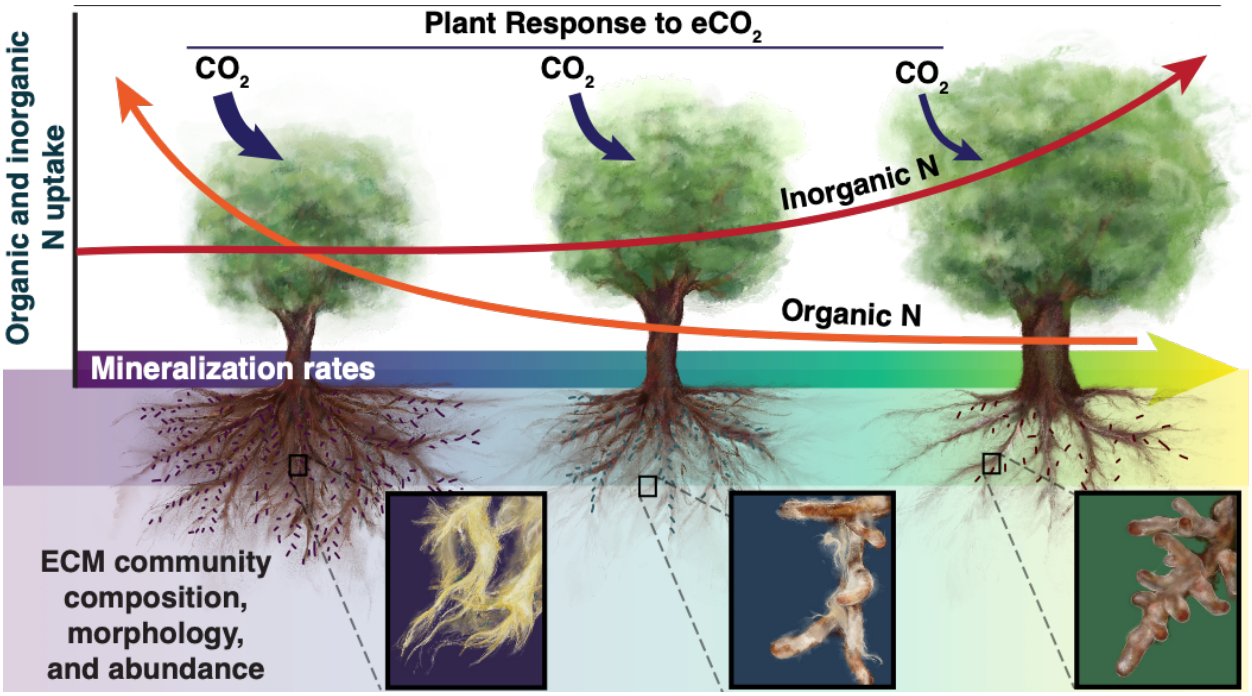

Figure 4-1 Conceptual framework of the contribution of different N forms to plant growth (red and orange lines; y-axis) along a soil inorganic N availability gradient (x-axis). Dark blue arrows show the hypothesized relativized effects (arrow width) of historic increases in atmospheric CO_2 (eCO_2) on tree growth. ECM community composition, hyphal morphology and abundance (speckles on tree roots) differ along the gradient. Note hypothesized turnover in the dominance of ECM taxa with extra-radical rhizomorphic hyphae and long-and medium-distance exploration morphologies. Illustration by Callie R. Chappell.

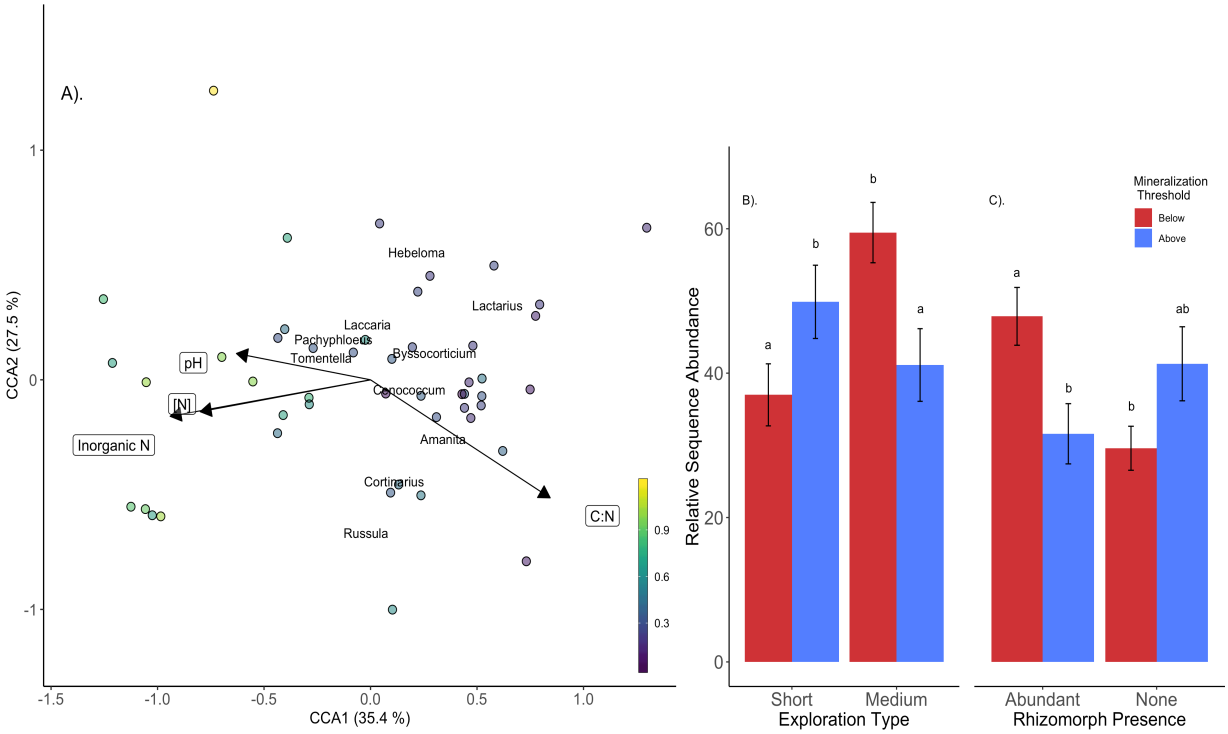

Figure 4-2 ***A.*** *Constrained correspondence analysis (CCA) depicting individual ectomycorrhizal (ECM) fungal communities from individual Q. rubra root-systems. Points are colored by rates of net N mineralization (μg g^{-1} d^{-1}). Plotted vectors (boxes) emerged as highly significant predictors of ECM community composition (GLM) and they constrain the ordination. Genus names are coordinates for ECM genera comprising more than 2% of total sequences. Axis percentages depict constrained variation.* ***B & C.*** *Tradeoffs in the relative community-wide abundance of dominant ectomycorrhizal (ECM) hyphal morphotypes above (blue) and below (red) the soil mineralization threshold. Soil threshold (0.46 μg g^{-1} d^{-1}) identified using community change point analysis (TITAN). Error bars (SE) depict variation across individual root-systems. Subscripts depict significance at $\alpha < 0.05$ for panel B, and $\alpha < 0.1$ for panel C.*

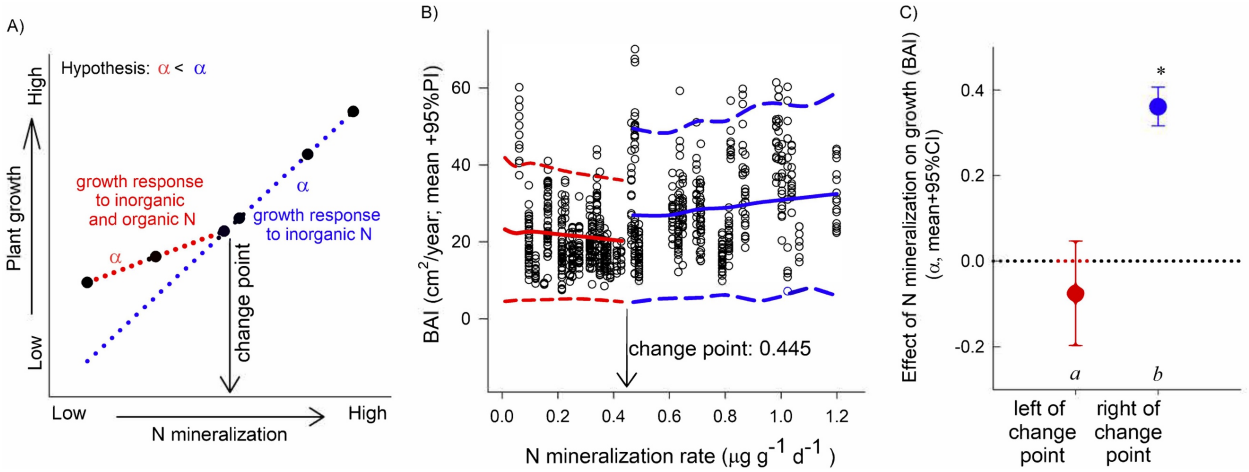

Figure 4-3 ***A.*** *Representative analysis of tree growth as a function of N mineralization rates. The change point analysis identifies the occurrence and location of the inflection point, if any, and the value of the slope parameters on each side.* ***B.*** *Basal Area Increment (BAI), from 54 Q. rubra trees along the studied N mineralization gradient (circles). Red and blue lines indicate estimated BAI mean and 95% CI above and below the identified change-point.* ***C.*** *Slope parameters are significantly different to each other (95% CIs do not overlap). Asterisks indicates parameter is different from zero (95% CI does not overlap with zero).*

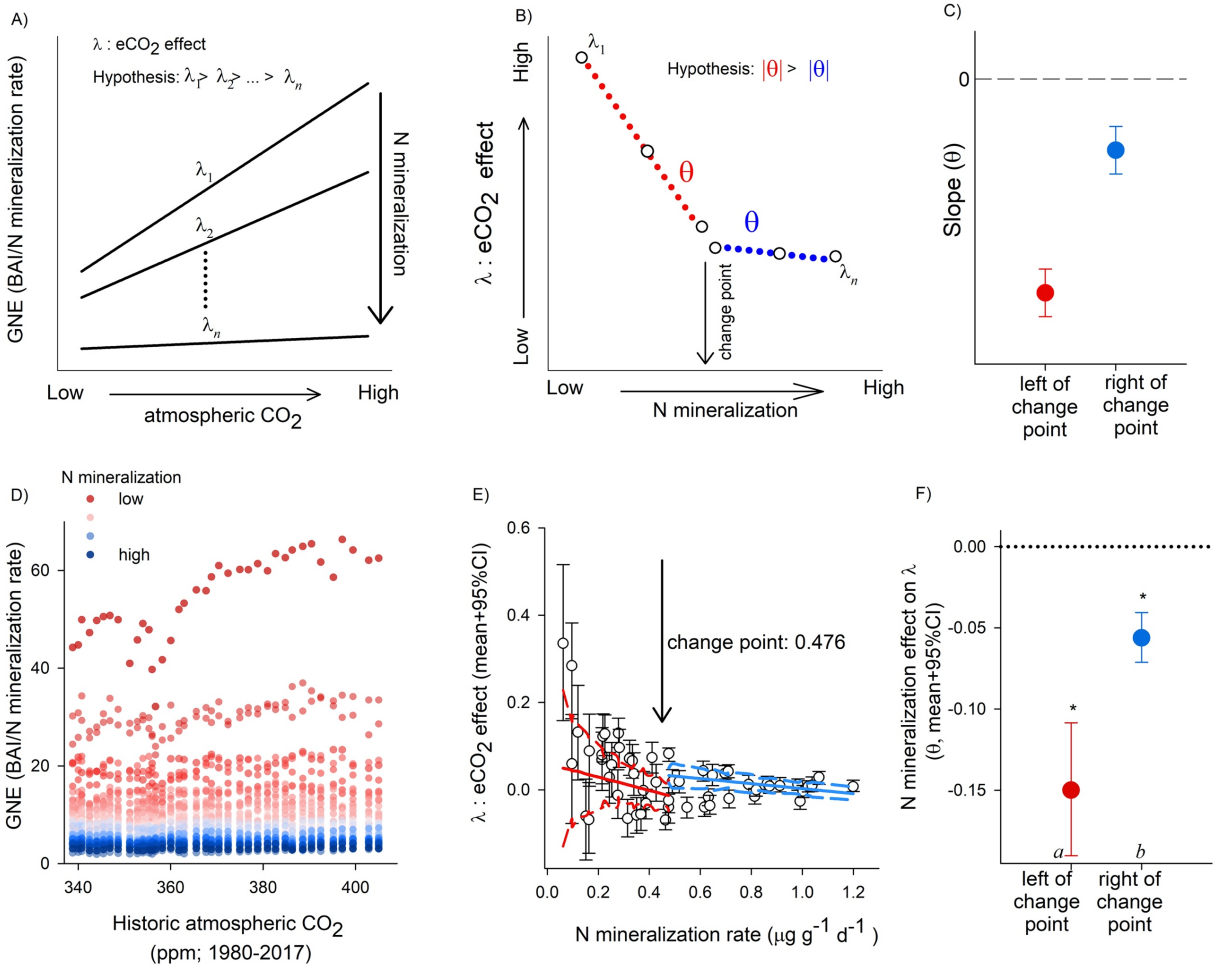

Figure 4-4 ***A.*** *Representative analysis framework of growth-N efficiency index (GNE) as a function of increasing concentrations of historic atmospheric CO_2 at each point along the net N mineralization gradient (different lines and their relative slopes).* ***B.*** *Conceptual diagram of the effects of eCO_2 (λ) on plant growth; change point analysis will detect an inflection point along the gradient, if any.* ***C.*** *Differences in* ***θ*** *derived from the red and blue portion of panel B, indicate change in slope values.* ***D.*** *Actual data collected from 54 trees from the past 38 years. Individual points represent estimated annual GNE values colored by rates of net-N mineralization.* ***E.*** *Individual points represent individual trees response to eCO_2 (model slopes) over the study period. Red and blue lines denote Bayesian change-point model with plotted 95% CI (dashed lines).* ***F.*** *Denotes mean and 95% CI for the red and blue slopes depicted in panel E; different letters denote significant differences between slopes, asterisks indicate significant differences from zero (95% CI do not include zero).*

Supplementary Information

Tree Core Sampling and Preparation

In May 2018, we measured tree diameter at breast height (1.3 m; DBH) in cm, then extracted growth cores from the North and South aspect of each individual at DBH using 5.15 mm Haglöf increment borers. The samples were dried overnight at 100° C. We mounted tree cores on cradles and sanded then by hand progressively from 100 to 600 grit. The mounted cores were digitized for measurement by scanning them on a flatbed scanner at a resolution of 1200 dpi. We digitally measured yearly ring width (growth) of the scanned tree cores using the Cybis CooRecorder program at a precision of 0.001 mm. We then used the program Cybis CDendro for individual cross dating and chronology assembly by site. Crossdating was achieved when TTest values were greater than 5 for matching target samples using the P2YrsL normalization method. We created master ring width lists that were summed by stem to reflect the average yearly growth of each individual using cross dated North & South aspects. We estimated historical DBH of focal trees at each year using the yearly ring width from our master chronologies.

Soil and Leaf Analyses

Total free primary amines (TFPA) availability (primarily amino acids and amino sugars) were measured using unincubated 2M KCl extracts following (Darrouzet-Nardi et al. 2013). TFPA is expressed as μmol leucine equivalents (leucine was used as standard); estimates of TFPA availability should be considered relative indices of labile organic N availability in soil solution (Fig. S13). Soil was dried 105°C and total C and N contents (% of dry mass) were determined using combustion analysis on a LECO TruMac CN analyzer (Fig S5 & S14; LECO Corporation, St. Joseph, MI, USA). Soil pH was determined for 2:1 deionized water-soil slurries with an Accumet 15 pH meter (Fig S15; Fisher Scientific, Waltham, MA, USA). Senesced (Oi horizon), and green leaves (~7 leaves each), were deveined, homogenized, dried at 60°C and ground using a ball mill. Leaves were analyzed for leaf N at the UC Davis Stable Isotope Facility using a PDZ Europa ANCA-GSL elemental analyzer interfaced to a PDZ Europa 20-20 isotope ratio mass spectrometer (Sercon Ltd., Cheshire, UK).

DNA extraction and PCR

CTAB from each root-tip sample was removed prior to lyophilization at -50°C. Lyophilized root-tips were homogenized and the totality of each root-tip sample was split into 20-25mg

components and each component was placed in a lysis-tube with three sterilized 2.38mm metal beads. Each lysis tube also contained 800µl of Buffer AP1 and 4µl of RNase A from a Qiagen DNeasy Plant Mini Kit. Tubes were vortexed and placed in a 65°C waterbath for 20 minutes. DNA was then extracted using the Qiagen DNeasy Plant Mini Kit following manufacturers recommended protocol. DNA extraction replicates were combined and DNA yield was assessed using gel electrophoresis. Assessment of DNA quality was conducted using a Nanodrop Spectrophotometer (Thermo Fisher). The Quant-iT PicoGreen dsDNA Assay Kit (LifeTechnologies) and a BioTek SynergyHT Multi-Detection Microplate Reader (BioTek Instruments) were used to quantify DNA concentrations prior to PCR.

The ITS2 region was amplified using Illumina dual-indexed primers 5.8S Fun and ITS4 Fun (Taylor et al. 2016). The forward and reverse primer each contained the appropriate Illumina Nextera adaptor, linker sequence and error correcting Golay barcode for use with the Illumina MiSeq platform. All PCRs were performed in triplicate following Taylor et al. (2016), using Phusion High Fidelity DNA Polymerase and master mix (New England BioLabs). Each PCR contained 6 µl High Fidelity Phusion 5 × buffer, 0.75 µl each primer (10 µm initial concentration), 0.42 µl dNTPs (20 $mmol^{-1}$ initial concentration of each dNTP), 1.5 µl of template DNA (mean concentration 3.76 ng/µl, SD=2.82) and 0.23 µl of Taq (2 U/µl) brought to a final volume of 20 µl with molecular-grade water. PCR conditions consisted of an initial denaturation step at 94°C for 3 min, followed by 27 cycles of the following: 30 s at 94°C, 45 s at 57°C and 90 s at 72°C followed by a final extension step of 72°C for 10 min. PhiX oligonucleotides were spiked for base diversity.

Taxonomic Identification of Fungi

All sequence processing was performed using QIIME (4.2019) The dada2 pipeline was implemented in QIIME in order to denoise sequences, detect chimeras, remove PhiX contaminants and infer absolute sequence variants (ASV) (Callahan *et al.,* 2016). The beginning of each read was trimmed 10bp due to low sequence quality. A total 6,869,462 of filtered sequences (mean= 5.64 x 10^5, *SD*= 1.39 x 10^5 sequences per sample) were assigned to operational taxonomic units (OTU) using the dynamic (97-99% sequence similarity) UNITE database (v.8) (Nilsson *et al.,* 2019) after the reference taxonomic dataset was trained scikit-learn naive Bayes machine-learning algorithm (Bokulich et al. 2018).This dynamic classification system captures evolutionary-variation among fungal clades in sequence similarity (Garnica et

al. 2016). The resulting dataset was rarefied with 24,021 sequences, OTU that could not be assigned to Fungi, and appeared less than twice across all samples were removed. The resulting BIOM file was used for all subsequent statistical analyses (McDonald et al. 2012).

After filtering and processing, sequence-based rarefaction curves were highly asymptotic (Fig. S9), implying that sequencing depth was adequate to capture the diversity of fungi encountered in our samples. Individual root-systems hosted a mean of 27 ECM OTU (SE = 0.95), and an average of 80% sequences per sample consisted of ECM taxa (SE = 0.020%). This is likely a slight under-estimation of per-sample ECM sequence abundance, because fungal taxa with questionable or uncertain biotrophic associations, although detected from ECM root-tips samples, were not scored as ECM (Lodge et al. 2014)

We used the DEEMY (characterization and DEtermination of EctoMYcorrhizae) database (http://www.deemy.de/) to gather trait information on the exploration type (hyphal foraging distance) and rhizomorph formation of ECM fungal species (OTU) present in our dataset. When fungal species in our study were not represented in DEEMY, congeners were surveyed and, if 90% of the entries agreed, consensus trait values were assigned to that taxon. This classification system is supported by the fact that foraging-related functional traits for fungal hyphae are typically conserved at the genus level (Agerer 2001). This also allowed incorporation of ECM taxa that could only be identified to genus (Moeller et al. 2014). Long-distance foraging types were rare in our study system, composing less than 7% of ECM-derived sequences in each sample (SE = 1.38) and were removed from subsequent analyses. We were able to assign morphological hyphal trait data for 28 ECM genera comprising more than 93% all identified ECM sequences.

TITAN 2

Threshold Indicator Analysis was used to detect ECM community level threshold responses – community change points- along the continuous soil N mineralization gradient, using the TITAN2 package in R (Baker and King 2010). Only validated ECM genera were used in this analysis, and taxa that occurred in less than five samples, less than five times were removed following (Baker and King 2010). Community-level changes are strongest where either sum (z−) or sum (z+) reaches a maximum. Evidence for a community-level threshold is obtained when (a) many species exhibit similar change points, (b) a large maximum zscore occurs relative to sums elsewhere on the gradient and (c) zscore maxima across bootstrap replicates occupy a relatively

narrow range of environmental values. We conducted this analysis after Hellinger transformation using 2000 bootstrap and permutation replicates. We used relative cutoff and threshold scores of 0.85, Indvals were calculated using the relative abundance obtained by the ratio of summed abundance in each partition to the total, to address skew. A total of 16 genera were identified as pure and reliable indicators (Fig. S13).

Generalized Linear Models (mvabund

To test how the abiotic elements of soil affected the composition of the fungal community, we fitted generalized linear models (GLMs) with the "manyglm" function in mvabund version 4.0.1 (Wang et al. 2012) and performed multivariate analyses of deviance with Hellinger transformed OTU abundances (i.e. ANOVA for models with non-normal error distributions; Warton *et al.,* 2015). GLMs explicitly model the mean-variance relationship of ecological counts (Warton *et al*., 2015), and can be used to reveal the strength and significance of the relationship between a predictor and the response variable (Paliy and Shankar 2016).Notably, inorganic N supply was a highly significant predictor of ECM community composition (GLM: $Wald_{adj}$: 4.86, P <0.001). Soil C:N (GLM:$Wald_{adj}$: 5.10, P < 0.001), pH (GLM: $Wald_{adj}$: 4.42, P < 0.05) and soil N (GLM:$Wald_{adj}$: 4.01, P < 0.05) were also significant predictors of ECM community composition.

Analysis of BAI response to N mineralization rates

These analyses were run in JAGS 3.4 (Plummer 2003) using the rjags package in R (R Development Core Team 2013). Three chains were run until convergence of the parameters, ~50,000 iterations, and run again for another 50,000 to estimate posterior parameter means, variances and covariances, after thinning every 100th iteration.

rjags analysis code

BAI analysis

```
model{

  for(i in 2:I){  #individuals
    J[i]<-step(miner[i]-cp)

    for(y in yearBeg[i]:109){  #years
```

```
   bai[y,i]~dlnorm(D[y,i],tau1[y,i])
   bai.h[y,i]~dlnorm(D[y,i],tau1[y,i])
   D[y,i]<- alpha[1]+(alpha[2]+alpha[3]*J[i])*(miner[i])+alpha[4]*log(dbh[y,i])+alpha[5]*bai[y-
1,i]+YRE[y]
   tau1[y,i]<-1/(a+b*log(dbh[y,i]))
  }
  }

  #priors
  cp~dunif(0,1.25) # range of values in the data 0.06-1.19
  a~dlnorm(1,0.001)
  b~dnorm(0,0.001)

  for(i in 1:5){
   alpha[i]~dnorm(0,0.001)
   }

  alphacom<-alpha[2]+alpha[3] #slope after the change point

    for(y in 1:108){#year
     YRE[y]~dnorm(0,TT)
     }

TT~dgamma(0.0001,0.0001)

}
```

Analysis of GNES

```
model{
```

```
 for(i in 1:N){
  GNES[i]~dnorm(B[i],tau[indv[i]])
  GNES.h[i]~dnorm(B[i],tau[indv[i]])

  B[i]<- beta[indv[i]]+lambda[indv[i]]*CO2[i]+YRE[Year[i]]
 }

 #priors

 for(i in 1:NN){ #individuals
  beta[i]~dnorm(0,0.001)
  lambda[i]~dnorm(0,0.001)
  tau[i]~dgamma(0.0001,0.0001)
 }

  for(y in 1980:2017){#year
   YRE[y]~dnorm(0,TT)
   }

TT~dgamma(0.0001,0.0001)
 }
```

Analysis of the slopes

```
model{

 for(i in 2:NN){
 J[i]<-step(minerS[i]-cp)

 Ltau[i]<-1/(Lsd[i]*Lsd[i])

 Lambdamean[i]~dnorm(L [i],Ltau[i])
```

```
Lambdamean.h[i]~dnorm(L[i],Ltau[i])
L[i]<-theta[1]+(theta[2]+theta[3]*J[i])*(minerS[i])
}

#priors
for(i in 1:3){
  theta[i]~dnorm(0,0.001)
 }
 thetacomb<-theta[2]+theta[3]
 cp~dunif(0,1.25)
```

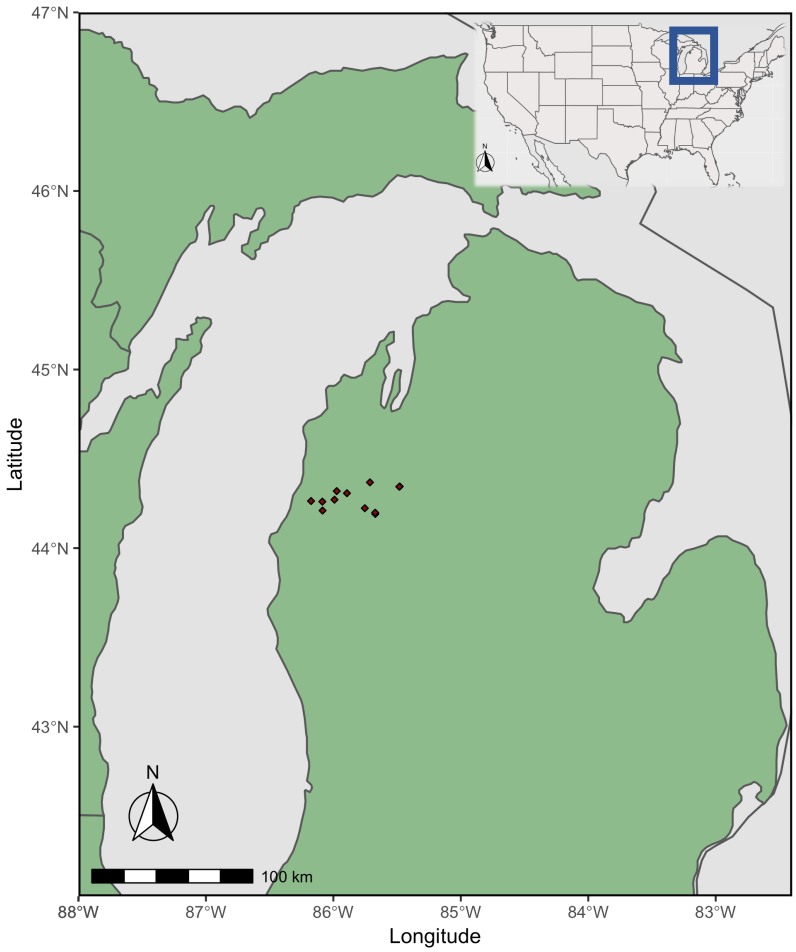

Supplementary Figure 4-1 Map of the twelve forest stands in Wexford and Manistee Counties, Manistee National Forest, Michigan, USA. Inset: continental United States and location of Michigan, blue box. Sites are extensively described in; Zak et al., 1986; Zak & Pregitzer 1990.

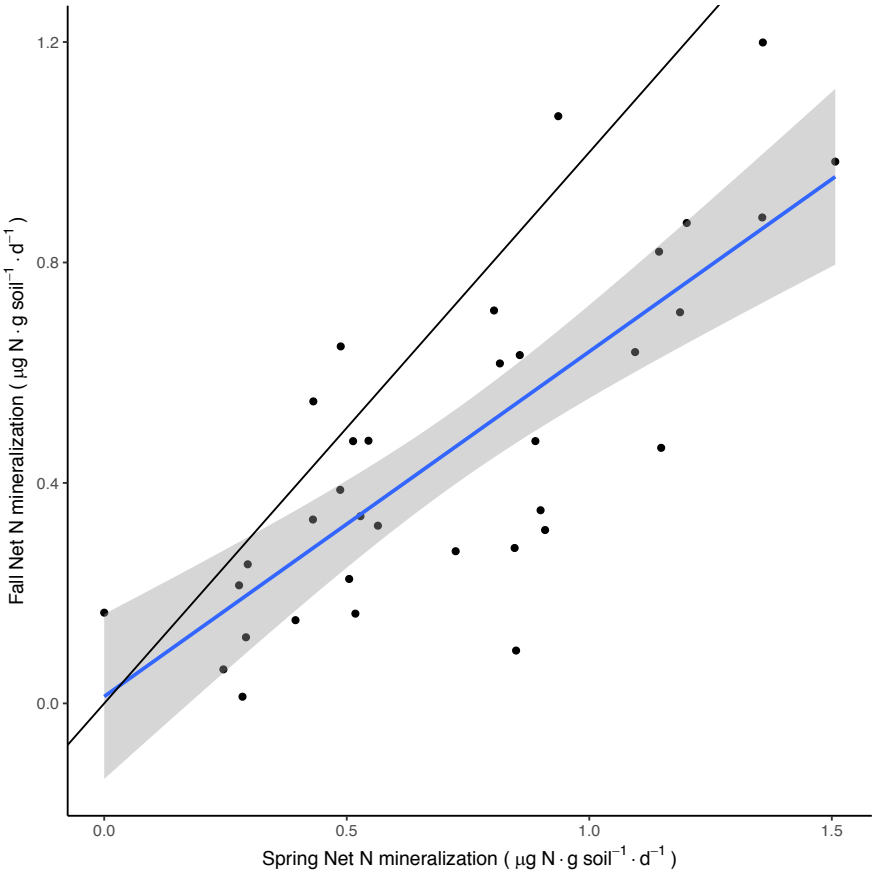

Supplementary Figure 4-2 Relationship between Spring and Fall mineralization rates, sampled from the base of the same individual trees (R^2_{adj}: 0.58. P <0.001). Black line is 1:1 plot.

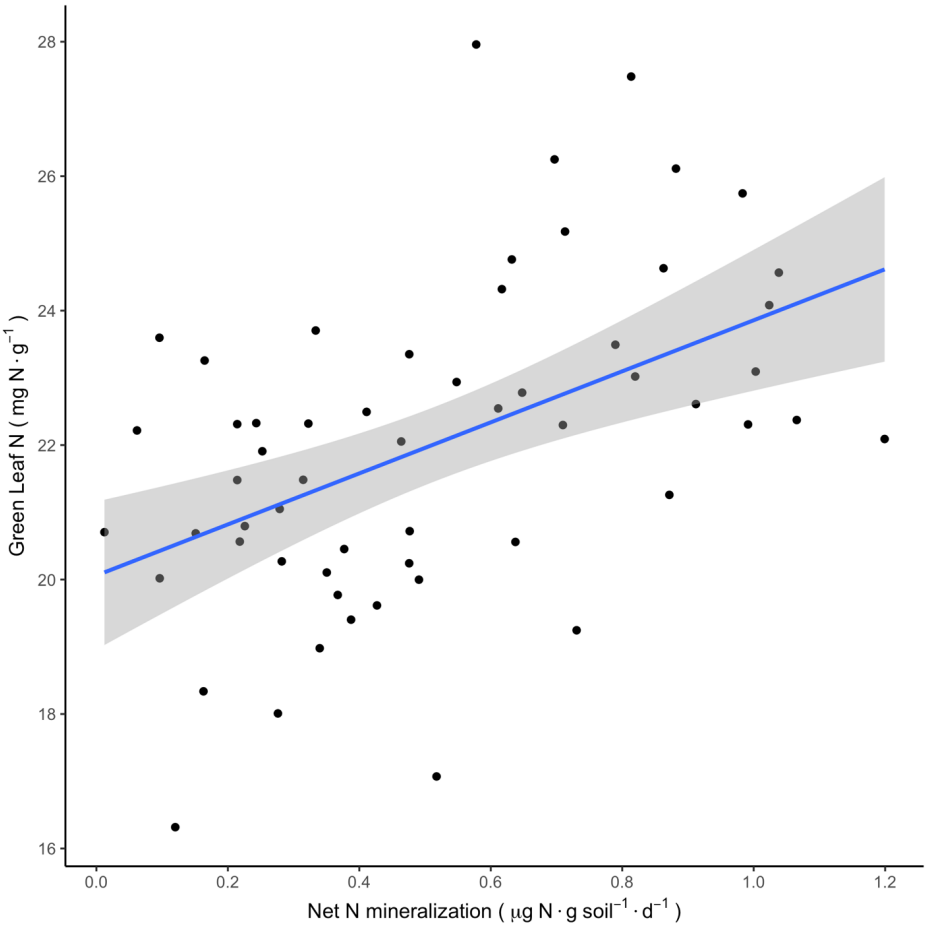

Supplementary Figure 4-3 Green-leaf nitrogen content from the 60 northern red oak trees along the inorganic N gradient (R^2_{adj} = 0.36, P <0.001).

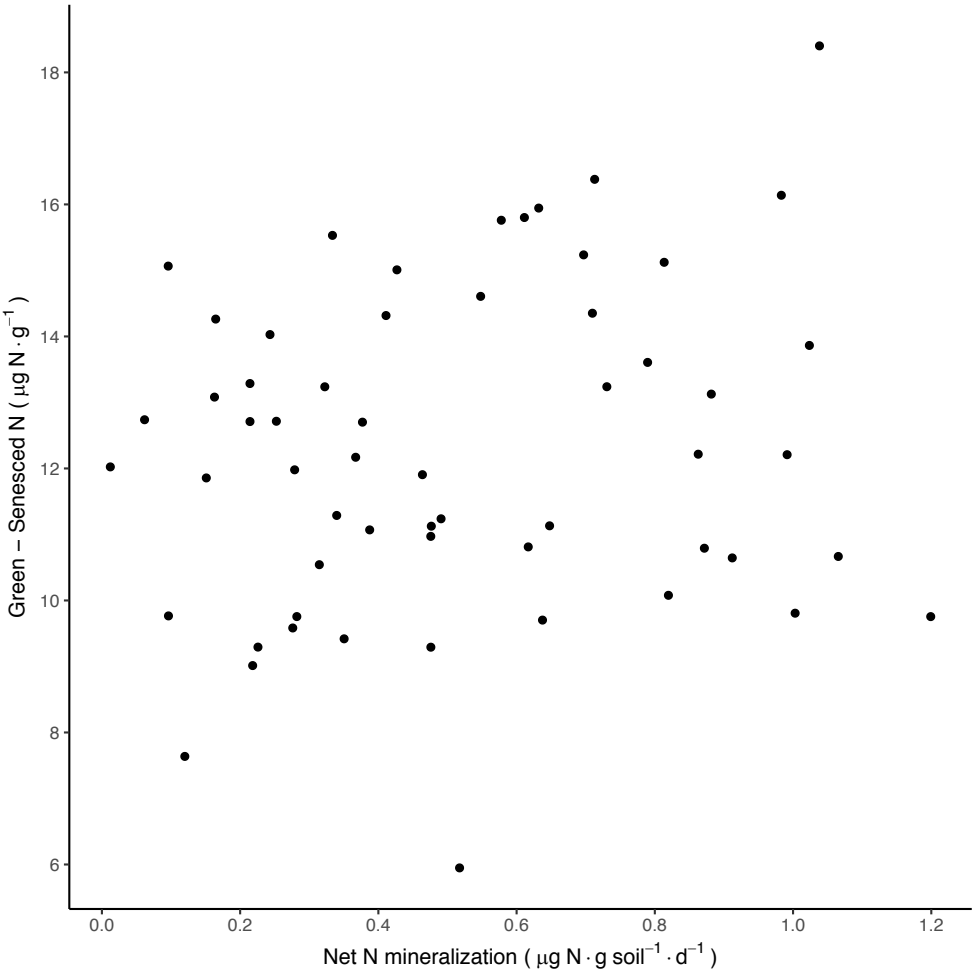

Supplementary Figure 4-4 Translocation of N into leaves, calculated as the difference between green leaf N and senesced leaf N (P > 0.2).

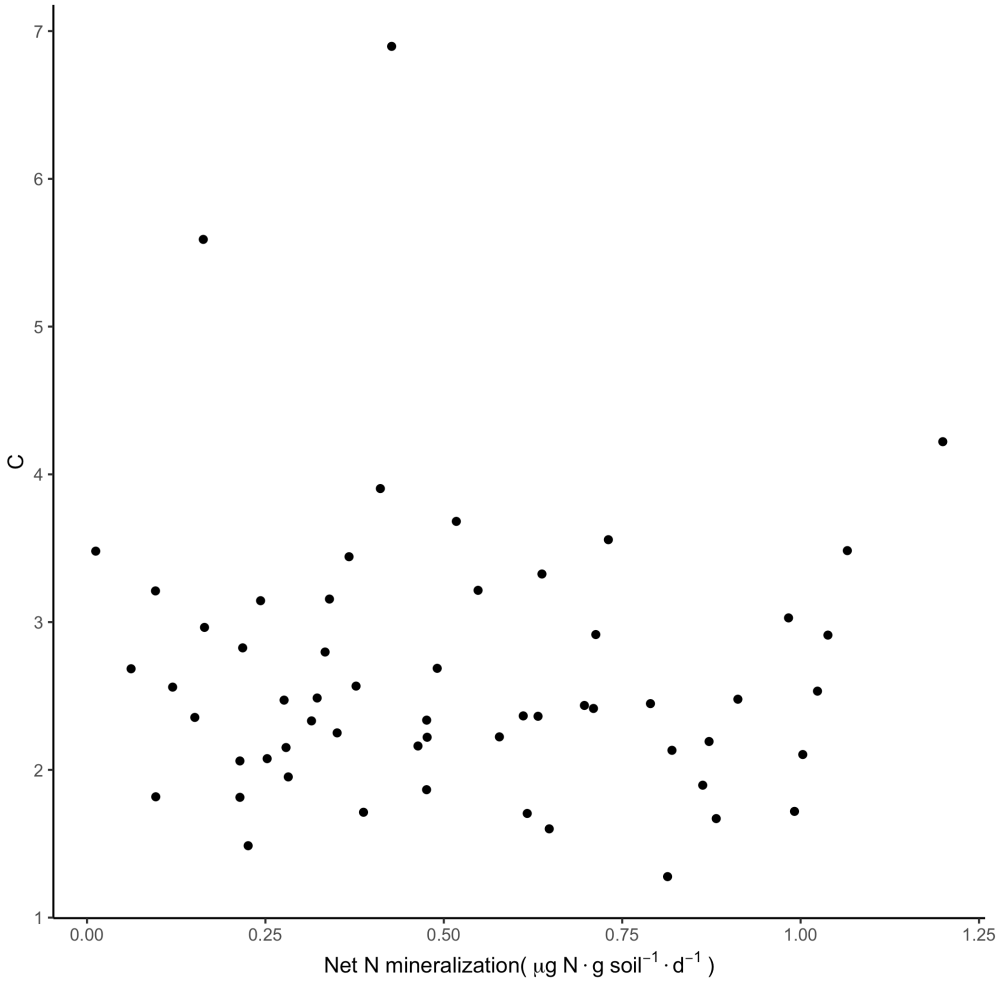

Supplementary Figure 4-5 Percent carbon (C) of bulk soil across the studied gradient (P > 0.6)

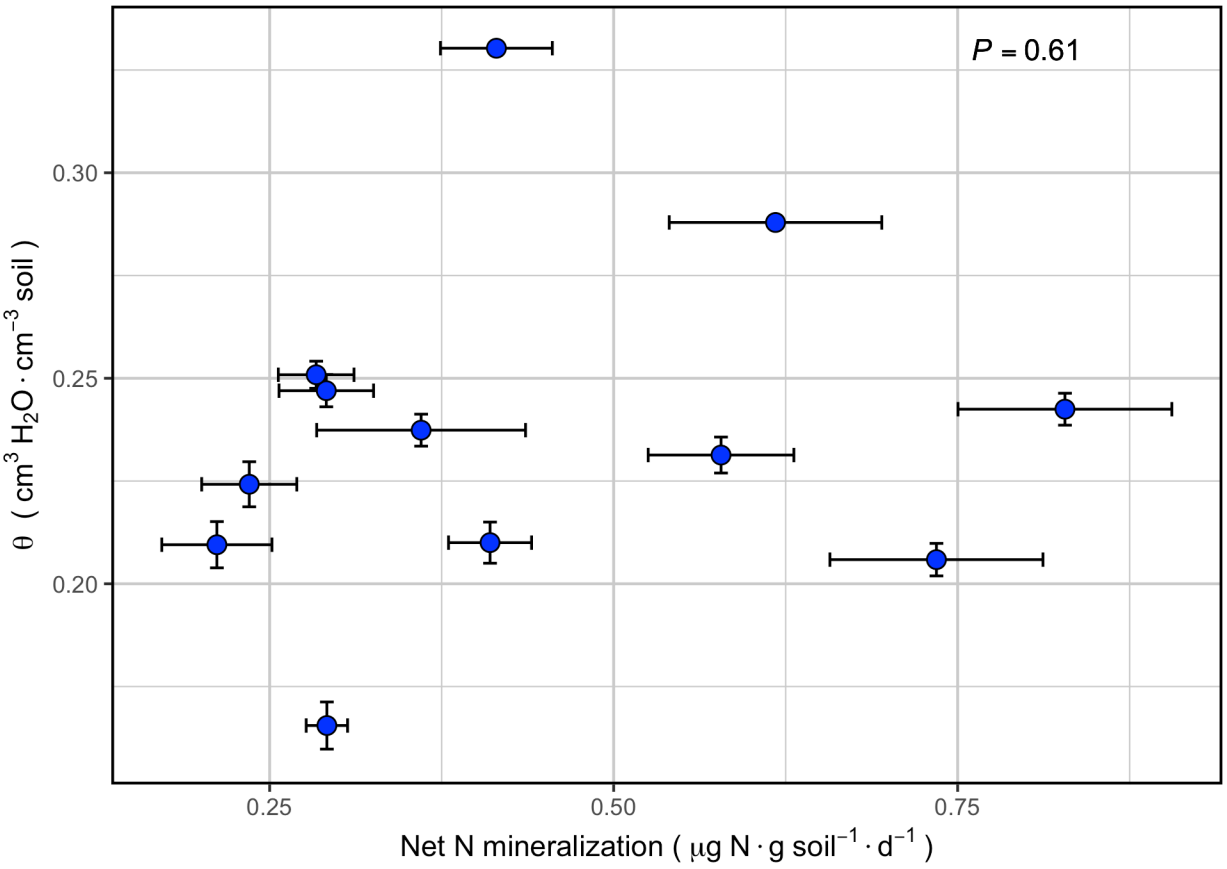

Supplementary Figure 4-6 No observed linear change in volumetric water content across the studied soil gradient. Points indicate site-level means for the 12 studied sites.

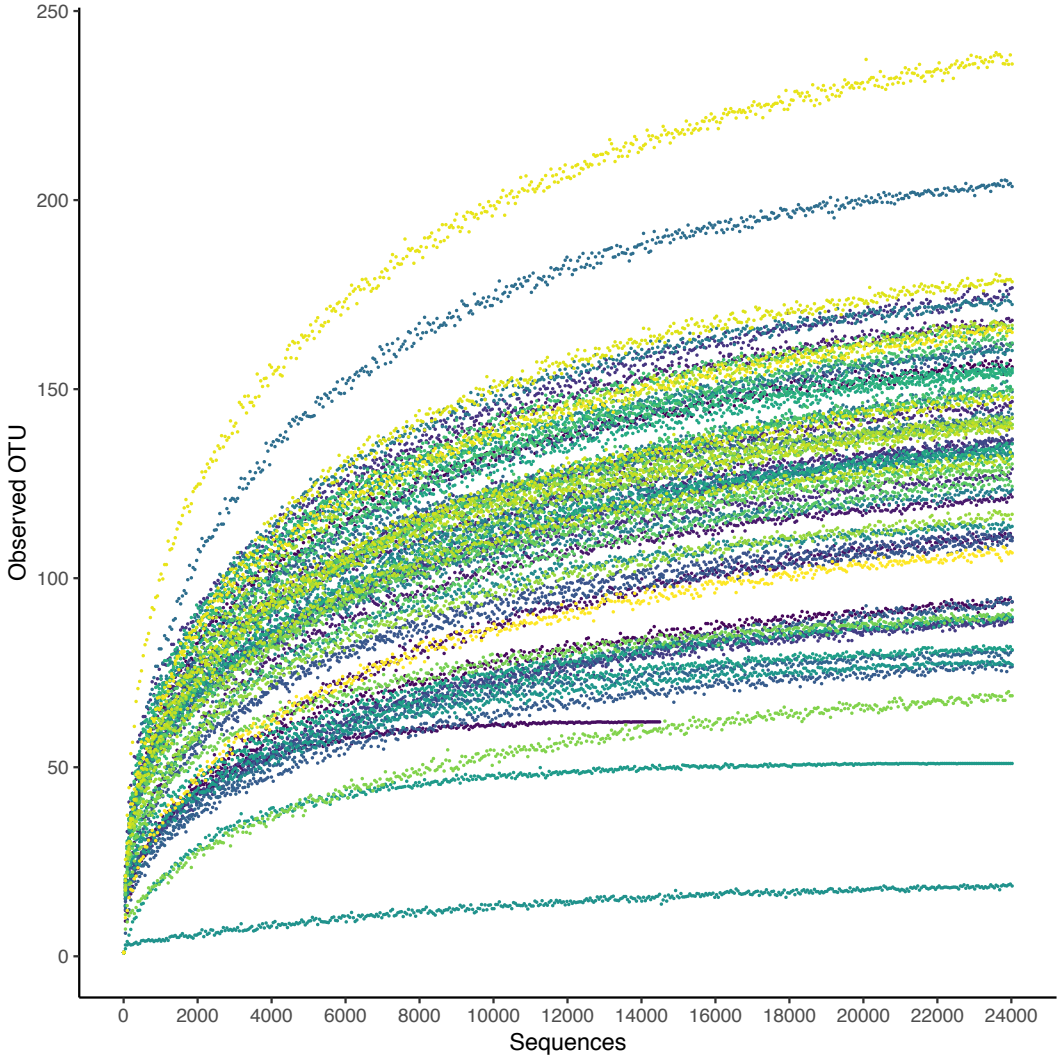

Supplementary Figure 4-7 Sequence rarefaction curves (24,021 sequences), were nearly asymptotic for all individual samples (i.e. root systems; colors). One sample with fewer overall sequences (~14,500 sequences) was removed from subsequent analyses.

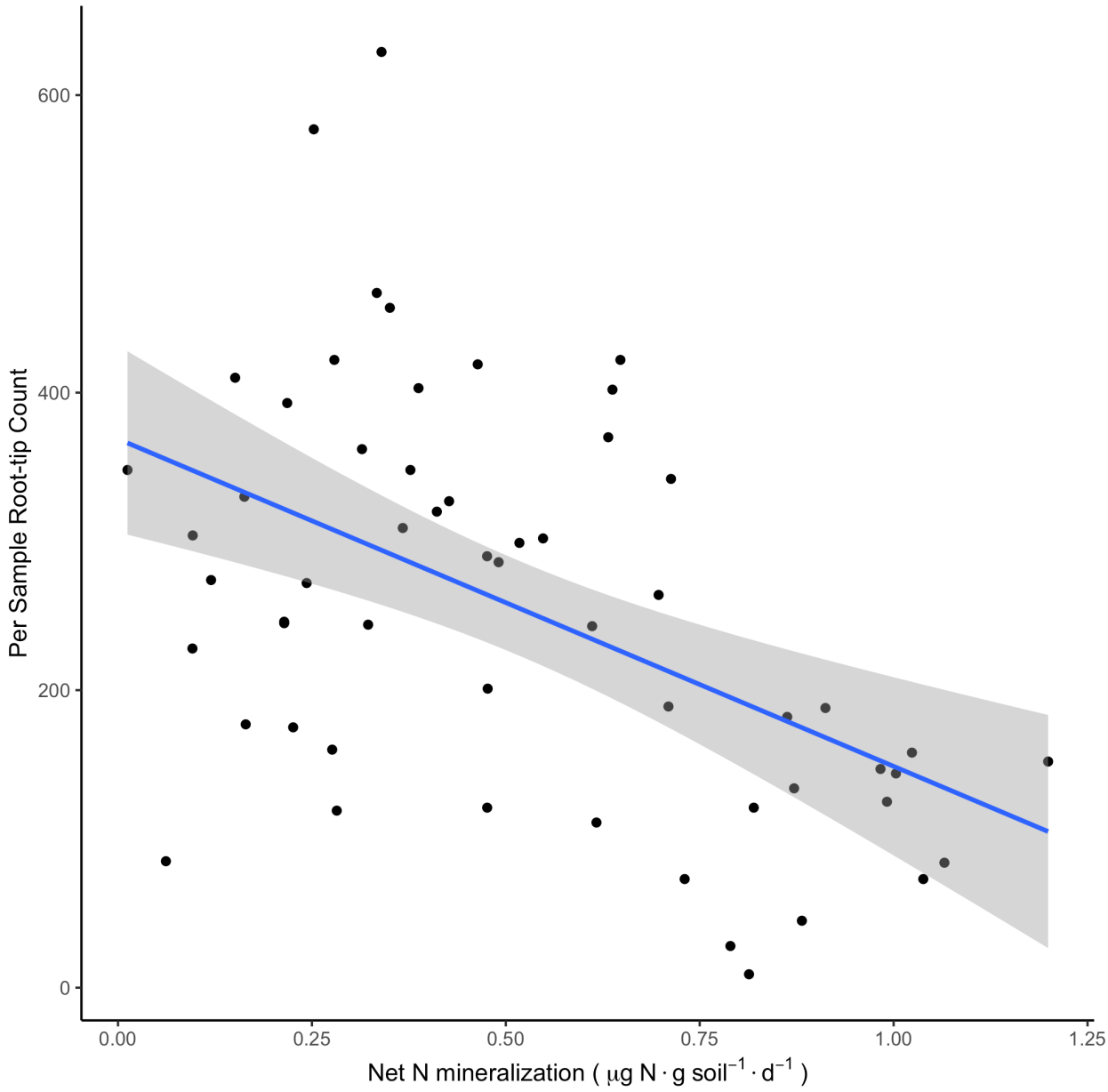

Supplementary Figure 4-8 Number of colonized ectomycorrhizal (ECM) root-tips on northern red oak individuals across the studied soil gradient: $R^2_{adj} = 0.25$, $P < 0.001$.

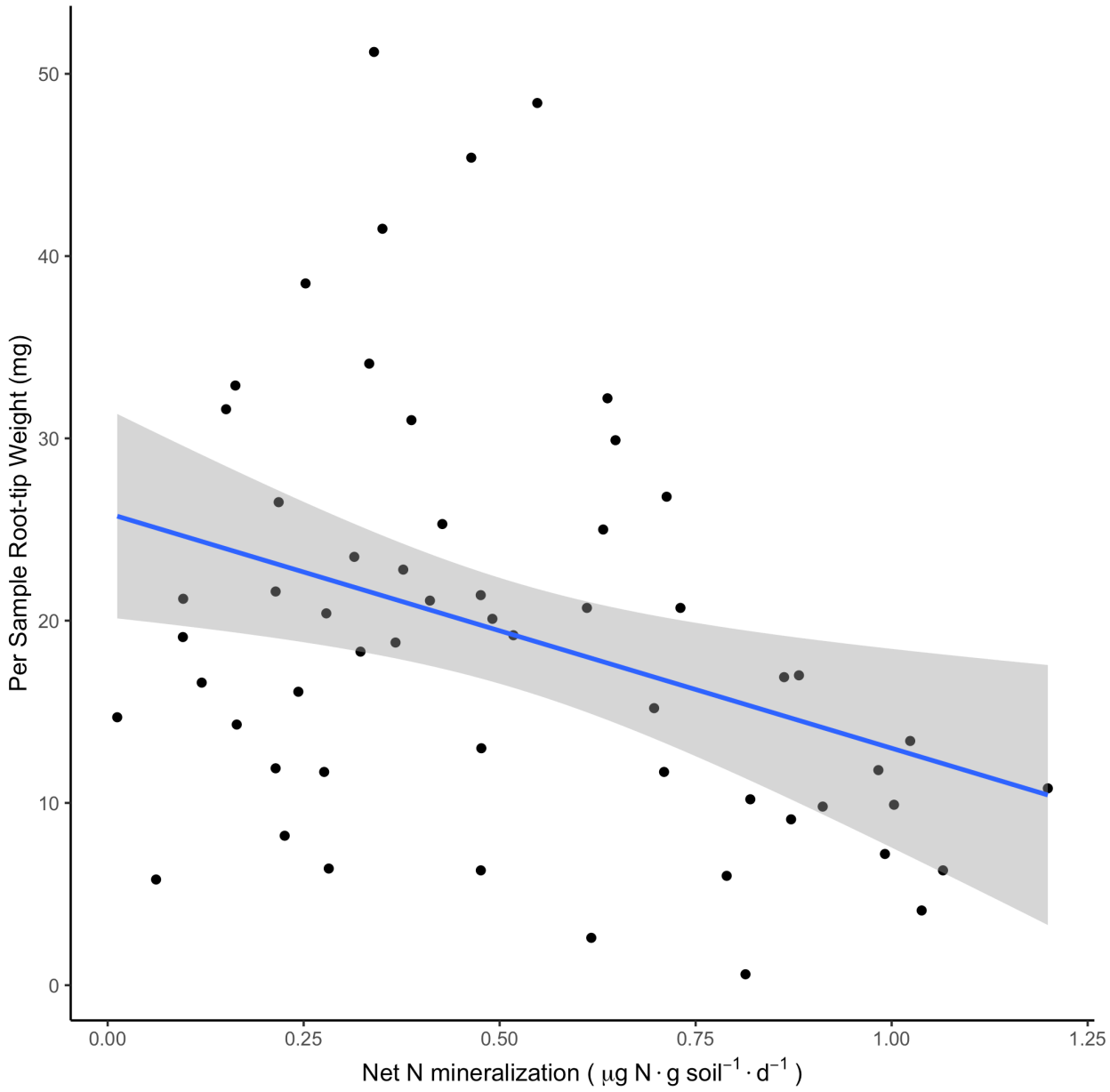

Supplementary Figure 4-9 Freeze-dried weight of ectomycorrhizal (ECM) root-tips collected from northern red oak individuals across the studied inorganic N gradient: $R^2_{adj} = 0.10$, $P<0.01$.

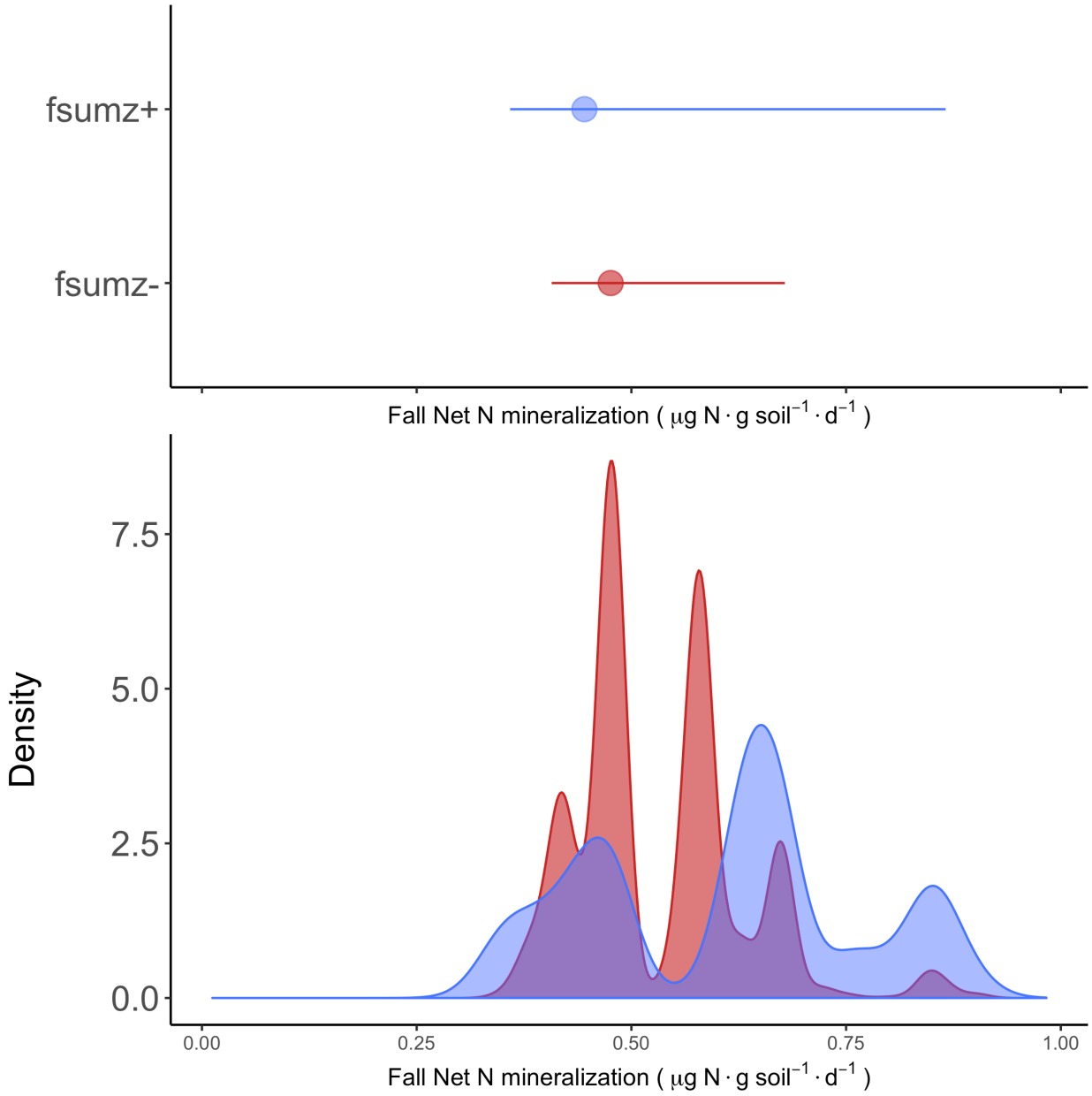

Supplementary Figure 4-10 Community change points changes with ECM sequences clustered at the genus level. Blue indicates taxa with (z+) scores, red indicates taxa with (z-) scores. Community change point = 0.47μg g^{-1} d^{-1} (z+) and 0.45 μg g^{-1} d^{-1} (z-) scores, showing the observed (z+) and (z-) maxima as circles with the 95th percentile of their distributions as horizontal lines. The bottom panel shows the estimated probability densities across all booststrap replicates.

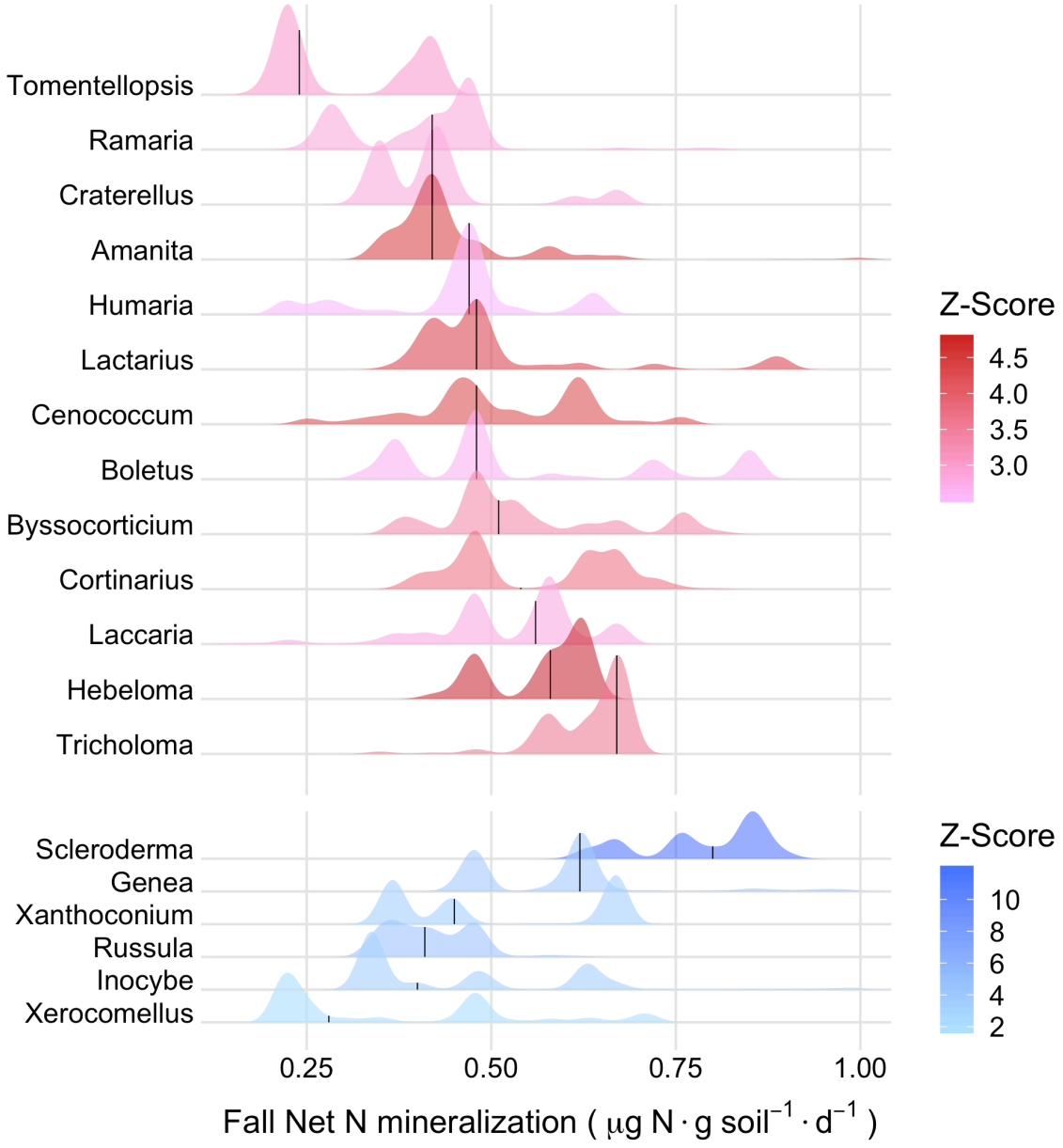

Supplementary Figure 4-11 ECM taxon change point ridges, showing negative (red) and positive (blue) z-scores, for pure and reliable taxa > 0.70. Plot depicts probability density function for all boostraps used in the model (2000). Vertical line for certain genus corresponds to the change point for each individual genus that was pure and reliable (0.85) of all bootstrap replicates in a consistent direction (either increasing or decreasing). For plotting purposes, purity and reliability of 0.70 was chosen.

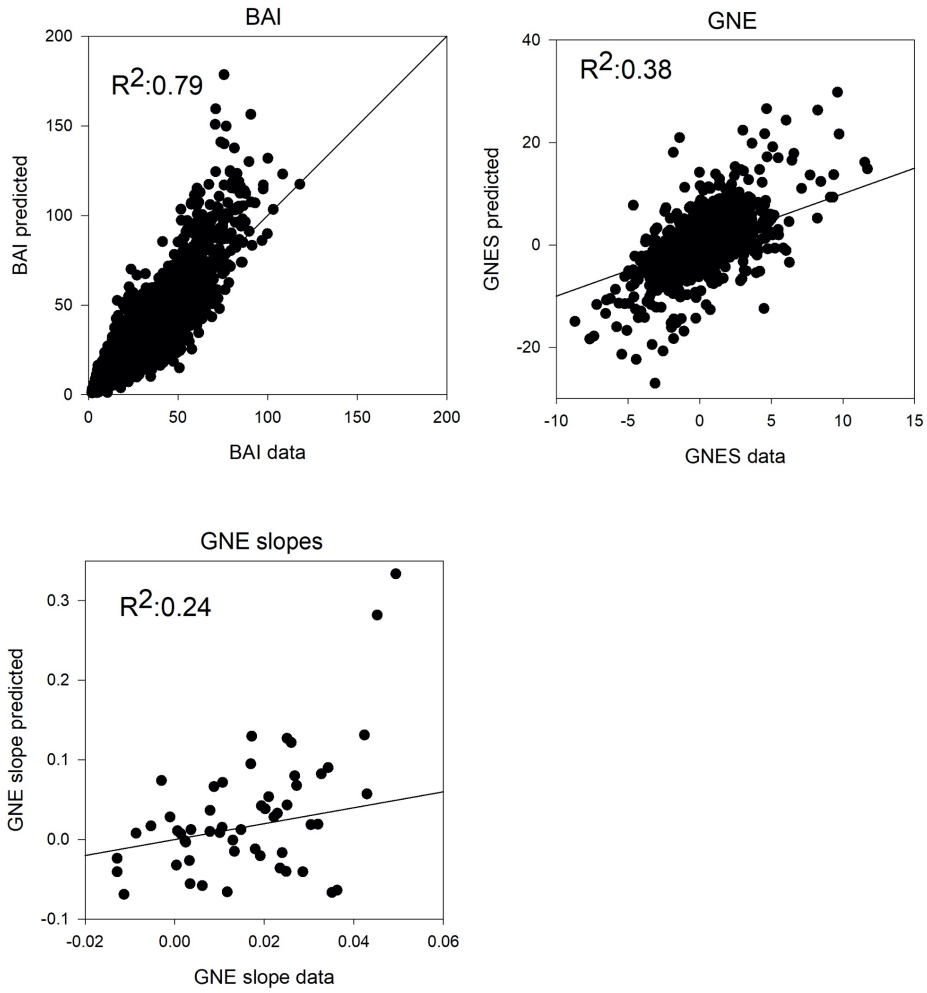

Supplementary Figure 4-12 Model fit, goodness of fit (predicted versus observed [in our case calculated data]) for our three analyses of plant growth. Solid line indicates the 1:1 relationship between the two variables. BAI = Basal Area Increment. GNES= standardized Growth Nitrogen Efficiency. See methods for calculation and estimations of parameters.

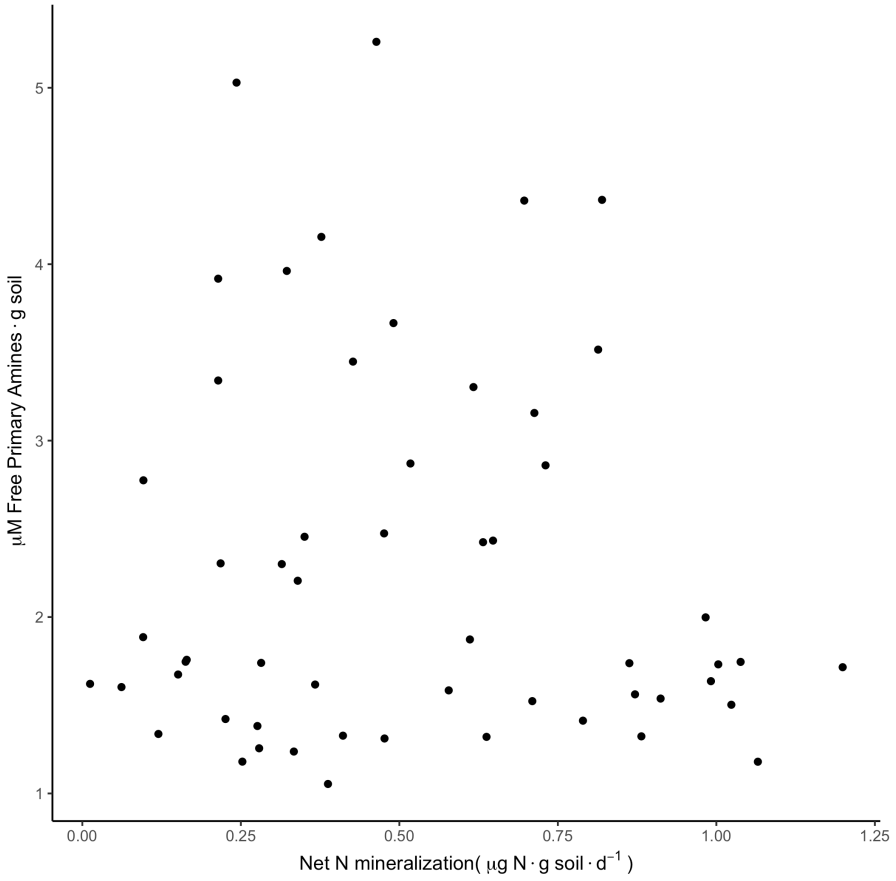

Supplementary Figure 4-13 Soil inorganic N availability is a poor predictor of total free primary amines present in soil solution (P>0.56)

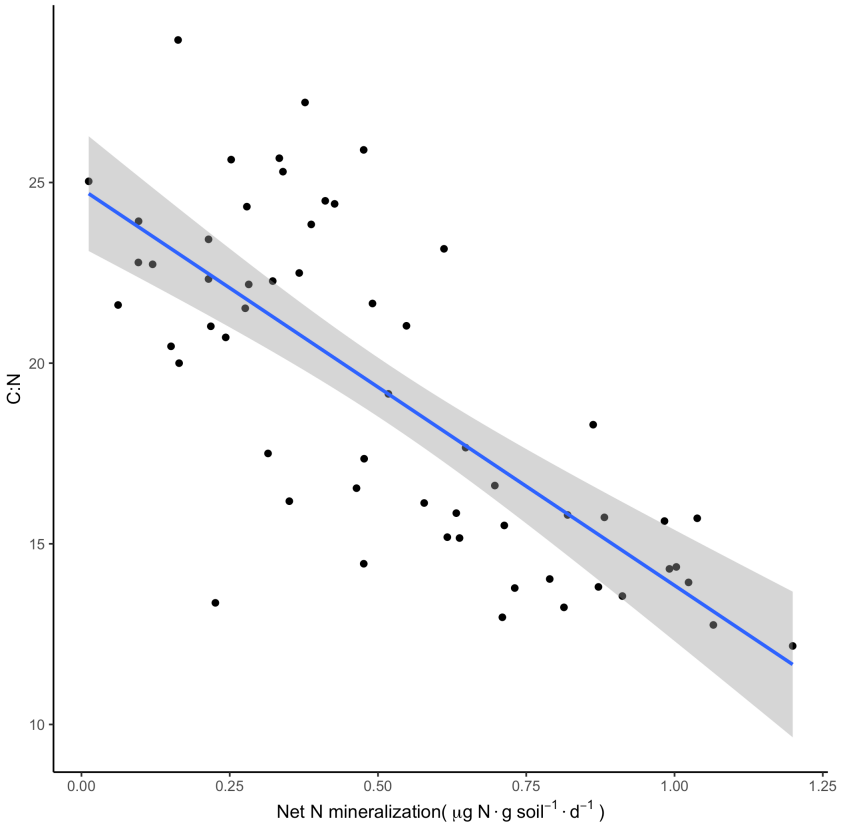

Supplementary Figure 4-14 C:N is negatively correlated with soil inorganic N availability ($P < 0.001$ $R^2_{adj} = 0.53$).

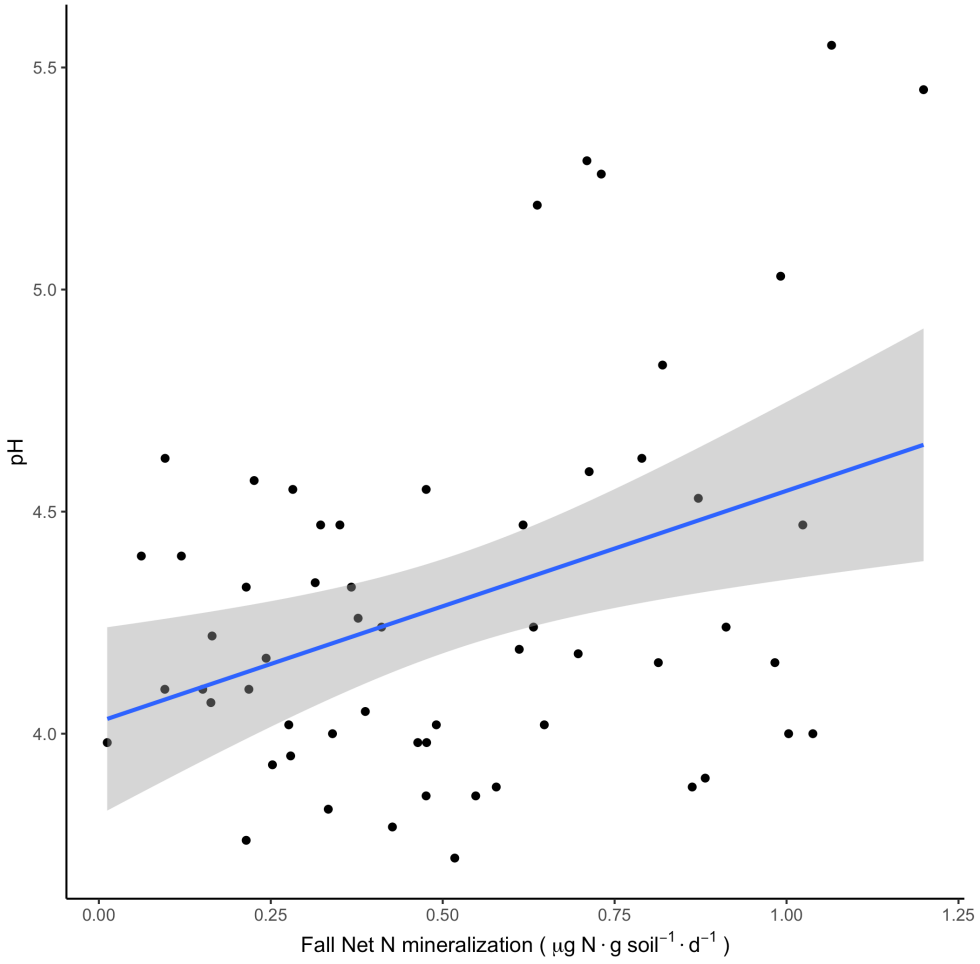

Supplementary Figure 4-15 Correlation between soil mineralization rate and soil pH ($P < 0.001$ $R^2_{adj} = 0.12$).

Table 4-1 Analysis of BAI, parameter posterior means, SD, and 95%CI

Parameter	mean	SD	2.5%	97.5%
$\alpha 1$ intercept	-1.2237	0.0510	-1.3195	-1.1168
$\alpha 2$ slope before change point	-0.0756	0.0622	-0.1967	0.0469
$\alpha 3$ difference in slope	0.4368	0.0471	0.3451	0.5292
$(\alpha 2+\alpha 3)$ slope after change point	0.3612	0.0232	0.3162	0.4070
$\alpha 4$ ln(dbh)	0.1847	0.0150	0.1553	0.2140
$\alpha 5$ BAIS	1.1895	0.0148	1.1593	1.2169
Change point	0.4453	0.0106	0.4278	0.4628
a intercept var	0.2574	0.0197	0.2203	0.2967
B ln(dbh)	-0.0385	0.0056	-0.0495	-0.0280
$\sigma 2$ year RE	42.3425	7.5604	29.3199	59.0738

Table 4-2 Analysis of GNES slopes parameter posterior means, SD, and 95%CI.

Parameter	mean	SD	2.5%	97.5%
$\theta 1$ intercept	0.0589	0.0068	0.0455	0.0719
$\theta 2$ slope before change point	-0.1489	0.0218	-0.1903	-0.1084
$\theta 3$ difference in slopes	0.0928	0.0159	0.0635	0.1245
$(\theta 2+\theta 3)$ slope after change point	-0.0560	0.0079	-0.0712	-0.0406
Change point	0.4763	0.0002	0.4760	0.4766

Supplementary References

Agerer, R., 2006. Fungal relationships and structural identity of their ectomycorrhizae. *Mycological progress*, *5*(2), pp.67-107.

Baker, M.E. and King, R.S., 2010. A new method for detecting and interpreting biodiversity and ecological community thresholds. *Methods in Ecology and Evolution*, *1*(1): 25-37

Bokulich, N.A., Kaehler, B.D., Rideout, J.R., Dillon, M., Bolyen, E., Knight, R., Huttley, G.A. and Caporaso, J.G., 2018. Optimizing taxonomic classification of marker-gene amplicon sequences with QIIME 2's q2-feature-classifier plugin. *Microbiome*, *6*(1): 90

Darrouzet-Nardi, A., Ladd, M.P. and Weintraub, M.N., 2013. Fluorescent microplate analysis of amino acids and other primary amines in soils. *Soil Biology and Biochemistry*, *57*: 78-82.

Garnica, S., Schön, M.E., Abarenkov, K., Riess, K., Liimatainen, K., Niskanen, T., Dima, B., Soop, K., Frøslev, T.G., Jeppesen, T.S. and Peintner, U., 2016. Determining threshold values for barcoding fungi: lessons from Cortinarius (Basidiomycota), a highly diverse and widespread ectomycorrhizal genus. *FEMS Microbiology Ecology*, *92*(4).

Ibáñez I., Zak, D.R., Burton, A.J. and Pregitzer, K.S. 2018. Anthropogenic nitrogen deposition ameliorates the decline in tree growth caused by a drier climate. *Ecology, 99*:411-420

Lines ER, Zavala MA, Purves DW, Coomes DA. 2012. Predictable changes in aboveground allometry of trees along gradients of temperature, aridity and competition. *Global Ecology and Biogeography*, *21*(10):1017-28.

Lodge, D.J., Padamsee, M., Matheny, P.B., Aime, M.C., Cantrell, S.A., Boertmann, D., Kovalenko, A., Vizzini, A., Dentinger, B.T., Kirk, P.M. and Ainsworth, A.M., 2014. Molecular phylogeny, morphology, pigment chemistry and ecology in Hygrophoraceae (Agaricales). *Fungal Diversity*, *64*(1): 1-99.

McDonald, D., Clemente, J.C., Kuczynski, J., Rideout, J.R., Stombaugh, J., Wendel, D., Wilke, A., Huse, S., Hufnagle, J., Meyer, F. and Knight, R., 2012. The Biological Observation Matrix (BIOM) format or: how I learned to stop worrying and love the ome-ome. *Gigascience*, *1*(1): 2047-217x

Moeller, H.V., Peay, K.G. and Fukami, T., 2014. Ectomycorrhizal fungal traits reflect environmental conditions along a coastal California edaphic gradient. *FEMS microbiology ecology*, *87*(3): 797-806.

Nilsson, R.H., Larsson, K.H., Taylor, A.F.S., Bengtsson-Palme, J., Jeppesen, T.S., Schigel, D., Kennedy, P., Picard, K., Glöckner, F.O., Tedersoo, L. and Saar, I., 2019. The UNITE database for molecular identification of fungi: handling dark taxa and parallel taxonomic classifications. *Nucleic acids research*, *47*(D1): D259-D264.

NOAA 2019. Globally averaged marine surface annual mean data. ftp://aftp.cmdl.noaa.gov/products/trends/co2/co2_annmean_gl.txt retrieved November 15 2019.

Peltier, D.M., Fell, M. and Ogle, K., 2016. Legacy effects of drought in the southwestern United States: A multi-species synthesis. *Ecological Monographs*, *86*(3): 312-326.

Plummer, M. 2003. JAGS: a program for analysis of Bayesian graphical models using Gibbs sampling. Proceedings of the 3rd International Workshop on Distributed Statistical Computing. March 20-22 Vienna, Austria.

Plummer, M., A. Stukalov, and M. Denwood. 2018. Package 'rjags'. Bayesian graphical models using MCMC. R package version 408. https://CRAN.R-project.org/package=rjags

R Development Core Team. 2013. R: a language and environment for statistical computing. R Foundation for Statistical Computing, Vienna, Austria.

Taylor, D.L., Walters, W.A., Lennon, N.J., Bochicchio, J., Krohn, A., Caporaso, J.G. and Pennanen, T., 2016. Accurate estimation of fungal diversity and abundance through improved lineage-specific primers optimized for Illumina amplicon sequencing. *Appl. Environ. Microbiol.*, *82*(24): 7217-7226.

Wang, Y.I., Naumann, U., Wright, S.T. and Warton, D.I., 2012. mvabund–an R package for model-based analysis of multivariate abundance data. *Methods in Ecology and Evolution*, *3*(3): 471-474.

Warton, D.I., Blanchet, F.G., O'Hara, R.B., Ovaskainen, O., Taskinen, S., Walker, S.C. and Hui, F.K., 2015. So many variables: joint modeling in community ecology. *Trends in Ecology & Evolution*, *30*(12): 766-779.

Zak, D.R. and Pregitzer, K.S., 1990. Spatial and temporal variability of nitrogen cycling in northern lower Michigan. *Forest Science*, *36*(2): 367-380.

Zak, D.R., Pregitzer, K.S. and Host, G.E., 1986. Landscape variation in nitrogen mineralization and nitrification. *Canadian Journal of Forest Research*, *16*(6):1258-1263.

Chapter 5 Conclusions

- The polyphyletic evolutionary history of the ectomycorrhizal (ECM) lifestyle is key to understanding their role in the decay of soil organic matter (SOM).The ~85 independent lineages of ECM fungi possess a wide and uneven range of genes potentially encoding the decay of SOM. Understanding the presence of putative decay genes in ECM genomes is critical, however, further study of the expression of these genes under field settings, the conformation and activity of the enzymes they encode, and the fungal transfer of N-SOM to the plant host, is urgently needed to understand the contribution of N-SOM to plant growth. Unlike the monophyletic arbuscular mycorrhiza, genomic variation among ECM lineages is to be expected. The impact of this variation is critical to understanding their community impact on ecosystem function.
- The metagenomic evidence presented here represents a trait-based explanation for decades of work documenting the primacy of soil inorganic N availability in ECM community assembly. So called 'nitrophobic' ECM taxa, species that are often found in low inorganic N soils, have higher enzymatic potential to decay organic N bearing compounds. Similarly, I document that ECM communities inhabiting low inorganic N soils have greater genetic potential to obtain N-SOM. These patterns are likely to extend to boreal forests because similar patterns in community turnover have primarily demonstrated in such forest ecosystems. I employ metagenomic enabled trait-based approach to support the role of soil inorganic N as an environmental filter structuring ECM communities. Heterogeneity in plant C allocation to ECM fungi is likely to be a key component of the role of soil N availability as an environmental filter. The degree of variation in community weighted trait-means across a soil inorganic N gradient was comparable to studies of plant-trait covariance.
- Functional redundancy within microbial communities has been predicted to be 'inevitable', and here metagenomic analyses of ECM communities was used to detect a degree of redundancy at several scales of inference. However, for specific 'indicator'

gene families and when ECM decay was scaled by differences in biomass, ECM communities vary significantly in their genomic potential to decay SOM. I conclude that functional redundancy among ECM communities and microbial communities more generally, may arise as an artefact of specific levels of genomic and environmental inference.

- Several ECM lineages such as *Cortinarius* and *Piloderma* may play a disproportionate role in plant access to N-SOM via their production of Manganese Peroxidases (MnP). These ECM lineages evolved from white-rot saprotrophic progenitors, whereas many ECM taxa that that do not possess MnP, evolved from brown-rot or Ascomycete ancestors. These saprotrophic lineages never evolved class II peroxidases. MnP have been widely implicated in boreal in temperate ecosystems as key saprotrophic and ECM enzymes mediating the decay of SOM. Here I found that ECM communities were enriched in genes encoding this enzyme in low inorganic N soils.
- Dendrochronological evidence presented in Chapter 3, corroborate the predictions derived from Chapter 2. Bayesian models demonstrate that N-SOM appears to primarily contribute to plant growth in low inorganic N soils; shifts in the community weighted mean traits of ECM communities, independently confirm this mechanism. Together, shifts in the functional attributes of ECM communities may represent an overlooked basis for plant flexibility in nutrient foraging strategies, and this work broadly extends theory of optimal plant N foraging. This conclusion corroborates a hierarchy of plant preferences for distinct N sources, and emphasizes market-based perspectives on flexible plant C allocation for N via their ECM symbionts.
- I find strong support for the hypothesized role of plant uptake of N-SOM in positive plant response to eCO_2. Dendrochronological evidence supports positive response of *Quercus rubra* to eCO_2, however this response was only observed for trees inhabiting low inorganic N soils. Metagenomic insights derived for the primary nutrient uptake organs inhabiting these individual plants--ECM fungi--provides mechanistic evidence for plant uptake of N-SOM. Although ECM fungi may partially alleviate plant N limitation, by foraging for N-SOM, acquisition of this N source, likely carries enhanced C costs to the plant host. Critically, I demonstrate that heterogeneity in ECM community composition and function can differentially impact plant response to climate change. Predicting plant

response to eCO_2 requires further insight into the functional biogeographic structure of ECM communities at global scales.